NASA/CR—2010-215673

Closed Brayton Cycle Power Conversion Unit for Fission Surface Power Phase I Final Report

Robert L. Fuller
Barber-Nichols Inc., Arvada, Colorado

June 2010

NASA STI Program . . . in Profile

Since its founding, NASA has been dedicated to the advancement of aeronautics and space science. The NASA Scientific and Technical Information (STI) program plays a key part in helping NASA maintain this important role.

The NASA STI Program operates under the auspices of the Agency Chief Information Officer. It collects, organizes, provides for archiving, and disseminates NASA's STI. The NASA STI program provides access to the NASA Aeronautics and Space Database and its public interface, the NASA Technical Reports Server, thus providing one of the largest collections of aeronautical and space science STI in the world. Results are published in both non-NASA channels and by NASA in the NASA STI Report Series, which includes the following report types:

- TECHNICAL PUBLICATION. Reports of completed research or a major significant phase of research that present the results of NASA programs and include extensive data or theoretical analysis. Includes compilations of significant scientific and technical data and information deemed to be of continuing reference value. NASA counterpart of peer-reviewed formal professional papers but has less stringent limitations on manuscript length and extent of graphic presentations.

- TECHNICAL MEMORANDUM. Scientific and technical findings that are preliminary or of specialized interest, e.g., quick release reports, working papers, and bibliographies that contain minimal annotation. Does not contain extensive analysis.

- CONTRACTOR REPORT. Scientific and technical findings by NASA-sponsored contractors and grantees.

- CONFERENCE PUBLICATION. Collected papers from scientific and technical conferences, symposia, seminars, or other meetings sponsored or cosponsored by NASA.

- SPECIAL PUBLICATION. Scientific, technical, or historical information from NASA programs, projects, and missions, often concerned with subjects having substantial public interest.

- TECHNICAL TRANSLATION. English-language translations of foreign scientific and technical material pertinent to NASA's mission.

Specialized services also include creating custom thesauri, building customized databases, organizing and publishing research results.

For more information about the NASA STI program, see the following:

- Access the NASA STI program home page at *http://www.sti.nasa.gov*

- E-mail your question via the Internet to *help@sti.nasa.gov*

- Fax your question to the NASA STI Help Desk at 443–757–5803

- Telephone the NASA STI Help Desk at 443–757–5802

- Write to:
  NASA Center for AeroSpace Information (CASI)
  7115 Standard Drive
  Hanover, MD 21076–1320

NASA/CR—2010-215673

Closed Brayton Cycle Power Conversion Unit for Fission Surface Power Phase I Final Report

Robert L. Fuller
Barber-Nichols Inc., Arvada, Colorado

Prepared under Contract NNC08CA64C

National Aeronautics and
Space Administration

Glenn Research Center
Cleveland, Ohio 44135

June 2010

Acknowledgments

The author would like to acknowledge the support of the NASA Glenn Research Center.

This report contains preliminary findings, subject to revision as analysis proceeds.

Level of Review: This material has been technically reviewed by expert reviewer(s).

Available from

NASA Center for Aerospace Information
7115 Standard Drive
Hanover, MD 21076–1320

National Technical Information Service
5301 Shawnee Road
Alexandria, VA 22312

Available electronically at http://gltrs.grc.nasa.gov

Table of Contents

Table of Figures

Table of Tables

1. Summary and Introduction

1.1 Summary

A Closed Brayton Cycle power conversion system has been developed to support the NASA fission surface power program. The goal is to provide electricity from a small nuclear reactor heat source for surface power production for lunar and Mars environments. The selected media for a heat source is NaK 78 with water as a cooling source.

The Closed Brayton Cycle power was selected to be 12 kWe output from the generator terminals. A heat source NaK temperature of 850 K +/-25 K was selected. The cold source water was selected at 375 K +/-25 K. A vacuum radiation environment of 200 K is specified for environmental operation.

The prioritized goals for the power conversion system are contained in the NASA specification as follows:

- Close relevance to future flight designs, including the potential for 8 year service life
- Credible development path and maturation approach exist to achieve TRL 6 by FY 2012 with a reasonable cost
- Low development cost and risk
- Design extensible to Mars (materials and design strategies compatible with mars environment)
- High thermal-to-electric efficiency
- Minimum complexity
- Low mass and volume

The major components of the system are the power converter, the power controller, and the top level data acquisition and control unit. The power converter with associated sensors resides in the vacuum radiation environment. The power controller and data acquisition system reside in an ambient laboratory environment. Signals and power are supplied across the pressure boundary electrically with hermetic connectors installed on the vacuum vessel.

System level analyses were performed on working fluids, cycle design parameters, heater and cooling temperatures, and heat exchanger options that best meet the needs of the power converter specification. The goal is to provide a cost effective system that has high thermal-to-electric efficiency in a compact, lightweight package. A system level trade study was performed to optimize these competing factors in order to specify the various system components.

The power converter is a rotating turbine-alternator-compressor (TAC), NaK heater, gas-to-gas recuperator, and gas-to-water cooler.

The TAC consists of a centrifugal compressor, a two-pole permanent magnet alternator, and a radial in-flow turbine on a single shaft. The rotor is supported by gas foil journal and thrust bearings. The gas foils are coated to allow numerous startup and shutdown operations.

Labyrinth seals are utilized to limit turbine and compressor leakage into the generator cavity. The foil bearings are cooled by a combination of the labyrinth leakage flow from the compressor and also a secondary pumped loop that utilizes compressor inlet gas. The test unit would utilize o-rings and metallic c-seals for laboratory testing and be fully welded for the space-based version. The generator is cooled by the pumped secondary flow loop and also liquid cooling with a water jacket.

The NaK heater is a plate-fin type heat exchanger with NaK 78 heating the CO2 gas on the Brayton loop. The recuperator is a CO2/CO2 gas heat exchanger which preheats the gas from the compressor exit by utilizing waste heat from the turbine exit. The preheated compressor air enters the NaK heater to increase the gas energy content prior to entering the turbine. The CO2 to water cooler is used to expel the residual heat from the recuperator to cool the compressor inlet gas. The water is pumped to radiation cooler panels that expel the heat to the atmosphere. The system is piped and insulated with multi-layer insulation (MLI) to minimize heat loss.

The power controller utilizes a full-bridge interface to the alternator to allow motoring for startup and active rectification for power production. A buck/boost converter is utilized for conversion from the specified alternator output of 400 VAC to 120 VDC. The controller is liquid cooled and packaged in a 19-inch rack mount chassis.

Design decisions that resulted from the trade studies:

- Working fluid, carbon dioxide
- Maximum working pressure 689.5 kPa
- Pressure ratio 2:1
- Generator Efficiency 98%
- Recuperator Effectiveness 90%
- Turbine Efficiency 87%
- Compressor Efficiency 84%
- Shaft Speed 65 krpm

1.2 Introduction

The closed Brayton power converter was developed to support National Aeronautics and Space Administration goals of generating electricity using a nuclear heat source. While the use of closed Brayton cycle technology for space power is not new, the system proposed herein reflects modern technological improvements to satisfy a new specification and power goal. The system is packaged to be as compact is practical while insuring material stress limitations are not exceeded due to gravity, pressure, and thermal loading and cycling.

Closed Brayton cycle machinery has the ability to provide high reliability, good efficiency, and can operate for long periods as self-contained power sources for moon or Mars based missions. Development of the power conversion system focused on a compact system with a rotating turbine-alternator-compressor (TAC) power production. The TAC can operate in a 0 to 2 g environment in a variety of attitudes from horizontal to vertical and therefore could be used for not only terrestrial power, but space based power as well.

The power conversion system development includes analysis that simulates full power as well as partially power operation. The power controller for the TAC can provide rotating machine control during load steps and also operates as a state machine for startup, shutdown, normal operation, and fault handling modes.

2. Fluid and System Trade Study

2.1 Fluid Study

A study was performed to identify the best working fluid for use in the closed Brayton cycle power converter. The fluid selection was limited to those fluids known to be stable and remain a gas at working temperatures of 200 K to 875 K. Good thermodynamic and transport properties enable efficiency aerodynamic performance for the turbine and compressor as well as a direct impact on heat exchanger size and weight. Additionally, due to the long life, material compatibility is important. A non-reactive, inert gas is beneficial for material selection criteria. The fluids considered for this study were carbon dioxide, argon, nitrogen, and helium/xenon mixture. Helium was not considered due the low molecular weight causing extreme turbomachinery design challenges.

For this trade study, a simple recuperated Brayton cycle was used. The recuperator effectiveness is directly tied to the size of the recuperator heat exchanger and also dictates the optimum pressure ratio for a specific working fluid. A spreadsheet was utilized to perform the cycle analysis for the trade study. The spreadsheet is linked to Refprop (National Institute of Standards and Technology Property Database) to calculate the thermal and transport properties automatically. Figure 1 shows the cycle in graphical form and the cycle input sheet is shown in Figure 2. This is an example only and is not the final cycle design.

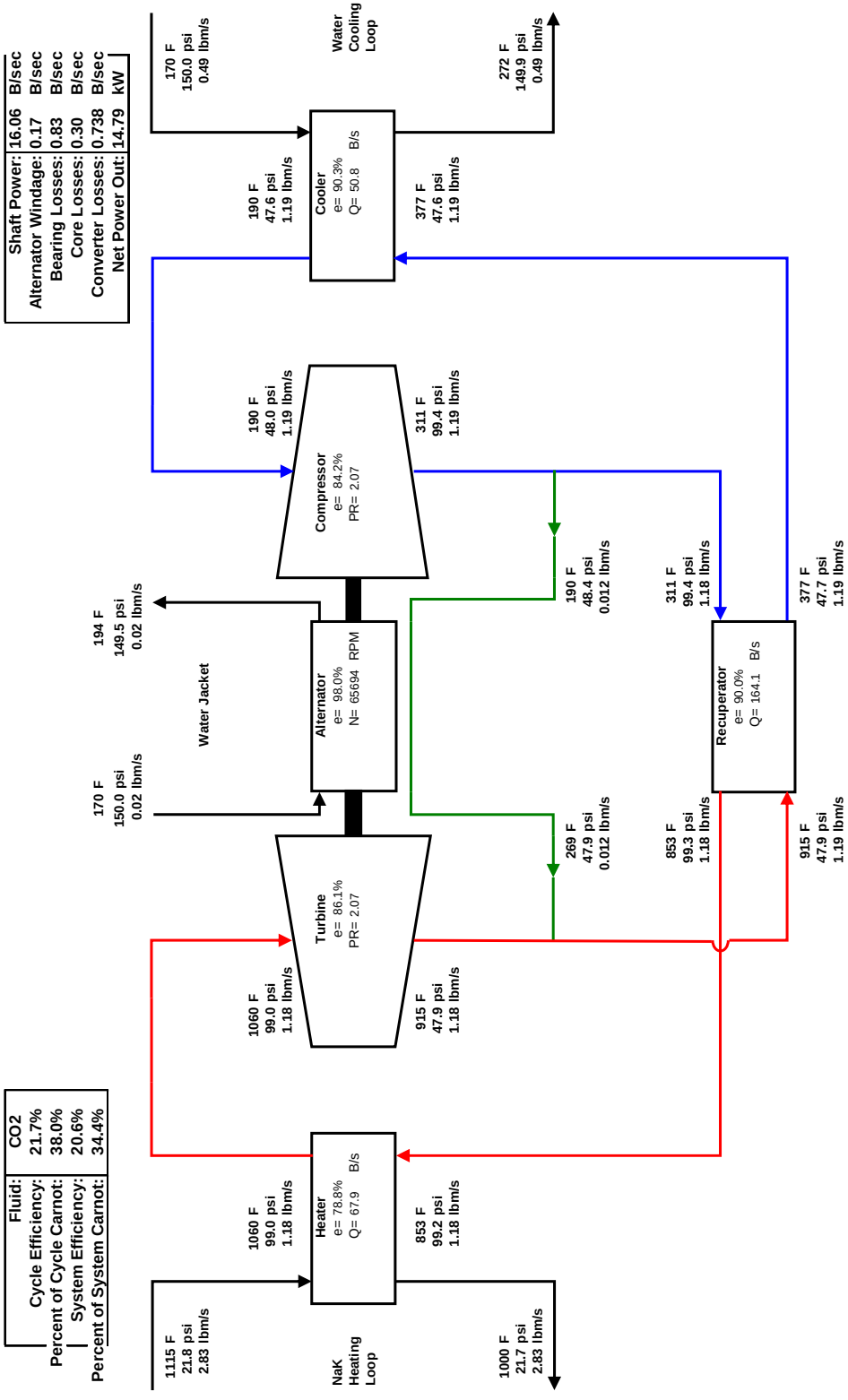

Figure 1: Cycle Diagram in Graphical Format Example (English Units Version)

	Temperature F	Pressure Psia	Density lbm/ft^3	Enthalpy B/lbm	Entropy B/ft-F
Turbine In	1060.000	98.956	0.267	463.162	0.821
Turbine Out	915.227	47.890	0.143	422.771	0.826
Recup Hot In	914.722	47.879	0.143	422.632	0.826
Recup Hot Out	377.144	47.720	0.235	283.585	0.698
Cooler In	377.140	47.637	0.234	283.585	0.698
Cooler Out	190.294	47.604	0.303	240.850	0.641
Comp In	190.330	48.032	0.306	240.850	0.640
Comp Out	311.291	99.405	0.534	267.457	0.645
Recup Cold In	311.289	99.372	0.534	267.457	0.645
Recup Cold Out	853.475	99.306	0.310	405.609	0.780
Heater In	853.474	99.227	0.310	405.609	0.780
Heater Out	1060.000	99.032	0.267	463.162	0.821
Heater In	1115.330	21.800	45.978		
Heater Out	1000.000	21.656	46.978		
Cooler In	170.330	150.000	60.814		
Cooler Out	272.100	149.946	58.203		
Jacket In	170.330	150.000	60.814		
Jacket Out	193.867	149.500	60.292		

Heater

	NaK	
Fluid		
mdot	2.833	lbm/s
Heat Transfer	67.913	B/s
LMTD	55.330	F
Pressure Drop	0.195	psi
effectiveness	78.85%	

Cooler

	Water	
Fluid		
mdot	0.494	lbm/s
Heat Transfer	50.754	B/s
LMTD	60.230	F
Pressure Drop	0.033	psi
effectiveness	90.35%	
efficiency	90.75%	

Cycle

	CO2	
Fluid		
Units	English	
Cycle Efficiency	21.73%	
System Efficiency	20.64%	
Cycle Carnot	57.23%	
System Carnot	60.00%	
Percent Cycle Carnot	37.97%	
Percent System Carnot	34.40%	
delta P hot	0.524	psi
delta P cold	0.283	psi

Turbine

speed	65694	rpm
mdot	1.180	lbm/sec
pressure ratio	2.066	
efficiency	86.07%	
power	47.661	B/sec

Compressor

	65694	rpm
speed		
mdot	1.1876497	lbm/sec
pressure ratio	2.070	
efficiency	84.23%	
power	31.600	B/sec
Pressure Balance	0.500	psid

Recuperator

	164.076	B/s
Heat Transfer		
LMTD	63.523	F
Pressure Drop - Hot	0.159	psi
Pressure Drop - Cold	0.066	psi
effectiveness	90.00%	
efficiency	90.00%	

Bearings

	0.5	psid
Bearing delta P		
Bearing Lube Percent	1.00%	
Bearing lube	0.012	lbm/s
Enthalpy Out	258.389	B/lbm

Generator

	98.00%	
gen efficiency		
conv efficiency	95.00%	
net turbine power	16.061	B/sec
windage loss	0.171	B/sec
bearing loss	0.833	B/sec
core loss	0.301	B/sec
converter loss	0.738	B/sec
gen power	14.756	B/sec
gen power	15.565	kW
conv power	14.018	B/sec
conv power	14.787	kW
full power	12	kW
percent power	123.23%	

Fluid Mass

Pipe 2	0.007	lbm
Pipe 3	0.053	lbm
Pipe 4	0.096	lbm
Pipe 5	0.077	lbm
Pipe 6	0.113	lbm
Pipe 1	0.060	lbm
Heater	0.297	lbm
Cooler	0.026	lbm
Recuperator-Hot	0.240	lbm
Recuperator-Cold	0.530	lbm
Hot Side	0.658	lbm
Cold Side	0.842	lbm
Total	1.500	lbm
Design Point	1.482	lbm
Mass Balance	0.018	lbm

Jacket

	Water	
Fluid		
mdot	0.02	lbm/sec
Delta P	0.5	psia
heat transfer	0.472	B/sec

Pipe Losses

Pipe 2	0.011	psid
Pipe 3	0.083	psid
Pipe 4	0.072	psid
Pipe 5	0.033	psid
Pipe 6	0.079	psid
Pipe 1	0.076	psid

Figure 2: Cycle Spreadsheet Input Screen Example (English Units Version)

Several caveats were placed on the fluid design trade study. All fluids were treated equally with fixed expected turbomachinery efficiency, recuperator effectiveness, generator efficiency, converter efficiency, and bearing losses. Windage losses were calculated as part of the analysis since it was easy to perform with this calculation imbedded in the worksheet and the variable windage that is inherent in gas selection.

The operating pressure was optimized for each fluid using an Excel based routine. This was done for all the working fluids under consideration for the three temperature ratios. The high temperature ratio is the highest NaK temperature and the lowest cooling water temperature. This results in the highest power output condition. The medium temperature ratio is the nominal NaK and cooling water temperature. This is the design point and per the specification should obtain 12 kWe of power from the generator. The low temperature ratio is the lowest NaK temperature coupled with the highest cooling water temperature. The recuperator effectiveness was set high with the knowledge that the actual recuperator sizing trade study would happen after the working fluid selection was performed. Therefore the overall cycle efficiency was optimistic relative to size/volume constraints placed in the specification after the project was initiated.

An initial survey of candidate operating gases was done to ascertain cycle efficiency and maximum operating pressure. The cycle spreadsheet used an internal optimization routing to find the maximum efficiency and operating pressure for a fixed recuperator effectiveness and temperature ratio. The gases considered were nitrogen, carbon dioxide, argon, and HeXe mixture. The data are shown in Figure 3. It is clear that the HeXe mixture allows the highest cycle efficiency. The optimum system operating pressure is similar for all gases except carbon dioxide, which is lower. The lower operating pressure should yield lighter pressure containment structure and therefore the power per unit weight for the system operating on carbon dioxide may be higher.

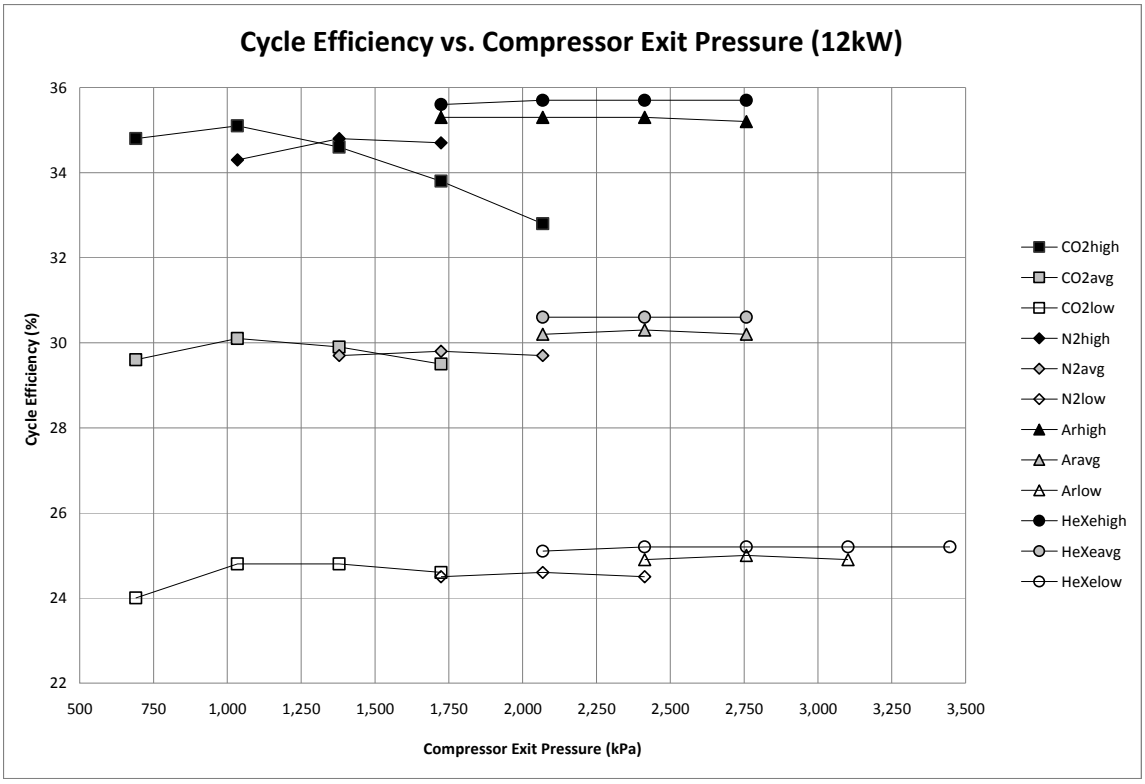

Figure 3: Cycle Efficiency vs Compressor Exit Pressure for Various Gases

The results of the fluid study at 12 kWe point to an obvious fluid choice, based on efficiency alone, of HeXe mixture. However given the cost of the HeXe fluid, it would probably be necessary to initially design the system for Argon use to test the TAC components due to the similar molecular weight of Argon and HeXe mixture. The heat exchangers would need to be larger to accommodate the Argon properties and therefore the test relevance to future flight needs would be compromised. Certainly the cost of Xenon may violate the need for a reasonable cost program.

With HeXe not a practical option for the goals of this program, Argon and Carbon Dioxide would be the next logical choices based on cycle efficiency alone. Given that Carbon Dioxide would operate at a lower system pressure it was concluded that carbon dioxide would be a better choice than either Argon or Nitrogen based on cycle efficiency and operating pressure, neglecting system level trade parameters such as heat exchanger size, turbine size, compressor size, operating speed, system weight, and other parameters.

An additional interest in fluid selection is the size and therefore the weight of the heat exchangers. The analysis was done utilizing the same spreadsheet that was formulated to yield an estimated size and weight for the heater, recuperator, and gas cooler. Figure 4 shows the gas cooler design sheet that was used for the analysis. Figure 5 shows the recuperator design sheet, and Figure 6 the gas cooler design sheet.

	Temperature F	Pressure Psia	Density lbm/ft^3	Enthalpy B/lbm	Entropy B/ft*F	Viscosity lbm/ft*s	Prandtl -	Thermal Conductivity B/hr*ft*F	Specific Heat B/lbm*F
Shell Side In	215.000	100.000	59.770	183.542	0.317	0.000186	1.718	0.393	1.008
Shell Side Out	227.706	98.600	59.442	196.357	0.336	0.000173	1.599	0.394	1.010
Shell Average	221.353	99.300	59.606	189.949	0.326	0.000180	1.659	0.394	1.009
Tube Side In	395.494	39.486	0.190	288.050	0.712	0.000015	0.731	0.018	0.239
Tube Side Out	225.000	39.474	0.238	248.655	0.661	0.000013	0.744	0.014	0.222
Tube Average	310.247	39.480	0.214	268.353	0.686	0.000014	0.737	0.016	0.231

Units	English
Reset Loops (0 then 1)	
Shell	1
Tube	1

	Tube Side	Shell Side	Units
Fluid	CO2	Water	
Mass Flow Rate	1.139	3.500	lbm/s
Velocity In	21.837		ft/s
Velocity Out	17.429		ft/s
Average Velocity	19.38562181	0.977337065	ft/s
Reynolds Number	9200	7849	-
Viscosity Ratio		1.032291085	-
Heat Capacity	0.262812721	3.530762691	B/s*F
Nusselt Number	31.12	61.02	-
Convection Coefficient	15.88	991.71	B/hr*ft^2*F
Pressure Drop Initial Estimate			
delta P/P in	0.03%	1.40%	
delta P	0.012	1.400	psi
Resulting Pressure	39.486	98.600	psia
Pressure Drop Final Estimate			
Roughness	0.000005		ft
Friction Factor	0.032	0.0024	- / ft^2/in^2
Major Pressure Drop	0.047	0.6228	psi
Minor Pressure Drop	0.013		psi
delta P/P in	0.15%	0.62%	
Resulting Pressure	39.53	99.37721861	psia
	Re > 10,000	Update f from Fig 29, Kern	

Heat Transfer	44.851	B/s			
Pinch 1	167.787	F			
Pinch 2	10.000	F			
LMTD	55.95076673	F			
UA (LMTD)	0.801615719	B/s*F			
UA (design)	0.829434947	B/s*F			
efficiency	94.67%	-			
effectiveness	94.46%	-			
Tube Thermal Conductivity	100	B/hr*ft*F	Aluminum alloy		
					wt kg
Shell Internal Diameter	8.000	in	*7.7*	shell	20.26704
Tube Length	64.000	in	*61.9*	tubes	94.03908
Baffles	10	-	*10*	total	114.3061 51.95733
Tube Internal Diameter	0.374	in			
Tube Wall Thickness	0.032	in			
Clearance	0.100	in			
Percent usable cross-section	90%				
Tube Outside Diameter	0.438	in			
Tube Pitch	0.538	in	(Triangle Pitch)		
Pitch Area	0.050	in^2			
Number of Tubes	360				
Tube Flow Area	39.549	in^2			
Baffle Space	5.818	in			
Shell Cross Flow Area	8.652	in^2			
Shell Hydraulic Diameter	0.291	in			
Tube Heat Transfer Area	27070.978	in^2			
Shell Heat Transfer Area	31703.445	in^2			
Volume	3485.073	in^3			
	2.017	ft^3			

Figure 4: Gas Cooler Design Spreadsheet

The gas cooler design sheet utilizes a tube shell heat exchanger calculation. The eventual heat exchanger technology chosen is plate/fin, but for a fluid trade study, the defining metric is the relative size for the various gases and therefore the tube/shell calculation is valid and is more widely represented in literature and therefore more reliable from the analysis perspective.

	Temperature F	Pressure Psia	Density lbm/ft^3	Enthalpy B/lbm	Entropy B/lbm*F	Viscosity lbm/ft*s	Prandtl -	Thermal Conductivity B/hr*ft*F	Specific Heat B/lbm*F		Units	English
Hot Side In	929.421	39.584	0.117	426.727	0.837170628	0.000023	0.724	0.032	0.277		Reset Loops (0 then 1)	
Hot Side Out	395.494	39.486	0.190	288.050	0.712024156	0.000015	0.731	0.018	0.239		Hot	1
Hot Side Average	662.457	39.535	0.153	357.389	0.775	0.000	0.727	0.025	0.258		Cold	1
Cold Side In	335.494	75.000	0.389	273.429	0.665449319	0.000014	0.736	0.017	0.235			
Cold Side Out	871.796	74.873	0.231	410.720	0.796617567	0.000022	0.724	0.030	0.274			
Cold Side Average	603.645	74.936	0.310	342.074	0.731	0.000	0.730	0.023	0.254			

	Hot Side	Cold Side	Units	
				442.208
Fluid	CO2	CO2		
Mass Flow Rate	1.1385	1.15	lbm/s	
Inlet Velocity	12.55266473	3.805549785	ft/s	
Exit Velocity	7.726347251	6.425215413	ft/s	
Reynolds Number	564	601	-	(600)
Pressure Drop Initial Estimate				
delta P/P in	0.25%	0.17%		
delta P	0.099	0.128	psi	
Resulting Pressure	39.584	74.873	psia	
Velocity Term	*5.0194E-05*	*8.11264E-06*	-	
Entrance Effect	*1.979364037*	*1.979364037*	-	
Flow Acceleration Effect	*-0.768970985*	*1.376760666*	-	
Core Friction Effect	*45.24729031*	*74.58383663*	-	
Exit Effect	*0.492020162*	*1.349630519*	-	
Delta P/P1	0.23%	0.06%	-	
Pressure Drop	0.09	0.05	psi	
Resulting Pressure	39.58	74.95	psia	
Nusselt Number	8.0	8.6	-	
Convection Coefficient	28.7	28.8	B/hr*ft^2*F	
m	96.5	96.8	?	
Fin Efficiency	0.559	0.558	-	
Fin Effectiveness	0.607	0.606	-	

Q	157.8838719	B/s	157.8839		
Pinch Hot	57.625	F			
Pinch Cold	60	F			
LMTD	58.80429358	F			
UA (LMTD)	2.684903811	B/s*F			
UA (Heat Exchanger)	3.024949401	B/s*F			
efficiency	90.72%	-			
effectiveness	90.30%	-			
Fin Thermal Conductivity	12.3	12.3	B/hr*ft*F	Stainless Steel	
Plate Thermal Conductivity	12.3		B/hr*ft*F		
Table 9.3 (Kays & London)					
Surface Designation	17.8-3/8W	17.8-3/8W			
Plate Spacing	0.0345	0.0345	ft		
Hydraulic Diameter	0.00696	0.00696	ft		
Fin Thickness	0.006	0.006	in		
Area/Volume Ratio	514	514	ft^2/ft^3		
Fin Area Ratio	0.892	0.892	-		
Frontal Area	2	2	ft^2	*1.9*	
Flow Length	1.4	1.4	ft	*1.3*	
Layers	1	1			
Plates per layer	10	10			
Width	0.796140493	0.796140493	ft		
Plate thickness	0.063		in		
Volume	2.8		ft^3		
Heat Transfer Area to Volume	223.0566038	223.0566038	ft^2/ft^3		
Heat Transfer Area	624.5584906	624.5584906	ft^2		
Free to Frontal Area Ratio	0.388118491	0.388118491	-		
Free Flow Area	0.776236981	0.776236981	ft^2		
Table 10.6 (Kays & London)					
St*Pr^2/3	0.0158	0.0158	-	Update for Reynolds Number	
Friction Factor	0.0738	0.0738	-		
Figure 5.4 (Kays & London)					
Entrance Loss Coefficient	1.13	1.13	-	Adjust for Reynolds Number and Free to Fron	
Exit Loss Coefficient	0.05	0.05	-		

8000	lb	Weight	89.70553592	kg	
75	ft^3				
106.6666667	lb/ft^3				
64.0753828					
29.125174	kg/ft^3				

Figure 5: Recuperator Design Sheet

The recuperator design is a plate fin type that utilizes correlations from "Compact Heat Exchangers", W.M. Kays and A.L. London, ISBN-10: 1575240602. The method utilized includes the proper heat transfer parameters, but does not include any structural analysis regarding the pressure containment boundary. Therefore the analysis is useful for relative size and weight from gas to gas, but not necessarily accurate in an absolute sense.

	Temperature F	Pressure Psia	Density lbm/ft^3	Enthalpy B/lbm	Entropy B/ft*F	Viscosity lbm/ft*s	Prandtl -	Thermal Conductivity B/hr*ft*F	Specific Heat B/lbm*F
Shell Side In	1070.000	20.000	46.371			0.000118	0.006	15.057	0.208
Shell Side Out	987.835	18.952	47.084			0.000125	0.006	15.152	0.208
Shell Average	1028.917	19.476	46.727			0.000122	0.006	15.105	0.208
Tube Side In	871.796	74.873	0.231	410.720	0.797	0.000022	0.724	0.030	0.274
Tube Side Out	1060.000	74.753	0.202	463.230	0.834	0.000025	0.723	0.035	0.284
Tube Average	965.898	74.813	0.216	436.975	0.815	0.000023	0.724	0.032	0.279

Units	English
Reset Loops (0 then 1)	
Shell	1
Tube	1

	Tube Side	Shell Side	Units
Fluid	CO2	NaK	
Mass Flow Rate	1.139	3.500	lbm/s
Velocity In	30.103		ft/s
Velocity Out	34.431		ft/s
Average Velocity	32.12174774	1.579635275	ft/s
Reynolds Number	9250	14875	-
Viscosity Ratio		0.996948943	-
Heat Capacity	0.317478429	0.727495432	B/s*F
Nusselt Number	30.09	12.87	-
Convection Coefficient	31.35	7939.34	B/hr*ft^2*F
Pressure Drop Initial Estimate			
delta P/P in	0.16%	5.24%	
delta P	0.120	1.048	psi
Resulting Pressure	74.753	18.952	psia
Pressure Drop Final Estimate			
Roughness	0.000005		ft
Friction Factor	0.032	0.0024	- / ft^2/in^2
Major Pressure Drop	0.195091	1.6385	psi
Minor Pressure Drop	0.037066		psi
delta P/P in	0.31%	8.19%	
Resulting Pressure	74.64	18.36152981	psia
	Re > 10,000	Update f from Fig 29, Kern	

(10,000)

Heat Transfer	59.783	B/s	
Pinch 1	116.038	F	
Pinch 2	10.000	F	
LMTD	43.25740042	F	
UA (LMTD)	1.382020938	B/s*F	
UA (design)	1.45124174	B/s*F	
effectiveness	94.95%	-	
Tube Thermal Conductivity	12.3	B/hr*ft*F	Stainless steel
Shell Internal Diameter	6.600	in	*6.6*
Tube Length	95.000	in	*90.5*
Baffles	15	-	*15*
Tube Internal Diameter	0.374	in	
Tube Wall Thickness	0.063	in	
Clearance	0.100	in	
Percent usable cross-section	90%		
Tube Outside Diameter	0.500	in	
Tube Pitch	0.600	in	(Triangle Pitch)
Pitch Area	0.058		
Number of Tubes	197	in	
Tube Flow Area	21.642	in^2	
Baffle Space	5.938	in	
Shell Cross Flow Area	6.531	in^2	
Shell Hydraulic Diameter	0.294	in	
Tube Heat Transfer Area	21989.295	in^2	
Shell Heat Transfer Area	29397.453	in^2	
Volume	3400.667	in^3	
	1.968	ft^3	

Figure 6: NaK Heater Design Sheet (Shell and Tube)

The results of this study, as seen in Figure 7, indicates that the HeXe heat exchanger sizing is the smallest. This is due to the excellent transport properties of the mixture. Since this gas mixture does not suit the cost of this program, the next choice is Carbon Dioxide. The Carbon Dioxide heat exchangers will be approximately 50% larger, but due to the lower pressure requirement, the anticipated weight will not scale with the same percentage. Clearly the Argon and Nitrogen heat exchangers are quite a bit larger and therefore Argon and Nitrogen are inferior relative to system weight and size. The data is presented at the low, medium, and high temperature ratios.

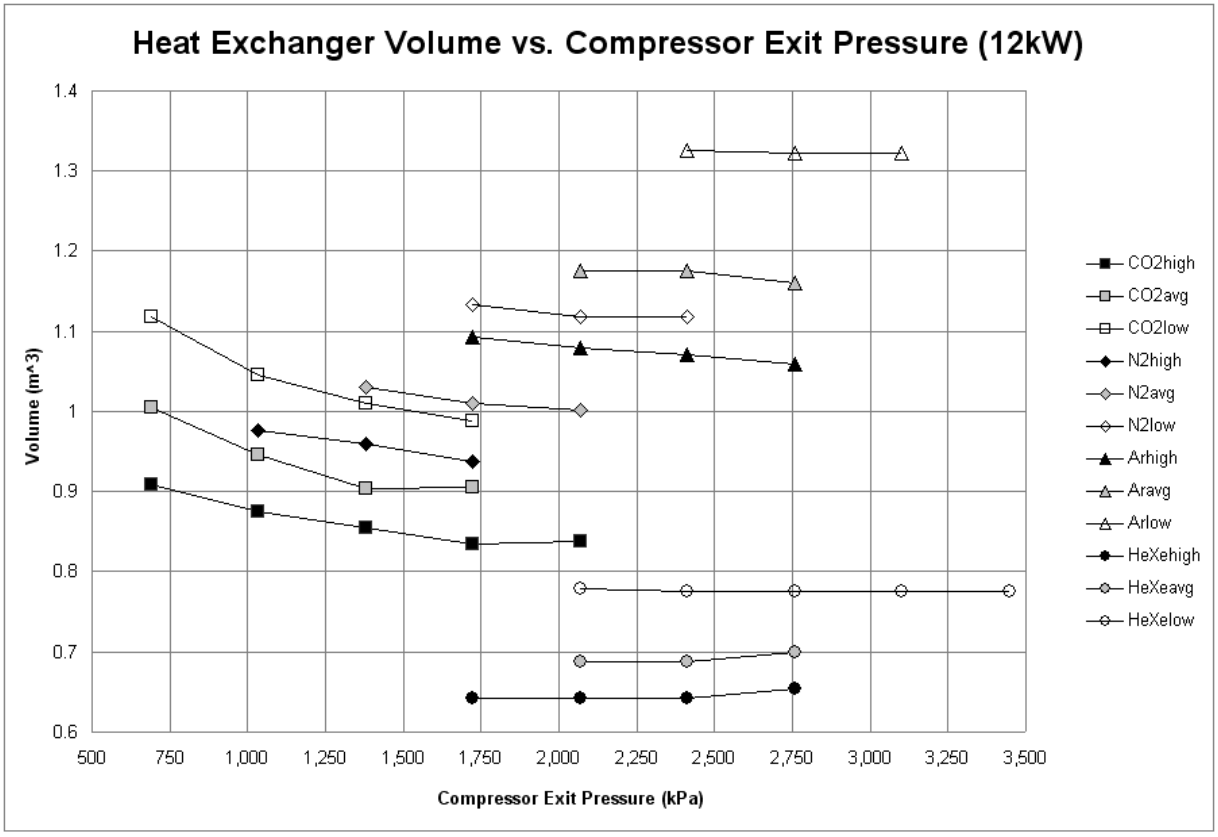

Figure 7: Heat Exchanger Volume vs. Compressor Exit Pressure at Various Temperature Ratios

Other figures of merit are the compressor and turbine efficiency. At the 12 kWe power range, the compressor and turbine wheel diameters become relatively small. This results in larger clearance losses due to practical machining tolerances and wheel clearances. Secondarily is the operating speed, slower speeds would mean heavier and larger equipment, but higher speeds may mean higher windage, bearings, and generator core losses. The shaft speed for the various gases and compressor exit pressures are shown in Figure 8. The turbine wheel diameter for various gases and operating pressures are shown in Figure 9. The compressor wheel diameters for various gases and operating pressures are shown in Figure 10. It is clear that Carbon Dioxide yields a higher shaft speed with similar turbine and compressor wheels sizes. With anticipated turbine and compressor efficiencies the same regardless of operating gas, then Carbon Dioxide would yield a much smaller alternator and therefore a much lower weight and volume TAC.

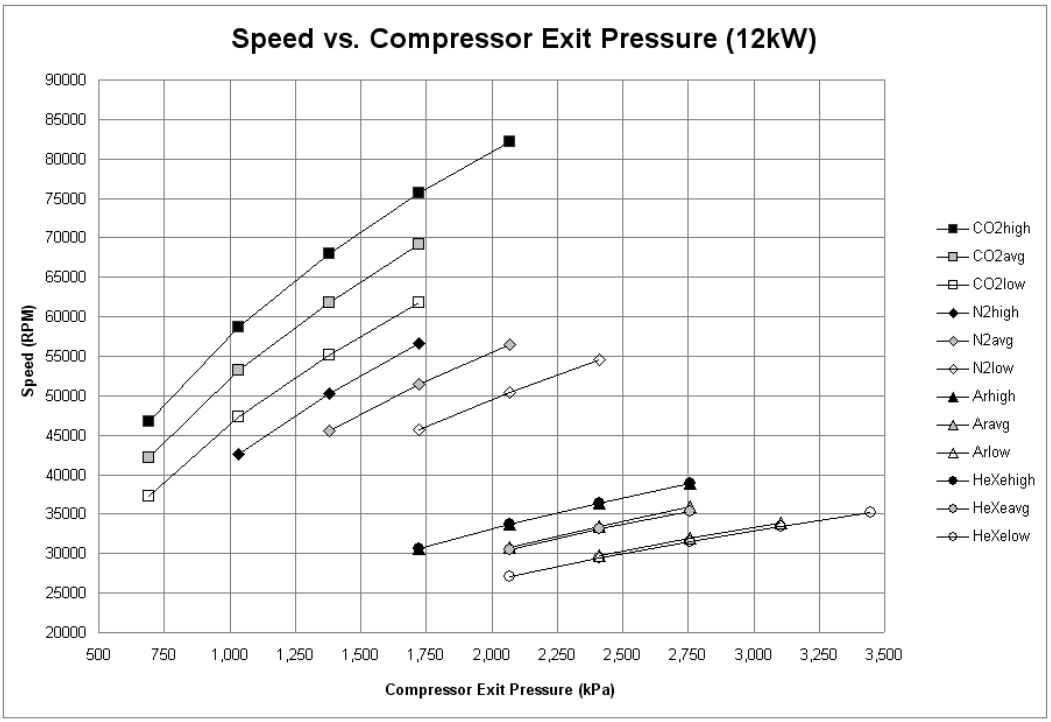

Figure 8: Optimum Shaft Speed versus Compressor Exit Pressure for Various Gases at low, average, and high temperature ratios.

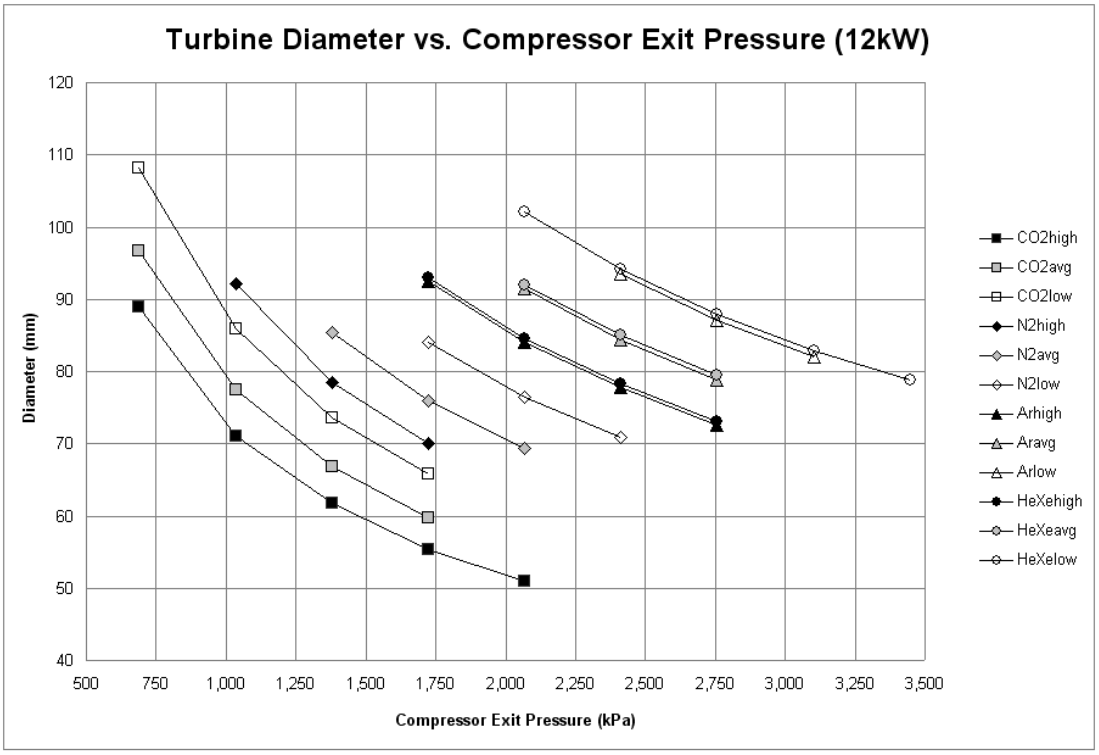

Figure 9: Turbine Wheel Diameter for various gases versus Compressor Exit Pressure for low, average, and high temperature ratios.

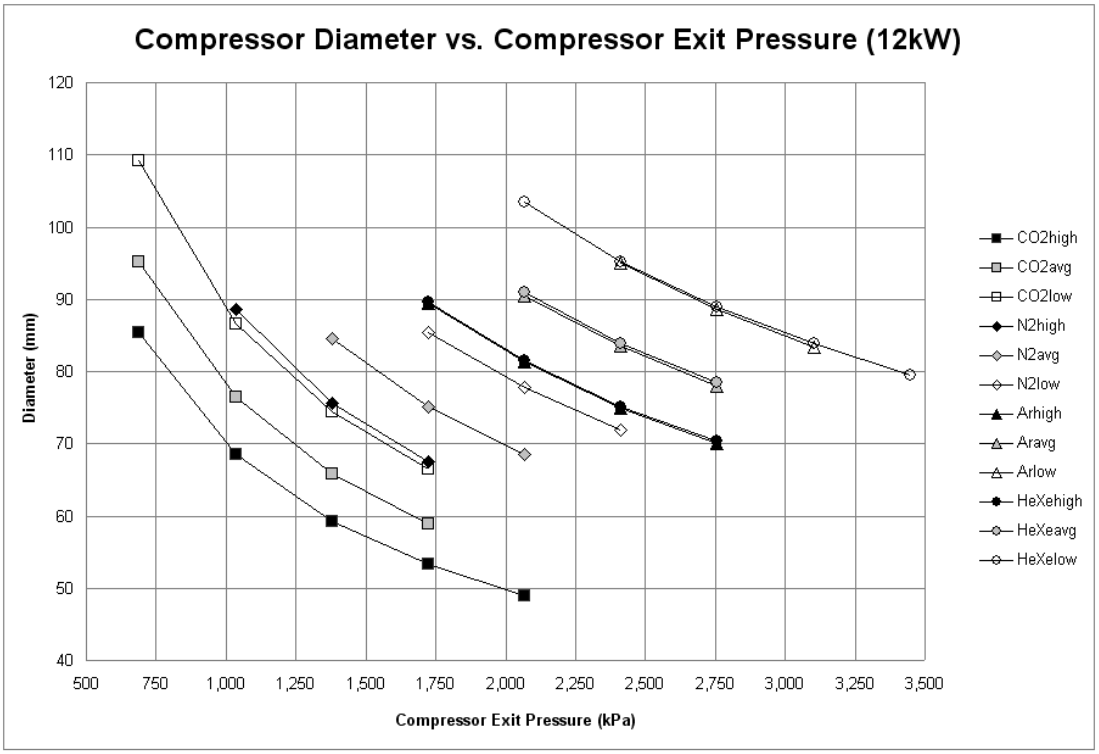

Figure 10: Compressor Wheel Diameter for various gases versus Compressor Exit Pressure for low, average, and high temperature ratios.

Additional analysis was performed for 6 kW, 12 kW, and 24 kW power converters. The Brayton cycle TAC has significant challenges to produce efficient power at lower power levels. This is primarily due to the small turbine and compressor wheel sizes and associated clearance losses. This lowers the overall efficiency for rotating machinery of this type. The anticipated cycle efficiencies with a larger 98% effective recuperator for various gases are seen in Figure 11.

The heat exchanger volume is also presented for the 6 kW, 12 kW, and 24 kW power levels for CO2, N2, Ar, and HeXe mixture, Figure 12. The heat exchanger sizes generally scale in a linear fashion with power level. Larger power levels could anticipate slightly lower weight per kW thermal transfer due to efficiency in pressure boundary construction.

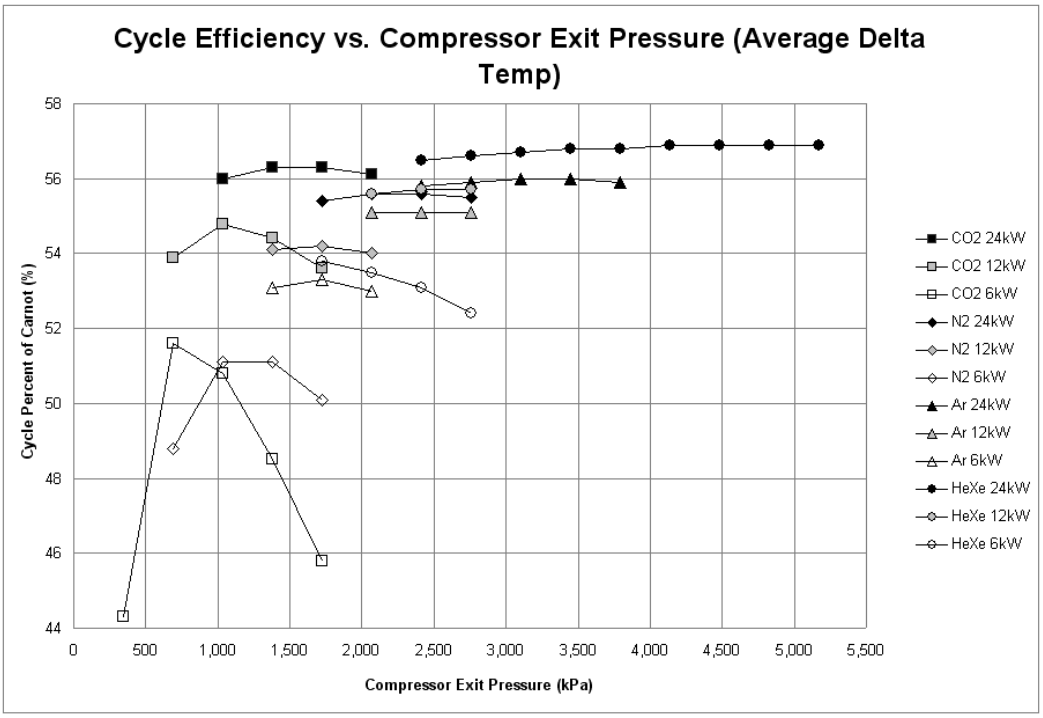

Figure 11: Cycle Efficiency vs. Compressor Exit Pressure for CO2, N2, Ar, and HeXe at 6 kW, 12 kW, and 24 kW.

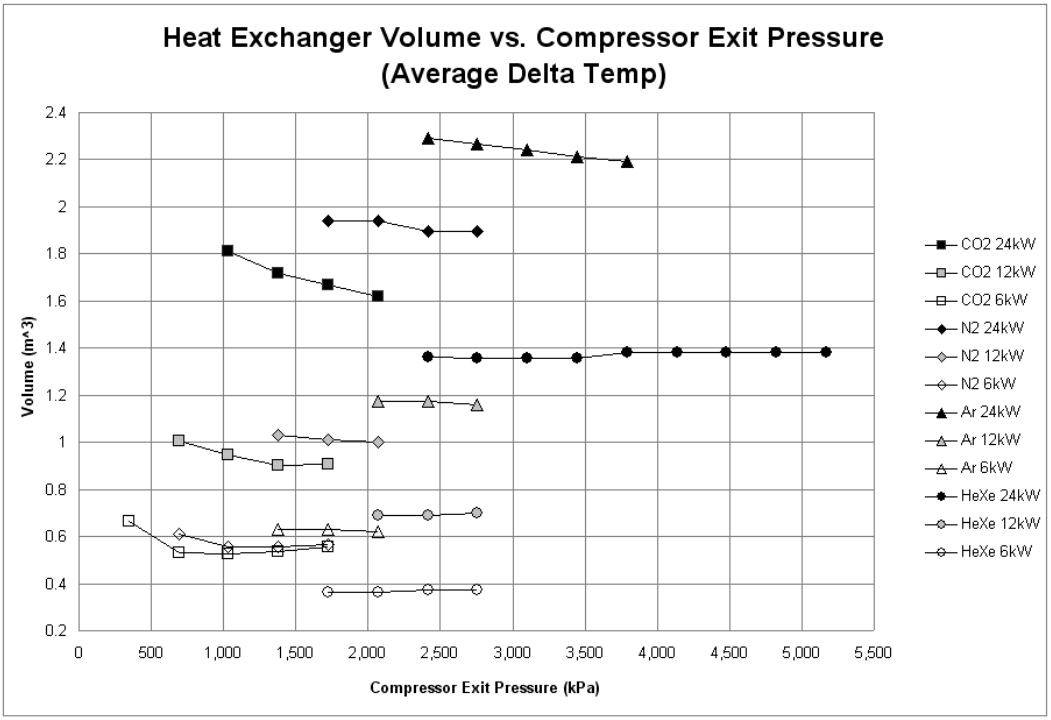

Figure 12: Heat Exchanger Volume vs. Compressor Exit Pressure for CO2, N2, Ar, and HeXe at 6 kW, 12 kW, and 24 kW.

Summary of Fluid Trade Study Information:

- Helium Xenon Mix
  - Best Efficiency
  - Lowest Heat Exchanger Volume
  - Low Weight
  - Most Expensive Fluid
- Argon
  - Comparable Efficiency to CO2
  - High Heat Exchanger Volume
  - High Weight
  - Reasonable Working Fluid Cost
- Carbon Dioxide
  - Good Efficiency
  - Moderate Heat Exchanger Volume
  - Low Weight (Lower Pressure and Smaller turbo-generator)
  - Least Expensive Fluid
  - Available on Mars at Low Pressure

The helium xenon system would provide the most efficient power conversion system, but on a kW/kg or kW/m^3 evaluation, it is not as clear for a 12 kWe power system. The TAC generator on HeXe would be approximately twice the size and roughly twice the weight primarily due to the lower shaft speed and larger alternator size. Secondarily the higher optimum operating pressure would lead to heavier pressure boundary containment. The prohibitive cost of the Xenon at approximately $1 US per gram (2008 price) does not fit the program goals as stated by NASA

The CO2 system is slightly heavier, but given the higher speed alternator, and relatively small heat exchanger sizes, it a good match for the program goals. It was selected primarily due to the advantageous cost of the working fluid

2.2 System Trade Study

The system trade study is used to identify the sensitivity of the various system components and parameters. The heat exchangers comprise the majority of the overall system volume and weight. The goal is to optimize the cycle efficiency relative to system specific weight and specific volume. Figure 13 identifies the influence of pressure ratio and heat exchanger volume on the overall cycle efficiency. It can be seen that a cycle efficiency reduction of 0.5-1% can reduce the heat exchanger size by 10-20% near the optimum point. This is an important consideration for a flight weight system. Figure 14 identifies the influence of recuperator effectiveness versus the overall cycle efficiency. Overlaid on this figure is the specific weight of the heat exchanger relative to recuperator effectiveness. An inflection point is obvious for the considered power levels of 6 kW, 12 kW, and 24 kW. For the 12 kW system, the inflection point is between 88-90% effectiveness. Larger recuperator effectiveness values can easily increase the heat exchanger weights by 50%.

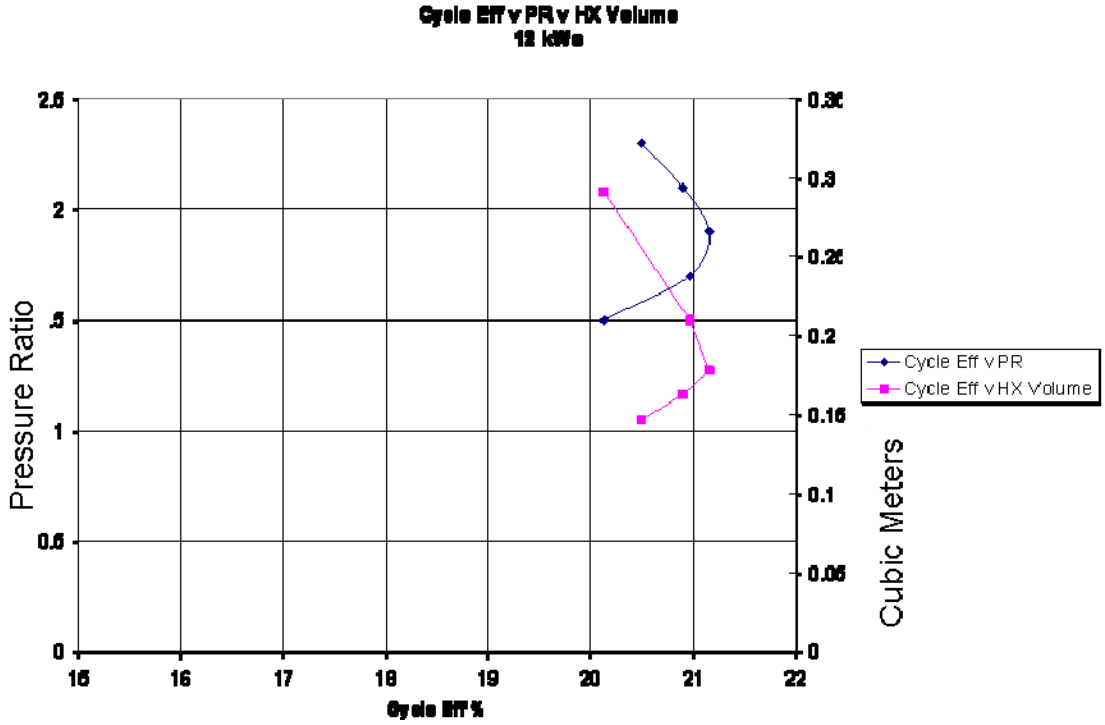

Figure 13: Cycle Efficiency vs. Pressure ratio and Heat Exchanger Volume

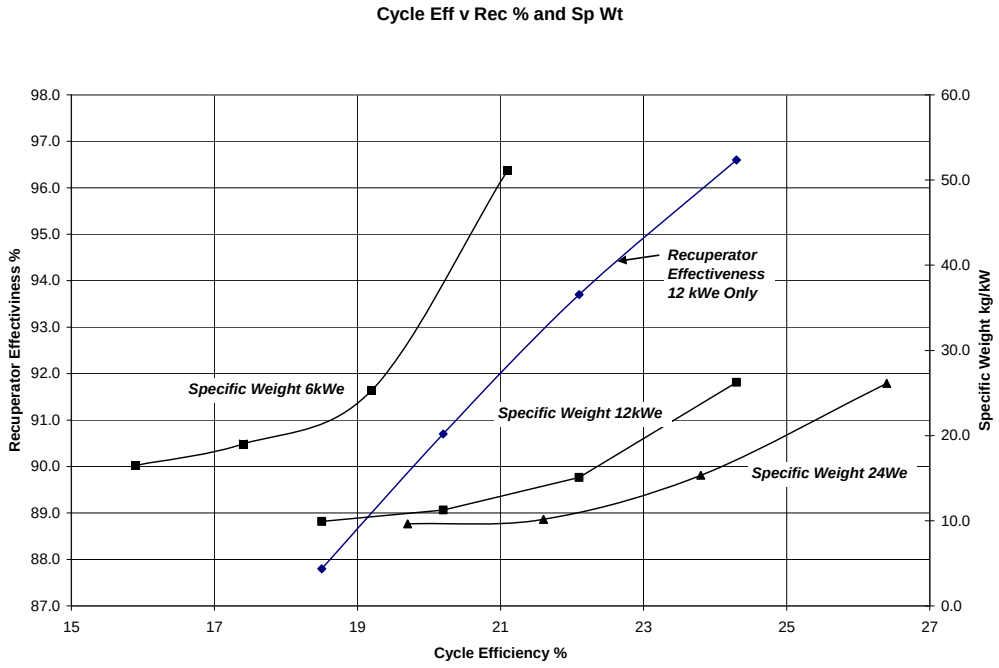

Figure 14: Cycle Efficiency vs. Recuperator Effectiveness and Specific Weight for 6 kW, 12 kW, and 24 kW Converters

Another sizing consideration is relative to the NaK to CO2 heat exchanger. NaK flow rate was not initially provided in the specification and was varied from 1.5 to 3.5 kg/s for the analysis to evaluate sensitivity. It is important to keep the CO2 temperature as close to the NaK temperature as possible without increasing the heat exchanger volume to an unacceptably large size. Figure 15 shows the effect of NaK Flow on cycle efficiency and NaK heater volume with a 5 deg K approach temperature.

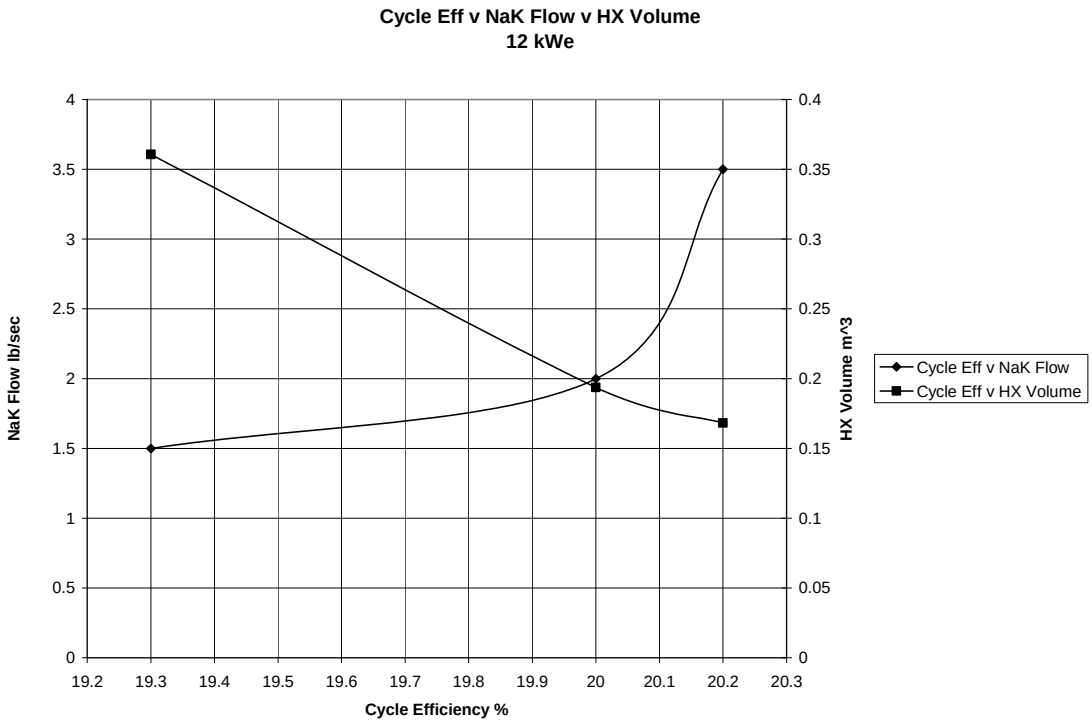

Figure 15: Cycle Efficiency vs. NaK Flow Rate and Heat Exchanger Volume

The system trade study identifies the important parameters regarding the effect of heat exchanger sizes and flow rates on cycle efficiency. At this point heat exchanger vendors were contacted regarding refining the designs relative to performance and fabrication.

3. Heat Exchanger Design

3.1 Recuperator Design

The recuperator is used to preheat the compressor exit gas prior to entering the NaK to gas heater. It utilizes the residual heat from the turbine exit gas. Niagara Thermal Products was contacted regarding the refinement of the recuperator design and ultimately provide a manufacturing quotation regarding this heat exchanger. The initial task was to confirm the Barber-Nichols recuperator design relative to performance, size, weight, and pressure drop estimates. Niagara Thermal Products identified several fin types that were tooled and available for use with this heat exchanger. The fin types offer different pressure drop and effectiveness options that are presented in Figure 16 and Figure 17.

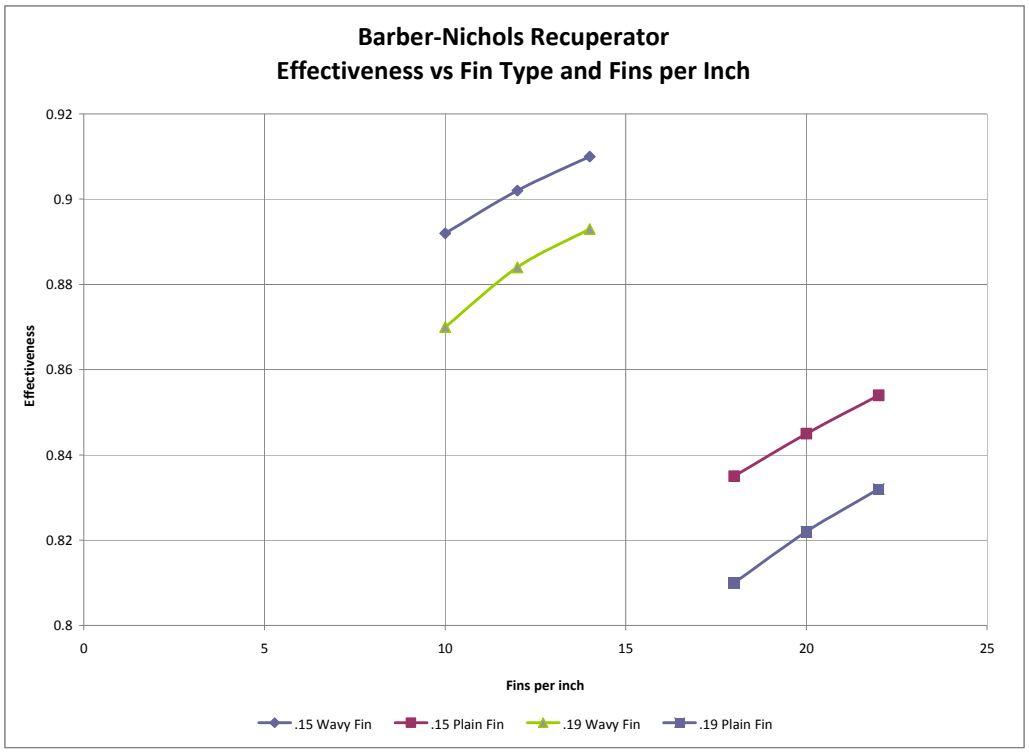

Figure 16: Fin Type/Pitch versus Recuperator Effectiveness

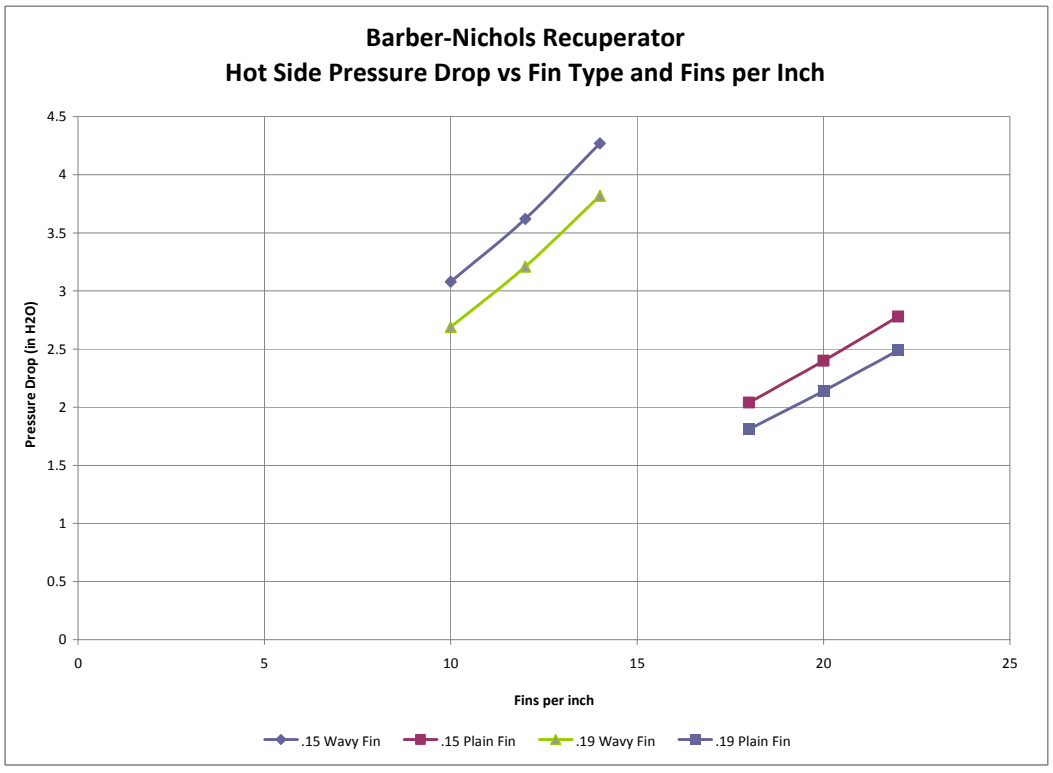

Figure 17: Fin Type/Pitch versus Pressure Drop

An effectiveness of 89-90% is required for high cycle efficiency so the choice is between the .19 wavy fin and the .15 plain fin. The .19 wavy fin was chosen based on lower pressure drop.

After fin selection, the recuperator design was finalized and the performance chart was constructed as seen in Figure 18.

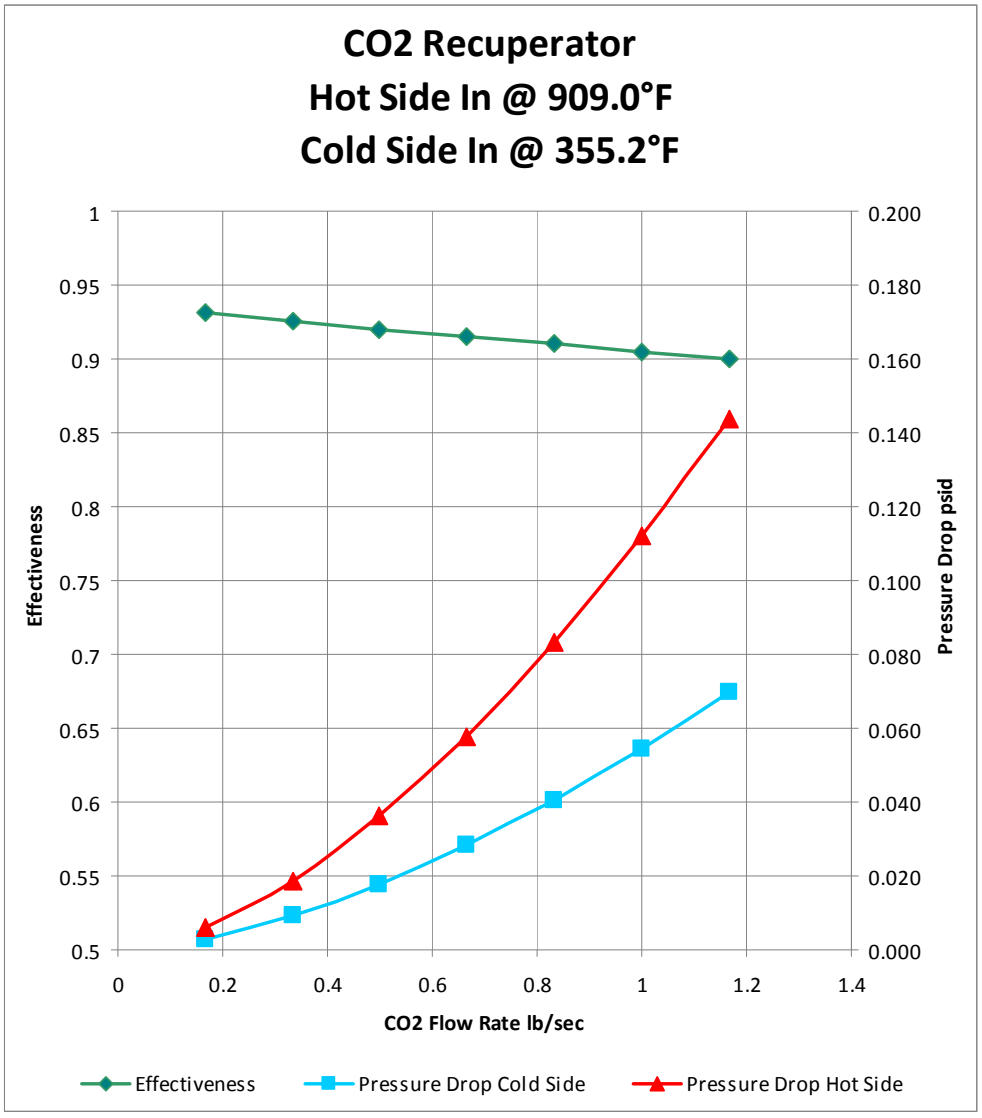

Figure 18: Recuperator Performance

The recuperator is a brazed construction with welded tank heads and manifolds. A preliminary design was provided by the manufacturer that indicated the approximate size and weight of the heat exchanger. Since the raised face flanges are not necessary in the final design, they were eliminated and the tank heads were modified to lower the estimated weight. The overall recuperator size is shown in Figure 19.

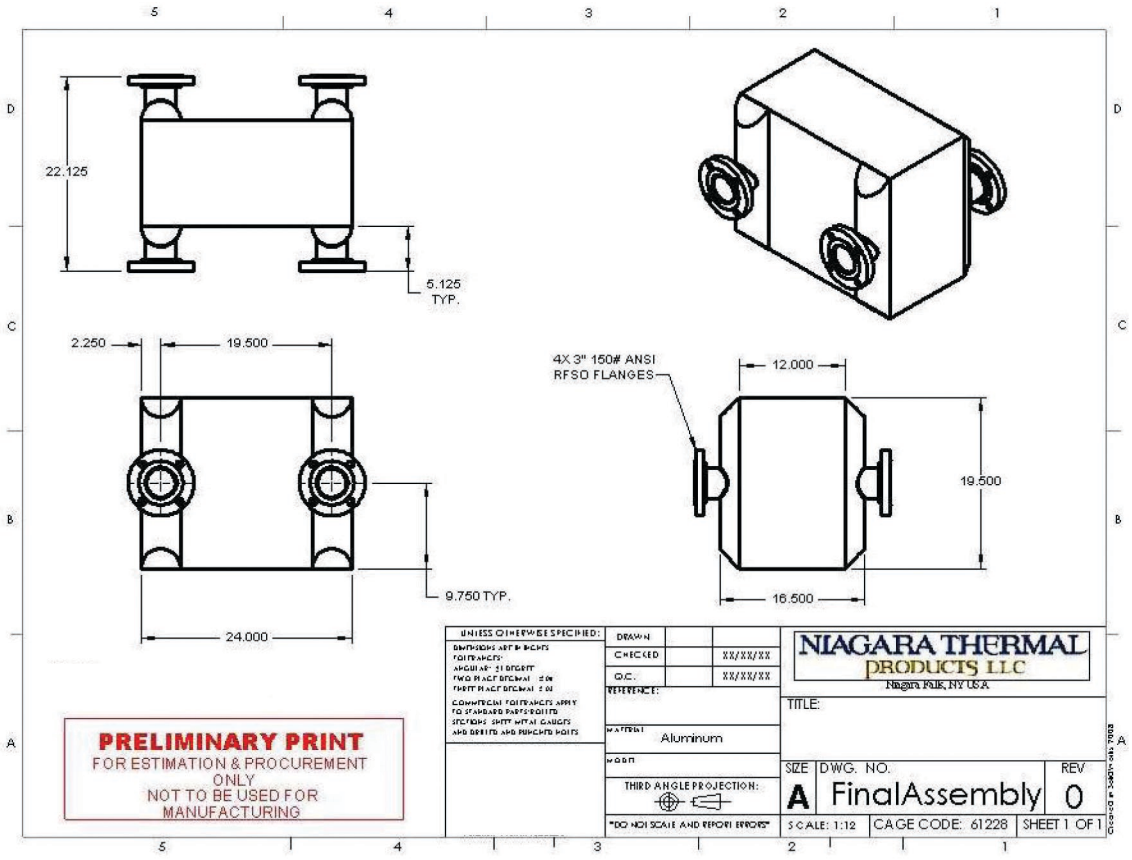

Figure 19: Overall Recuperator Size

3.2 Water/Gas Plate Fin Cooler

Niagara Thermal Products generated a compact water-to-CO2 gas cooler design. The heat exchanger is a plate/fin type much like the recuperator. The construction material is 316L stainless steel with AMS 4777 braze filler. The overall design is shown as given by the supplier in Figure 20. The ASME flanges will not be used and the weight is subtracted for those to come to a lower weight estimate. The supplier data sheet is shown in Figure 21 and the off design performance is shown in Figure 22.

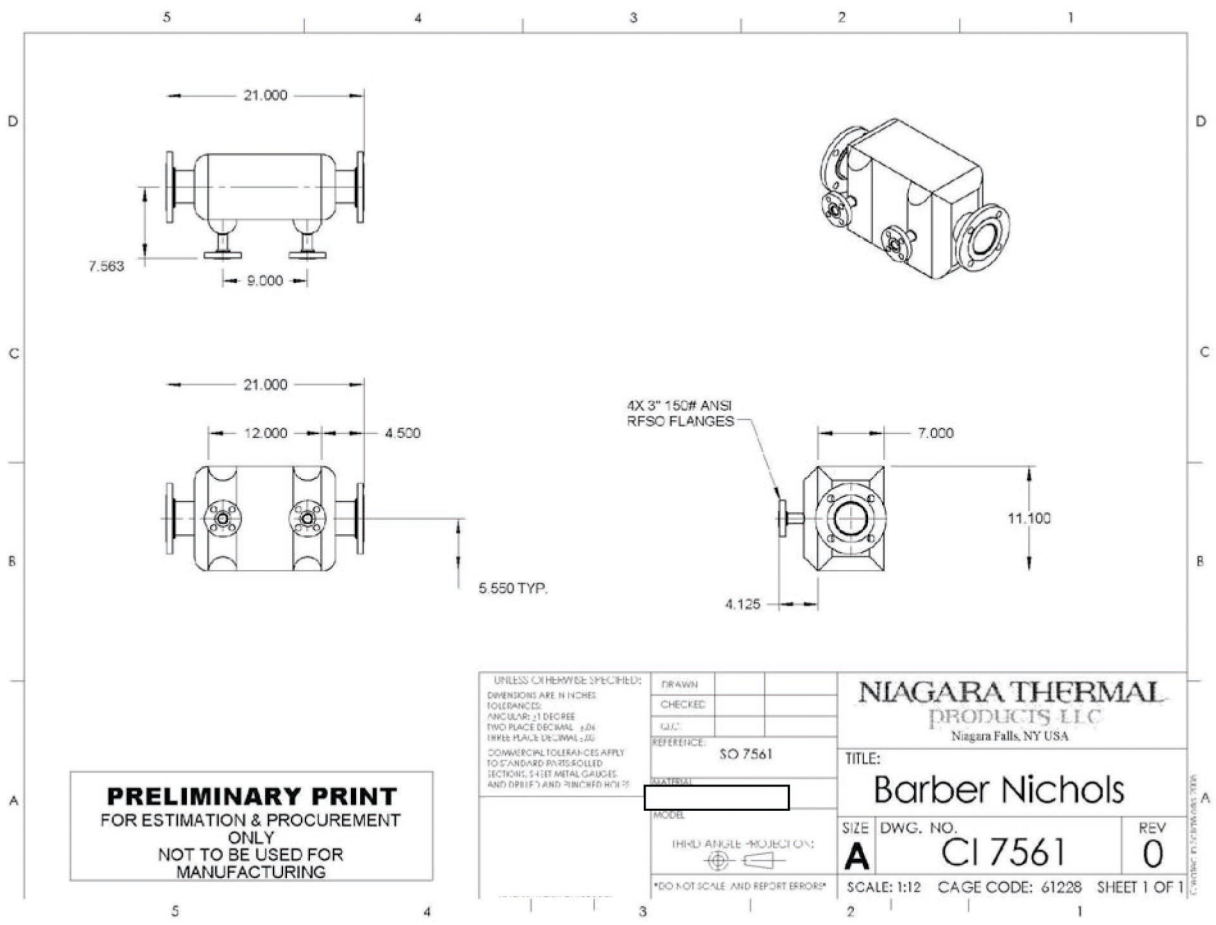

Figure 20: Water to CO2 Gas Cooler Dimensional Data

NIAGARA THERMAL PRODUCTS LLC	Inquiry: 28112
	Rev: 0
Heat Exchanger Data Sheet	Date: 11/18/08

Customer: Barber-Nichols

Customer P/N:

Description: CO2 / Water Cooler

Application:

Design File: 28112C30 Prepared by: Doug Turner

Function & Design:

The heat exchanger is designed to cool 1.1 lb/sec of CO2 Vapor at 415 ^{o}F using .825 lb/sec Water at 215.33 ^{o}F.

Construction:

Core:	316L Core Vacuum Brazed with AMS 4777 braze
Tanks	316L Fabricated and welded with ER 308L filler

Dimensions:

Core (W x H x D):	12.0" Wide x 11.1" High x 7.0" Deep (see sketch page 4)
Cold Side Fin:	.240" Louver Fin- 13 fpi
Hot Side Fin:	.060" Lance and Offset Fin- 20 fpi
Estimated Weight:	76 lbs(including tanks)

Testing:

	Cold Side	Hot Side
Leak Test Pressure:	100 psig	50 psig
Proof Test Pressure:	150 psig	75 psig

Maximum Leak Rate Allowed : 10^{-3} sccs helium

Figure 21: Water to CO2 Gas Cooler Data Sheet

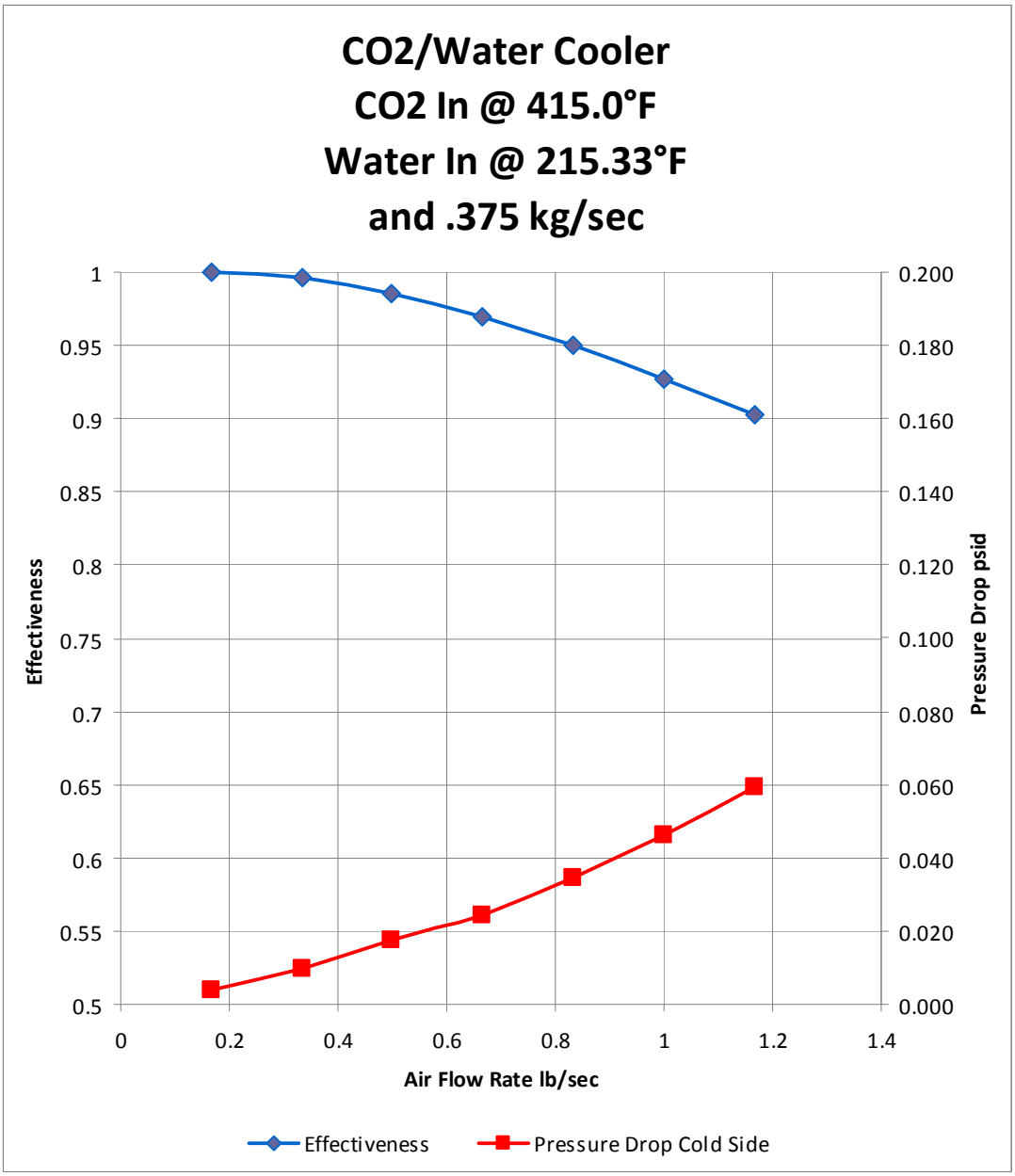

Figure 22: Water to CO2 Gas Cooler Performance Data

3.3 NaK Heater Design

3.3.1 Shell and Tube NaK Heater Design

The NaK heater operates at a temperature range of 825 K to 875 K. The flow rate was set at 1.75 kg/sec of NaK 78. Holtec International was selected to design the shell and tube heat exchanger. It was decided that a vendor with molten salt, and preferably NaK experience, be utilized. This limited the number of vendors that were available to consult on this heat exchanger. Holtec International was deemed the most capable supplier and

capable of only shell/tube type designs. Several iterations were done to trade pressure drop and heat exchanger size. The final shell/tube design sheet is shown in Figure 23.

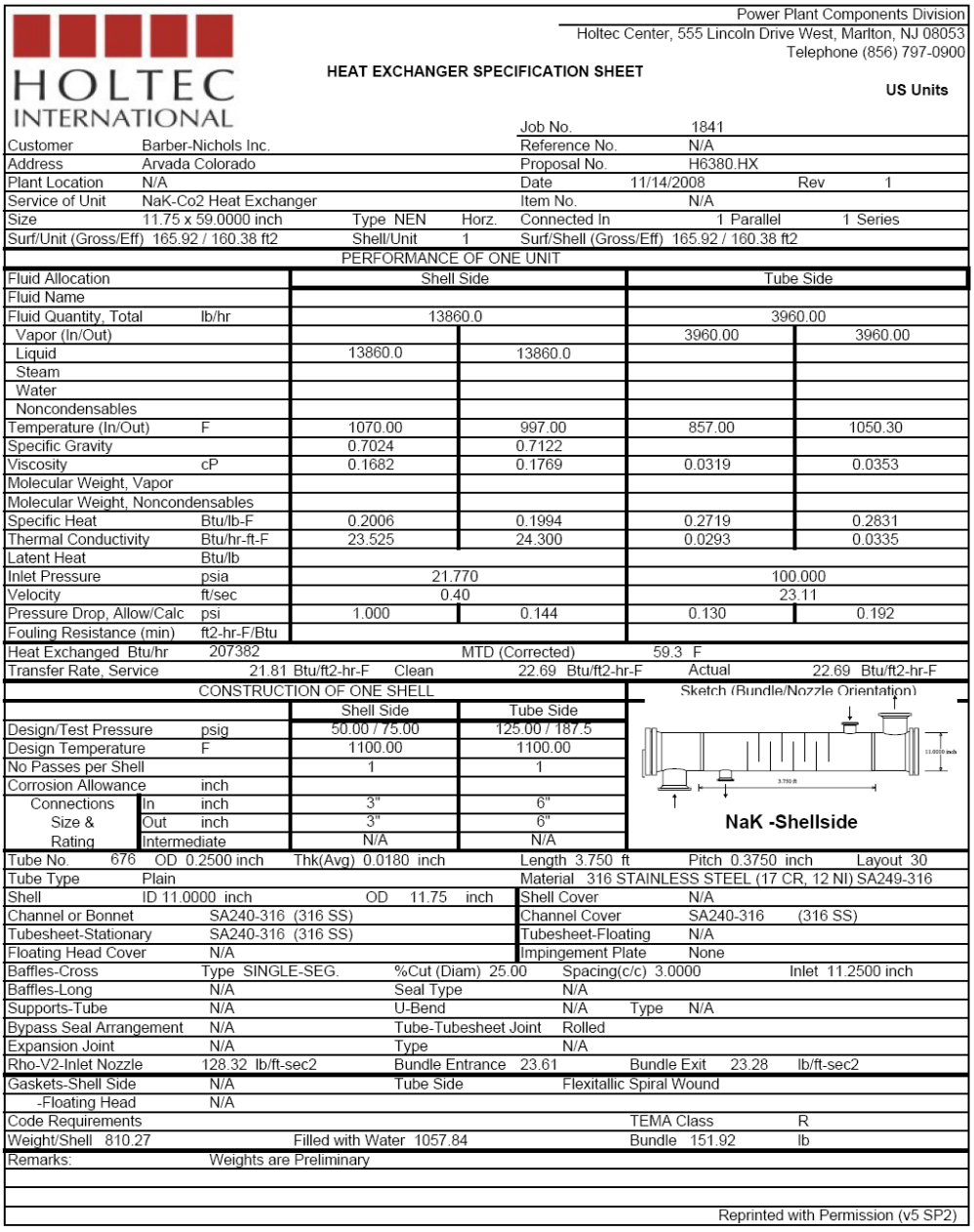

HOLTEC INTERNATIONAL

Power Plant Components Division
Holtec Center, 555 Lincoln Drive West, Marlton, NJ 08053
Telephone (856) 797-0900

HEAT EXCHANGER SPECIFICATION SHEET

US Units

Customer	Barber-Nichols Inc.			Job No.	1841		
Address	Arvada Colorado			Reference No.	N/A		
Plant Location	N/A			Proposal No.	H6380.HX		
Service of Unit	NaK-Co2 Heat Exchanger			Date	11/14/2008	Rev	1
Size	11.75 x 59.0000 inch	Type NEN	Horz.	Item No.	N/A		
Surf/Unit (Gross/Eff)	165.92 / 160.38 ft2	Shell/Unit	1	Connected In	1 Parallel	1 Series	
				Surf/Shell (Gross/Eff)	165.92 / 160.38 ft2		

PERFORMANCE OF ONE UNIT

Fluid Allocation		Shell Side		Tube Side	
Fluid Name					
Fluid Quantity, Total	lb/hr	13860.0		3960.00	
Vapor (In/Out)				3960.00	3960.00
Liquid		13860.0	13860.0		
Steam					
Water					
Noncondensables					
Temperature (In/Out)	F	1070.00	997.00	857.00	1050.30
Specific Gravity		0.7024	0.7122		
Viscosity	cP	0.1682	0.1769	0.0319	0.0353
Molecular Weight, Vapor					
Molecular Weight, Noncondensables					
Specific Heat	Btu/lb-F	0.2006	0.1994	0.2719	0.2831
Thermal Conductivity	Btu/hr-ft-F	23.525	24.300	0.0293	0.0335
Latent Heat	Btu/lb				
Inlet Pressure	psia	21.770		100.000	
Velocity	ft/sec	0.40		23.11	
Pressure Drop, Allow/Calc	psi	1.000	0.144	0.130	0.192
Fouling Resistance (min)	ft2-hr-F/Btu				

Heat Exchanged Btu/hr	207382	MTD (Corrected)	59.3 F	
Transfer Rate, Service	21.81 Btu/ft2-hr-F	Clean	22.69 Btu/ft2-hr-F	Actual 22.69 Btu/ft2-hr-F

CONSTRUCTION OF ONE SHELL

			Shell Side	Tube Side
Design/Test Pressure		psig	50.00 / 75.00	125.00 / 187.5
Design Temperature		F	1100.00	1100.00
No Passes per Shell			1	1
Corrosion Allowance		inch		
Connections Size & Rating	In	inch	3"	6"
	Out	inch	3"	6"
	Intermediate		N/A	N/A

Sketch (Bundle/Nozzle Orientation)

NaK -Shellside

Tube No. 676	OD 0.2500 inch	Thk(Avg) 0.0180 inch		Length 3.750 ft	Pitch 0.3750 inch	Layout 30
Tube Type	Plain			Material 316 STAINLESS STEEL (17 CR, 12 NI) SA249-316		
Shell	ID 11.0000 inch	OD 11.75 inch		Shell Cover	N/A	
Channel or Bonnet	SA240-316 (316 SS)			Channel Cover	SA240-316 (316 SS)	
Tubesheet-Stationary	SA240-316 (316 SS)			Tubesheet-Floating	N/A	
Floating Head Cover	N/A			Impingement Plate	None	
Baffles-Cross	Type SINGLE-SEG.	%Cut (Diam) 25.00		Spacing(c/c) 3.0000		Inlet 11.2500 inch
Baffles-Long	N/A	Seal Type		N/A		
Supports-Tube	N/A	U-Bend		N/A	Type N/A	
Bypass Seal Arrangement	N/A	Tube-Tubesheet Joint		Rolled		
Expansion Joint	N/A	Type		N/A		
Rho-V2-Inlet Nozzle	128.32 lb/ft-sec2	Bundle Entrance 23.61		Bundle Exit 23.28		lb/ft-sec2
Gaskets-Shell Side	N/A	Tube Side		Flexitallic Spiral Wound		
-Floating Head	N/A					
Code Requirements				TEMA Class	R	
Weight/Shell 810.27		Filled with Water 1057.84		Bundle 151.92	lb	
Remarks:	Weights are Preliminary					

Reprinted with Permission (v5 SP2)

Figure 23: Heat Exchanger Specification Sheet for NaK to CO2 Gas

The primary material of construction is 316 stainless steel. It contains the NaK on the shell side and the CO2 on the tube side. The heat exchanger is approximately 0.3 m diameter x 1.2 m long. The tube bundle contains 676 x 6mm tubes with a wall thickness 0.45mm.

This heat exchanger was deemed to be too heavy and not flight worthy. A search of an alternative vendor for a plate fin heat exchanger with NaK experience was not successful.

Niagara Thermal Products was capable of providing the heat exchanger, but had no experience in handling NaK.

3.3.2 Plate/Fin NaK Heater

Researching literature provided a basis for past molten salt heat exchanger designs for space applications. A previous NASA program for the SNAP reactor (1970's vintage) provided valuable information regarding proposed heat exchanger design types and material compatibility. A liquid metal design manual, "SNAP Technology Handbook", G.F. Burdi, NAA-SR-86 17, VOLUME I, REACTOR TECHNOLOGY, SNAP REACTORS, SNAP PROGRAM, TID-4500 (29th Ed.) M-3679 (34th Ed.) was utilized to provide material data and ultimately to design a plate fin heat exchanger that is much lighter weight than the shell/tube design.

Essentially, the thermal transfer of the NaK heater and the gas cooler are approximately equal. With the gas cooler design was used as a basis for scaling the NaK heater with a slight change in the braze material from AMS 4777 to AMS 4778 to remove the iron in the braze filler. All other parameters for pressure drop, thermal transfer showed this heat exchanger exceeded the specifications for the NaK heater. This drops the weight of the heat exchanger to below 30 kg and reduces the size to approximately 0.3m x 0.2m x 0.3m.

4. Cycle and Performance Analysis

After sizing the heat exchangers, an estimate of turbine and compressor performance can be made from a thermodynamic cycle simulation of the complete converter. Typically the cycle design will change slightly once the turbine and compressor performance is estimated. This design cycle also must include turbine and compressor stress estimates. This design cycle utilizes many areas of expertise from aerodynamics to stress to thermodynamics. Once the turbine and compressor designs are finalized, off performance maps are generated and implemented into the cycle design. The cycle design spreadsheet can then be used to estimate the performance for on and off design conditions.

The cycle spreadsheet calculates all state point data and displays losses and efficiencies for major components. The spreadsheet also calculates cycle efficiency as well as system efficiency. Cycle efficiency is defined as operating gas side efficiency. System efficiency includes the NaK and water side energy. The efficiency relative to Carnot is also provided.

4.1 Nominal Temperature Difference

The nominal temperature difference is specified at 850 K NaK inlet temperature to the heat exchanger at a 1.75 kg/sec flow rate (Figure 24). The water temperature for the nominal case is 375 K with a .8 lb/sec flow rate. The heat exchangers are designed for the nominal condition as is the turbomachinery. The spreadsheet is linked to both the heat exchanger and turbomachinery dynamically. This allows off design calculations to be performed in a relatively quick manner. It also balances the mass and pressure against

the turbine, compressor, and system design volumes to simulate actual steady state running conditions.

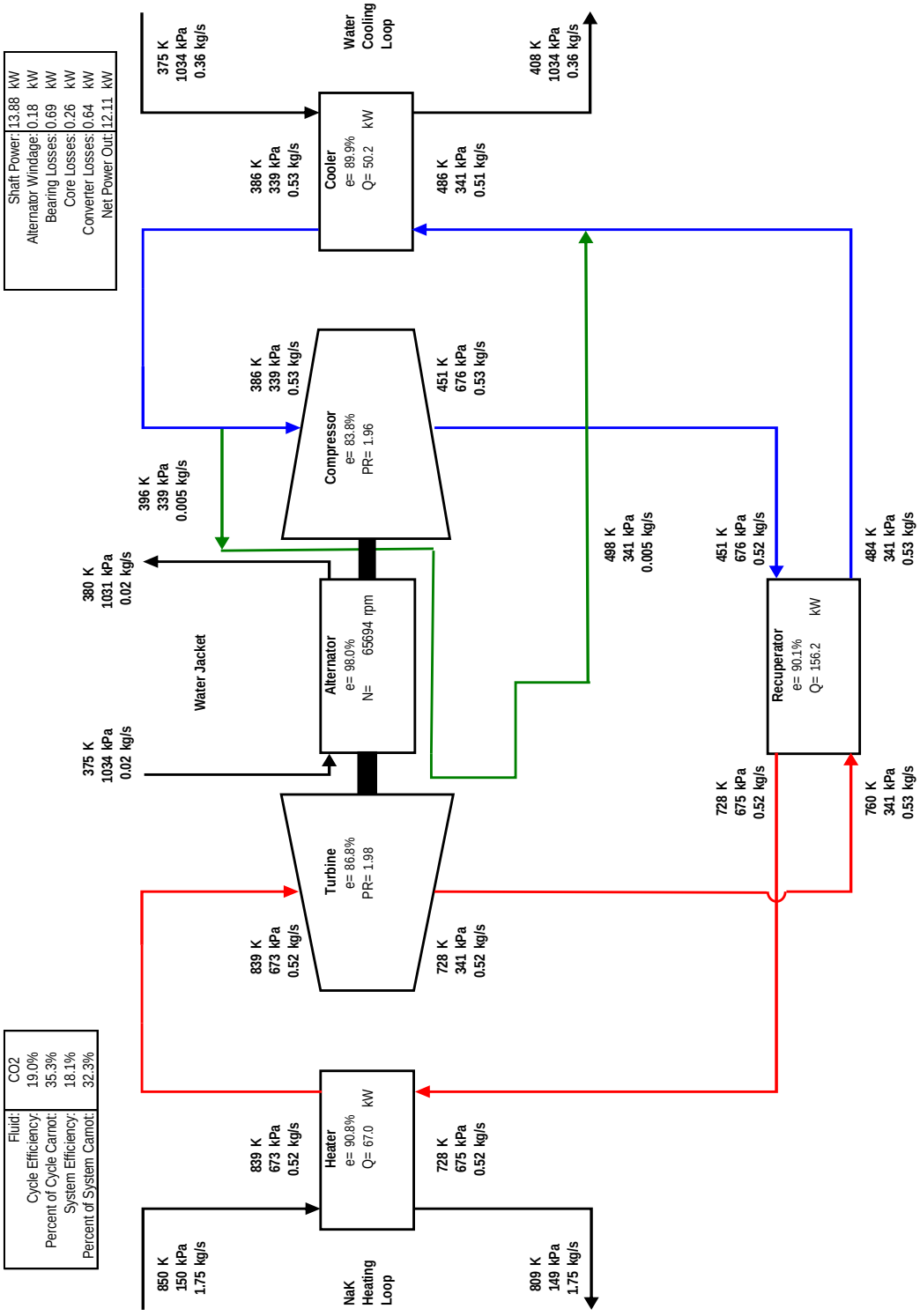

Figure 24: Thermodynamic Cycle State Points for Nominal Design Condition

The nominal condition operation results in a predicted system efficiency of 18.1%, with a cycle efficiency of 19.0%.

4.2 High Temperature Difference

The high temperature difference is specified at 875 K NaK inlet temperature to the heat exchanger at a 1.75 kg/sec flow rate. The water temperature for the nominal case is 325 K with a .375 kg/sec flow rate. The heat exchangers are designed for the nominal condition, as is the TAC, however the goal is to predict the performance of the power conversion system with the excess available heat. Again, the spreadsheet method is utilized so that the TAC and heat exchanger off-design characteristics can be met as a system with the proper heat and mass balance. Figure 25 shows the state points of the high temperature difference analysis.

The high temperature difference analysis results in a maximum power of 16.24 kWe from the power converter. The system efficiency is calculated at 21.4% and a cycle efficiency of 22.5%.

4.3 Low Temperature Difference

The low temperature difference is specified at 825 K NaK inlet temperature to the heat exchanger at a 1.75 kg/sec flow rate. The water temperature for the nominal case is 375 K with a .375 kg/sec flow rate. The heat exchangers are designed for the nominal condition, as is the TAC, however the goal is to predict the performance of the power conversion system with the minimum available heat. Again, the spreadsheet method is utilized so that the TAC and heat exchanger off-design characteristics can be met as a system with the proper heat and mass balance. Figure 26 shows the state points of the low temperature difference analysis.

The high temperature difference analysis results in a maximum power of 9.55 kWe from the power converter. The system efficiency is calculated at 16% and a cycle efficiency of 16.8%.

4.4 Off-Design Performance

The spreadsheet can also predict performance over a range of speeds. This analysis is useful to predict the initial charge pressure for the system and also the startup characteristics. The analysis also predicts the power produced as a function of TAC shaft speed. This allows the operator to select a speed and heat amount for operating off-design. The other control strategy is to operate the TAC at maximum speed and raise and lower the heat amount to effect part-load operation.

The maximum power produces versus shaft speed is presented in Figure 27. The analysis is done for the low, medium, and high temperature ratios. The startup power and pressure conditions are presented in Figure 28.

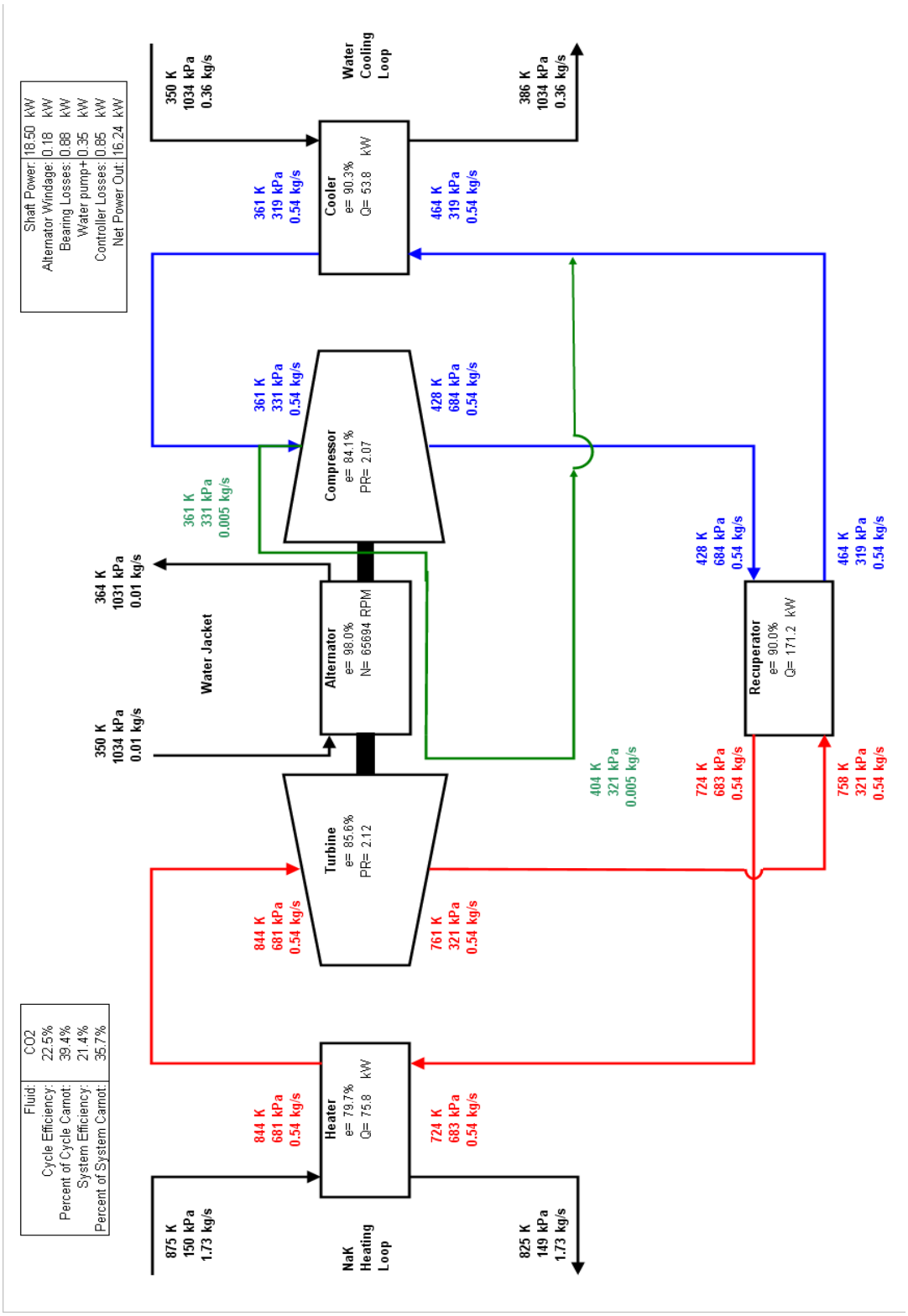

Figure 25: High Temperature Difference Performance Analysis

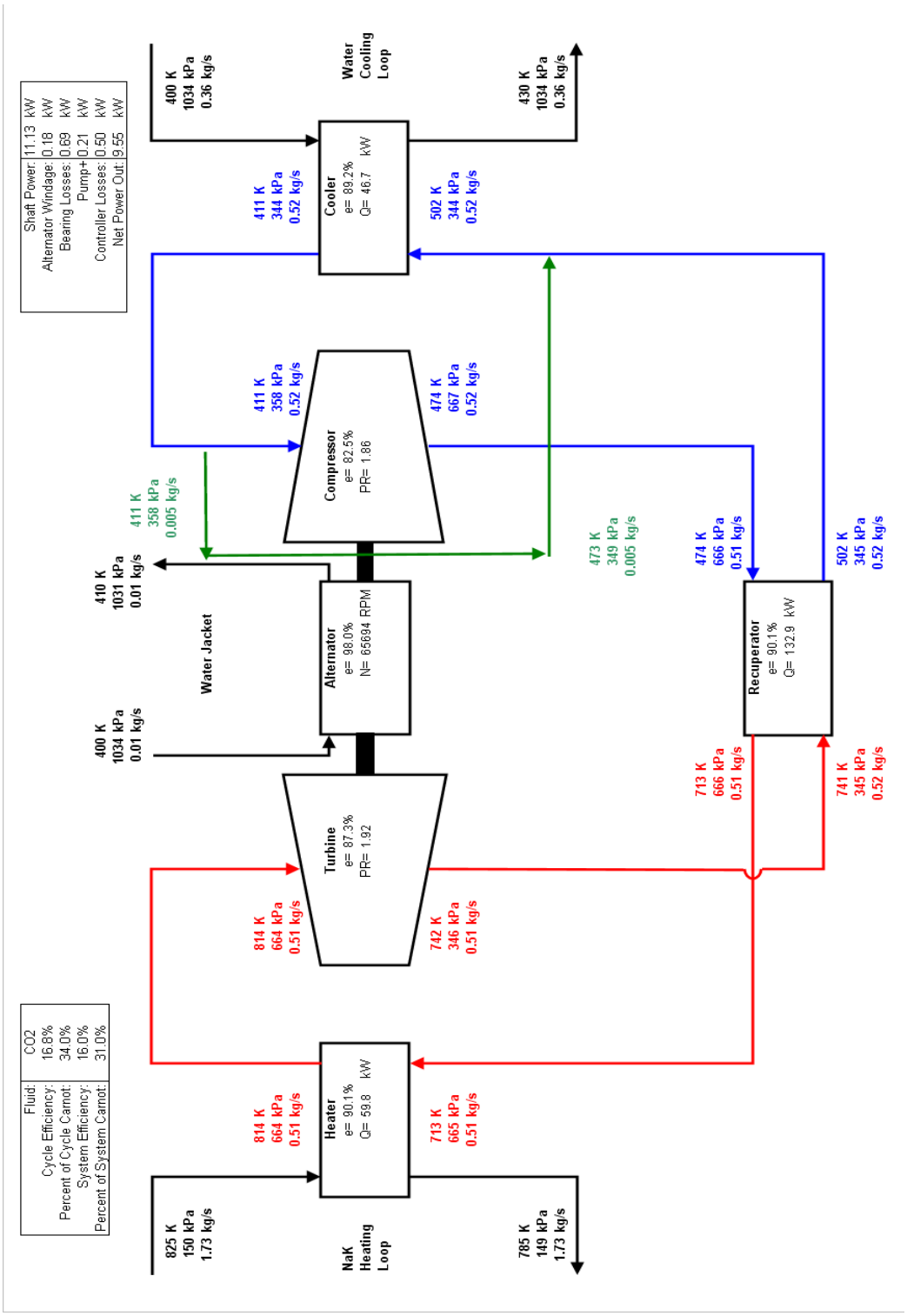

Figure 26: Low Temperature Difference Converter Performance

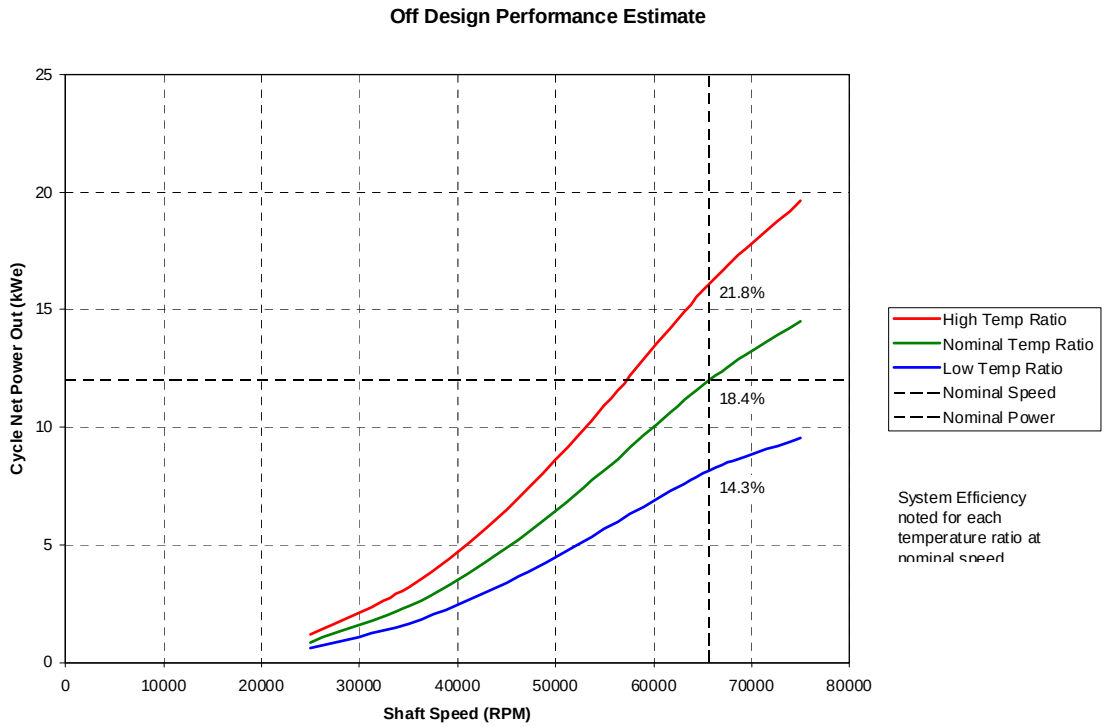

Figure 27: Cycle Power Output versus Shaft Speed for Specified Temperature Differences

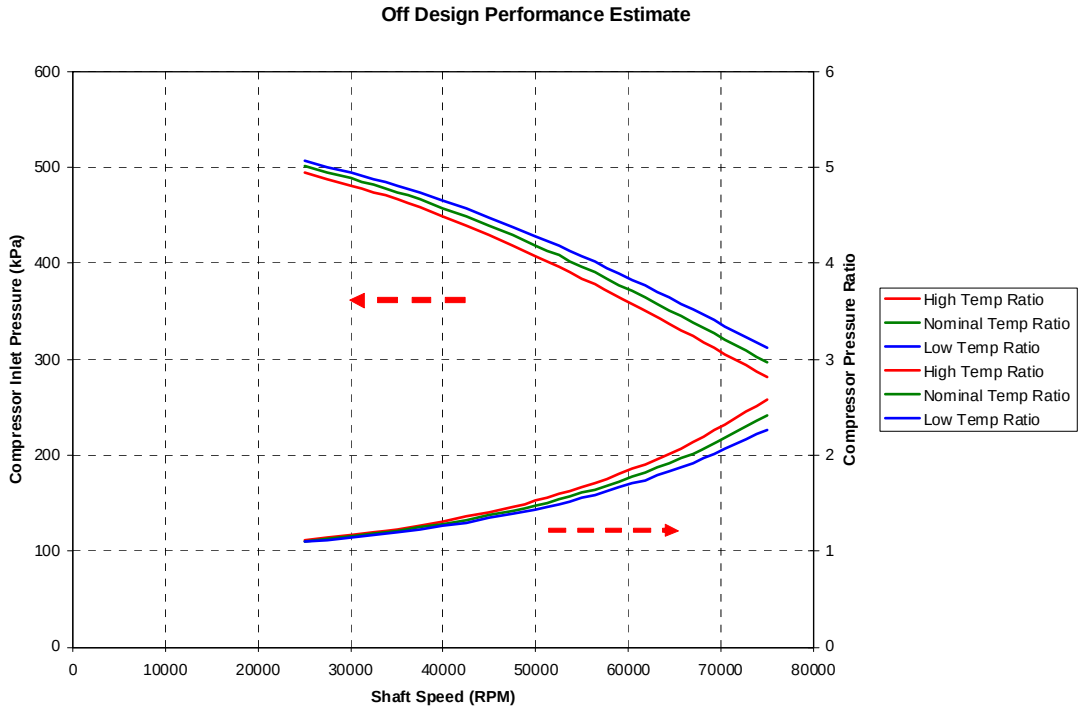

Figure 28: Off Design Performance Pressures versus Shaft Speed

5. Compressor Design

A centrifugal compressor is selected for high efficiency and a compact design. The centrifugal compressor operates as a single stage with a set of diffuser vanes to maximize pressure recovery and efficiency. The final design is shown in Table 1. A compressor intake side view with the shroud removed is shown in Figure 29.

Parameter	Design Value
Vaned-Island Diffuser [# vanes]	22
Impeller w/ Splitter Blades	7+7
Diameter Impeller-Exit mm	84. 78
Diameter-eye mm	37.11
Diameter-hub mm	9.75
Impeller Exit Blade Height mm	4
Exit Blade Angle [deg-from tang]	45
Impeller Clearance mm	.203

Table 1: Compressor Design Table

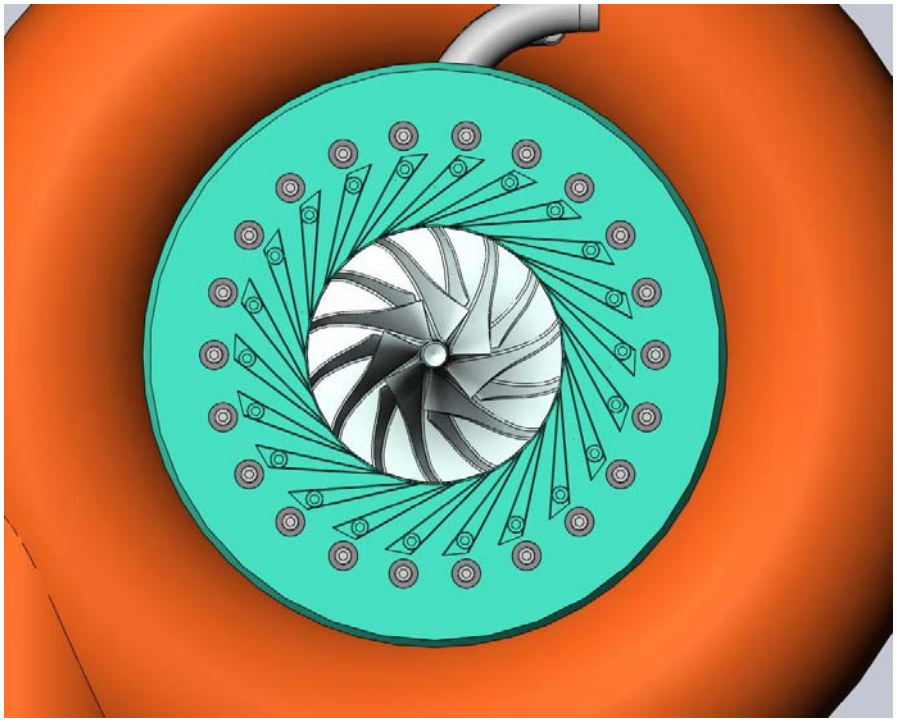

Figure 29: Front View Compressor and Vane Island Diffuser

The compressor was optimized for maximum efficiency by reducing operating clearances and specifying a high degree of surface finish on the compressor wheel and flow passages. The compressor wheel is manufactured from Inconel 718, enabling thin blade sections for increased performance.

A performance map of the compressor with thrust calculations is combined in Figure 30.

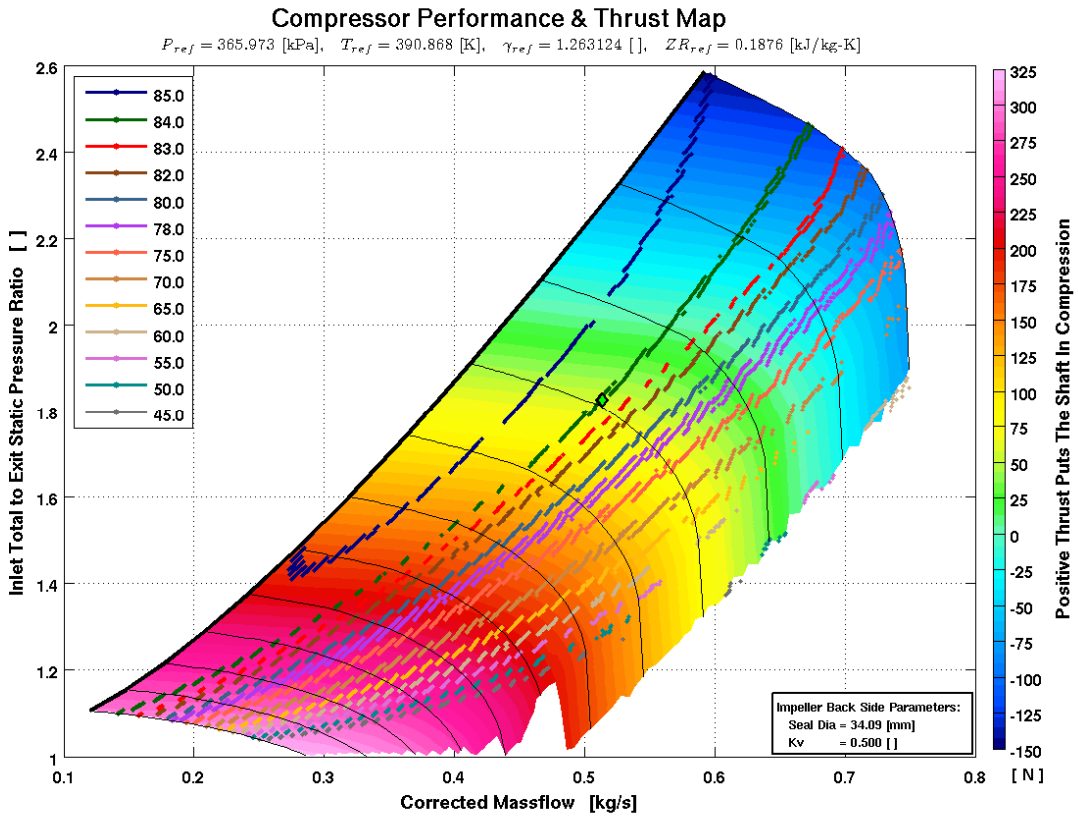

Figure 30: Compressor Performance Map with Thrust Calculations

The compressor wheel structural analysis is shown in Figure 31. The maximum blades are designed so that centrifugal effects do not produce blade bending. The aerodynamic loading is included, but is a very small value. The compressor wheel is manufactured of Inconel 718 with a yield strength of 986 MPa. The stress analysis is performed at an over speed of approximately 10%. This results in a large safety margin with a calculated burst speed of 150,000 rpm, over 2X operating speed.

Figure 32 is the blade interference Campbell diagram for the compressor wheel. The diagram shows all them modes generated by FEA analysis. Without presenting all the details, the wheel has not modes generated by the 1X, 2X, 3X, and 4X vibration signatures. The nozzle and blade passing frequency is quite high and no blade pass excitable modes are shown at operating speed. For this reason it is recommended to operate part load performance at a constant speed and not vary the speed. This will prevent wheel vibrations occurring at off-design speeds. The specification states a constant generator output voltage of 400 VAC and therefore the speed will need to be fixed.

Rotating - Compressor Wheel Structural Analysis

- Inconel 718 at 449.8 K
  - Ultimate Strength = 1179 MPa
  - Yield Strength = 986 MPa
- 10 % overspeed: 72,000 RPM
- Max Net Section Stress = 276 MPa
  - Ultimate SF = 4.30
  - Yield SF = 3.58
- Max Local Stress = 358 MPa
  - Ultimate SF = 3.29
  - Yield SF = 2.75
- Burst Speed = 150,000 rpm
  - Average tangential stress = 207 MPa

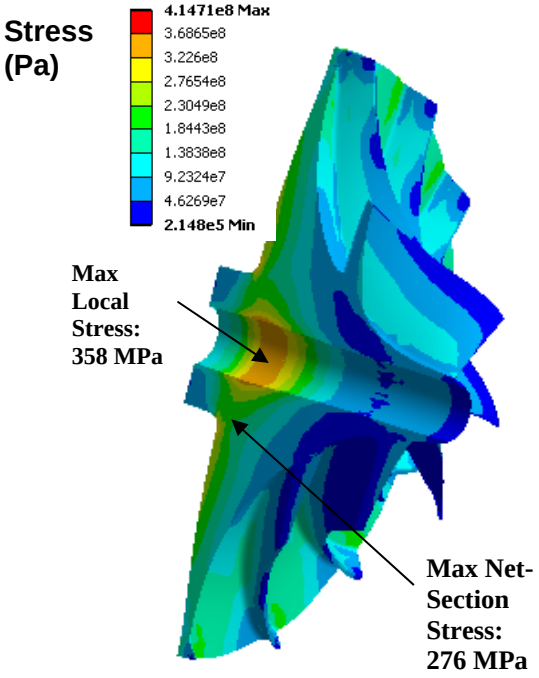

Figure 31: Compressor Wheel Stress Analysis at 10% Over-speed

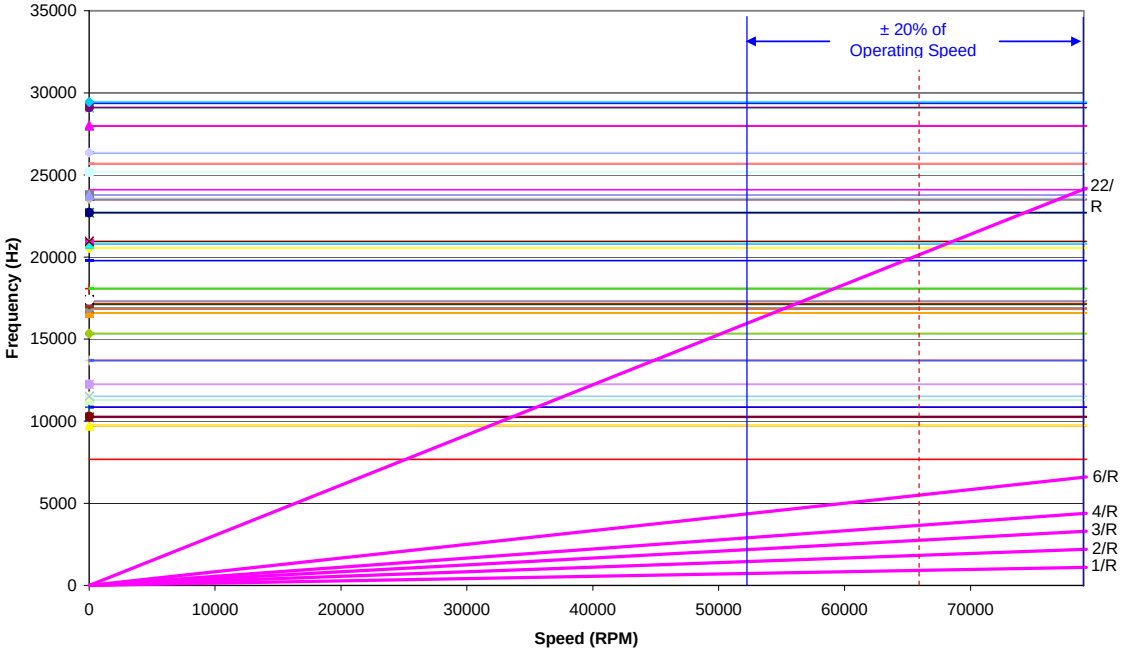

Figure 32: Compressor Wheel Campbell Diagram

6. Turbine Design

The turbine wheel is a radial inflow type. It utilizes nozzles to direct the flow at the optimum angle for high efficiency. The design dimensions and details are shown in Table 2. The front view with shroud removed is shown in Figure 33.

Parameter	Design Value
# Nozzles	13
# Blades	11
Diameter Turbine Inlet mm	89.6
Diameter Turbine Exit mm	61.1
Diameter Turbine Hub mm	23.2
Turbine Inlet Blade Height mm	18.92
Impeller Clearance mm	.203

Table 2: Turbine Design Dimensions

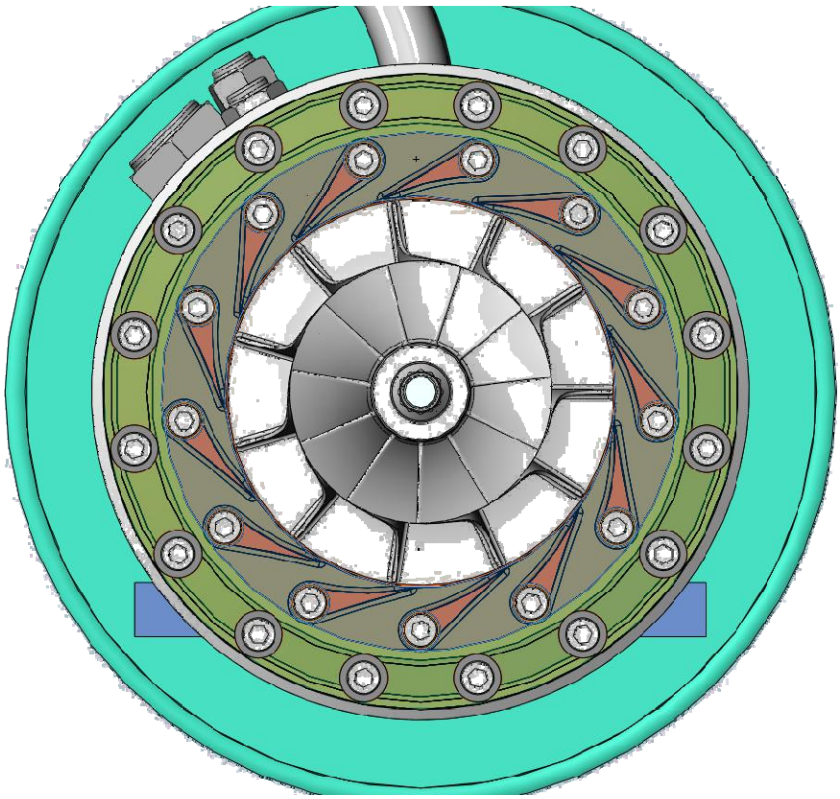

Figure 33: Turbine Exit View with Nozzles, Shroud Removed

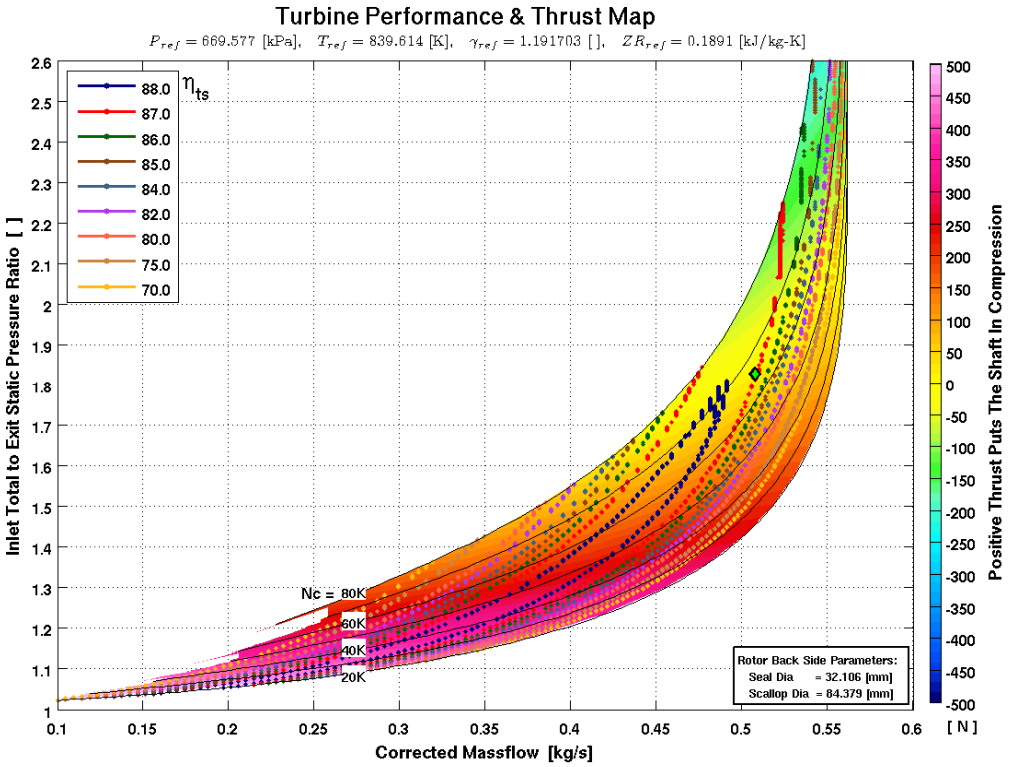

Figure 34: Turbine Performance and Thrust Map

The turbine performance indicates an efficiency of slightly higher than 87% (Figure 34). The turbine and compressor are on the same shaft and a compromise must be reached on overall performance. Slightly higher turbine efficiency could be reached at a different operating speed, but not enough to warrant two individual shafts. The thrust map is an important consideration and ideally is balanced with the compressor wheel thrust to neutralize the thrust load on the rotor support system.

The turbine wheel is made from Inconel 718 with yield strength at temperature of 931 MPa. This provides a 2:1 margin on burst speed. The analysis was performed at 10% over speed. The details of the stress analysis are shown in Figure 35. The interference Campbell diagram is shown in Figure 36. The 1x, 2x, 3x, and 4x modes are not excited, nor is the blade pass modes at the operating speed.

Rotating - Turbine Wheel Structural Analysis

- Inconel 718 at 810.9 K
  - Ultimate Strength = 1117 MPa
  - Yield Strength = 931 MPa
- 10 % over-speed: 72,000 RPM
- Max Net Section Stress = 207 MPa
  - Ultimate SF = 5.4
  - Yield SF = 4.5
- Max Local Stress = 400 MPa
  - Ultimate SF = 2.70
  - Yield SF = 2.25
- Burst Speed = 160,000 rpm
  - Average tangential stress = 173 MPa

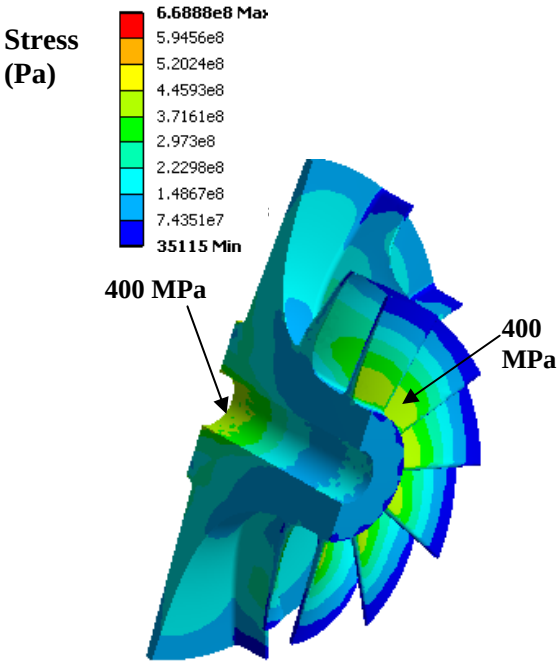

Figure 35: Turbine Stress Analysis

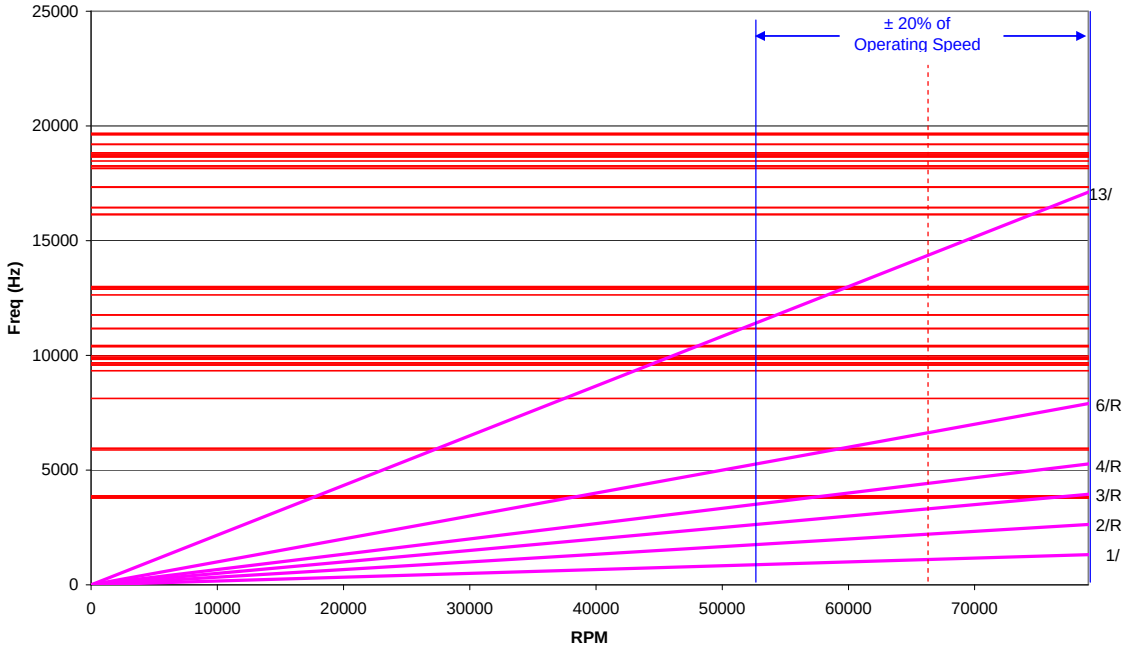

Figure 36: Turbine Wheel Interference Diagram

7. Alternator Design

The alternator is a permanent magnet design. It is a two pole (one pole pair) design using Samarium Cobalt magnets material shown in Figure 37. The magnets are cylindrical with a hollow center to provide a passage for a tie bolt. The magnets are kept in compression over the entire speed range by shrink fitting an Inconel 718 sleeve over the rotor structure. The magnet stresses are listed in Table 3. The stress analysis includes startup conditions at 200 K at results in 450 K at operating temperature.

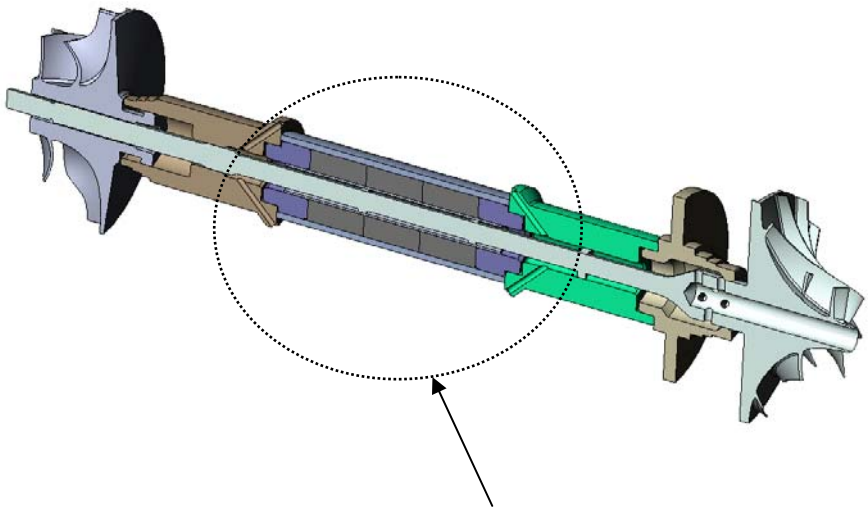

Figure 37: Permanent Magnet Section of Rotor

		TANGENTIAL STRESS			
CYLINDER	TOTAL	TOTAL	Due to	Due to	Due to
NAME	Cold	Hot	Press. - Cold	Press. - Hot	Speed
	Mpa	Mpa	Mpa	Mpa	Mpa
INNER-ID	-46.9193	-107.3	-133.3473	-193.728448	86.428
INNER-OD	-45.9428	-82.962	-79.2773646	-115.175041	33.3346
OUTER-ID	414.493	540.559	278.4071578	404.473031	136.086
OUTER-OD	329.916	431.498	224.3372224	325.919624	105.578
Inner SmCo	-550	Crush			
Outer Inconel 718	986	Yield			

Table 3: Magnet Stress Values

The alternator must be capable of high efficiency over the anticipated nominal and high temperature difference range. High efficiency of the alternator is important for overall cycle efficiency, but also to minimize the stator operating temperature. The performance map for the alternator is shown in Figure 38. The stator operating temperature defines the insulation method to meet the goal of 8 year life, or approximately 70,000 hours. Figure 39 indicates that the alternator will have sufficient life if the operating temperature is below 190 deg C with a goal of 180 deg C and is insulated to UL type N insulation.

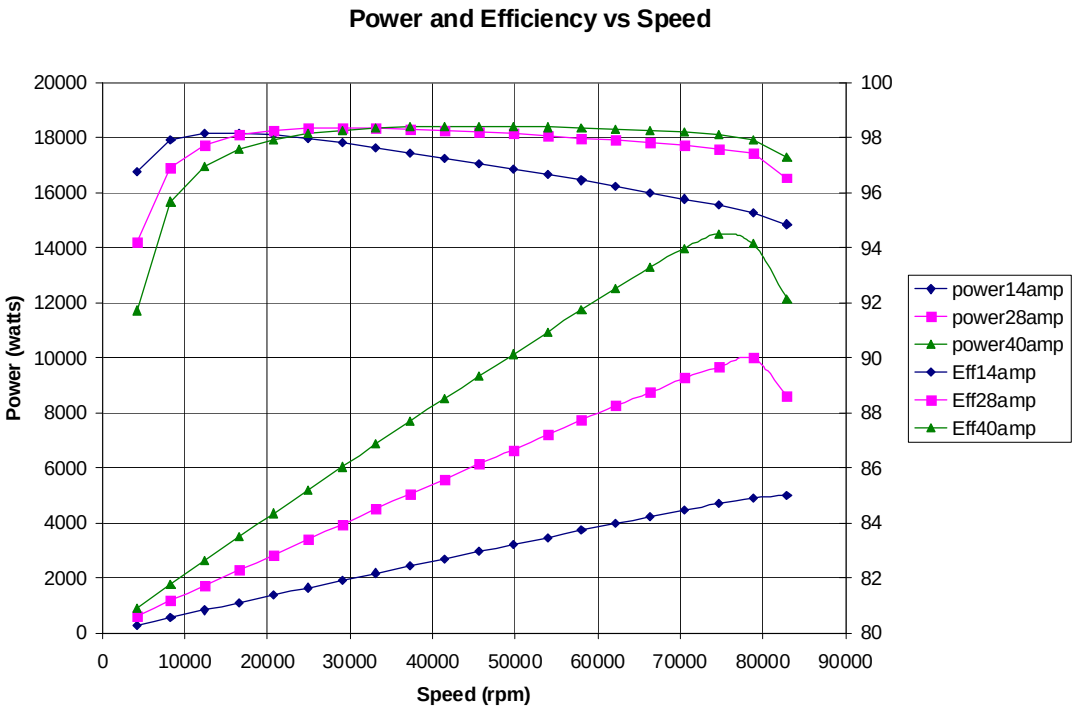

Figure 38: Alternator Performance Map

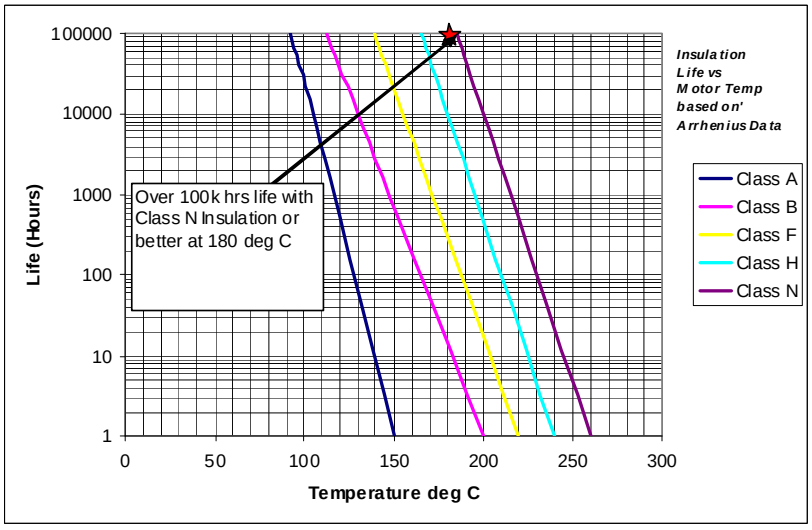

Figure 39: Insulation Life vs. Operating Temperature

The alternator stator is made from Hiperco 50 laminations, .006” thick. The properties of this material allow very low core losses in a small, lightweight package. The stator itself is wound with UL Class “N” materials. The stator has 18 slots in is wound in a sinusoidal fashion. The alternator must also act as a motor for power converter startup.

8. Turbine Alternator Compressor (TAC) Design

8.1 Overall Layout Section View

The overall layout is shown in Figure 40. The compressor is shown on the right end. The compressor inlet routes the flow into the compressor eye. The pressure is increased by the rotational speed and the flow exits the compressor wheel and diffuser vanes into a volute. The volute discharges the flow to the recuperator inlet on the power converter system. The heated gas then enters the turbine inlet plenum. The flow then travels through the turbine nozzles, into the turbine, and exits axially through the conical diffuser.

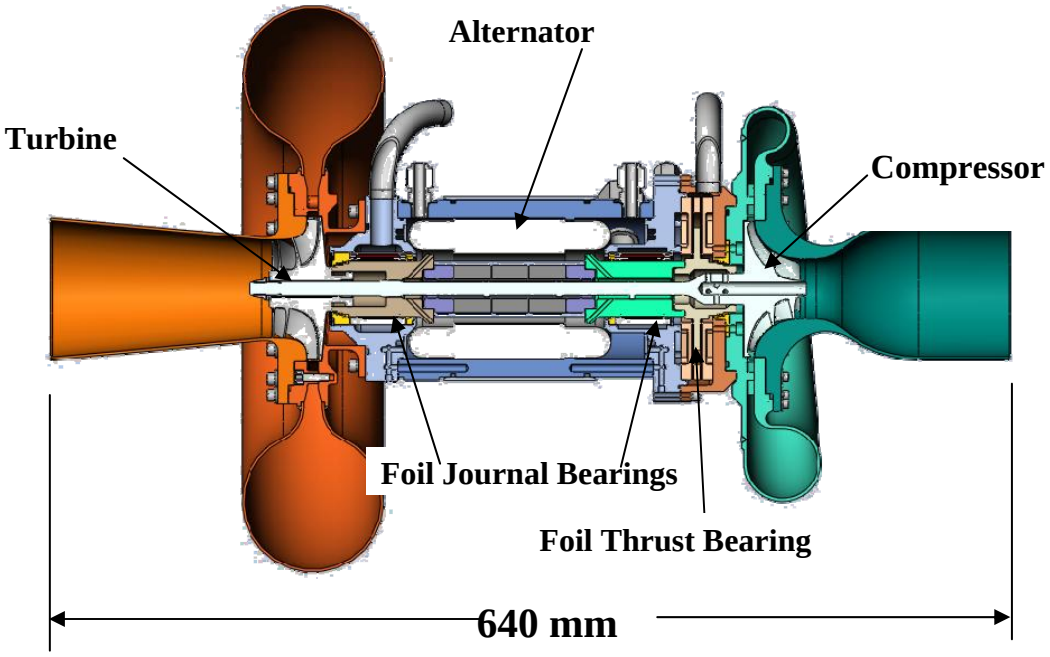

Figure 40: Overall TAC Layout

A closer view of the turbine end of the TAC is shown in Figure 41. The materials of construction are annotated and are primarily stainless steel and Inconel 625 or 718. Inconel 625 is utilized for welded construction to avoid the heat treatment and potential warping of components when using Inconel 718.

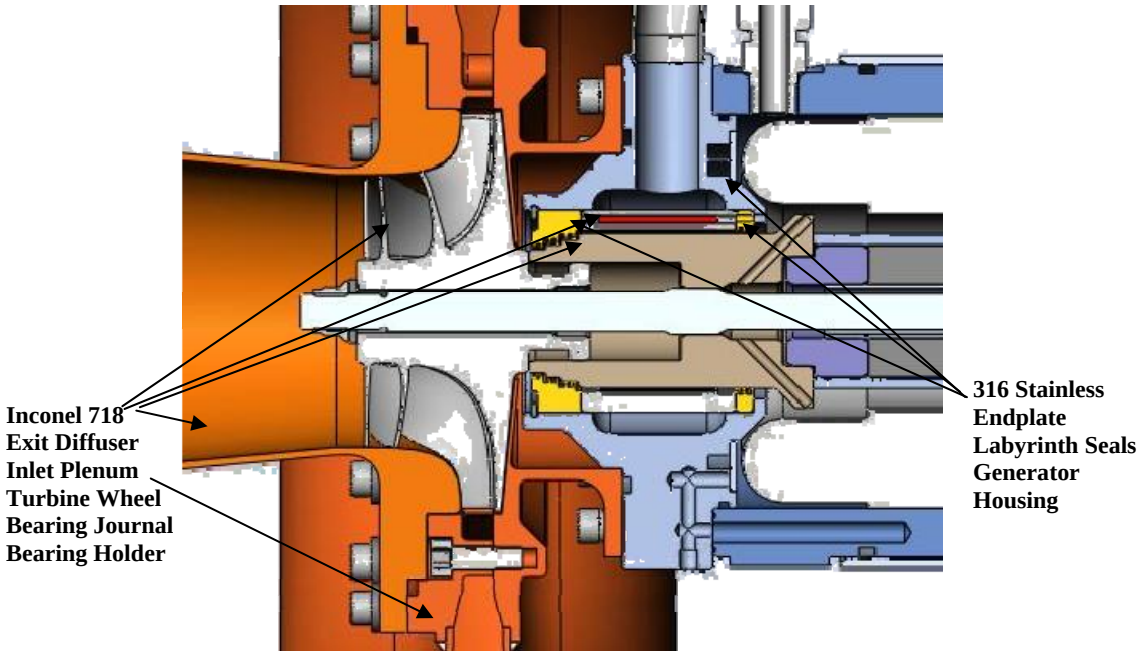

Figure 41: TAC Turbine End Close Up

The compressor end close up of the TAC is shown in Figure 42. Again the materials of construction are primarily stainless steel and Inconel alloys.

The TAC utilizes foil journal bearings and bi-directional thrust bearing. The overall thrust profile is shown in Figure 43. As the machine operates at higher pressures, the thrust profile may vary. The foil thrust bearing must compensate for the variable thrust profile.

The overall TAC weight breakdown is shown in Table 4. The major component weights are the alternator, inlet and exhaust volutes/plenums, and the main alternator housing. Smaller items are the generator rotor, bearings, end plates, seals, and the turbine and compressor wheels.

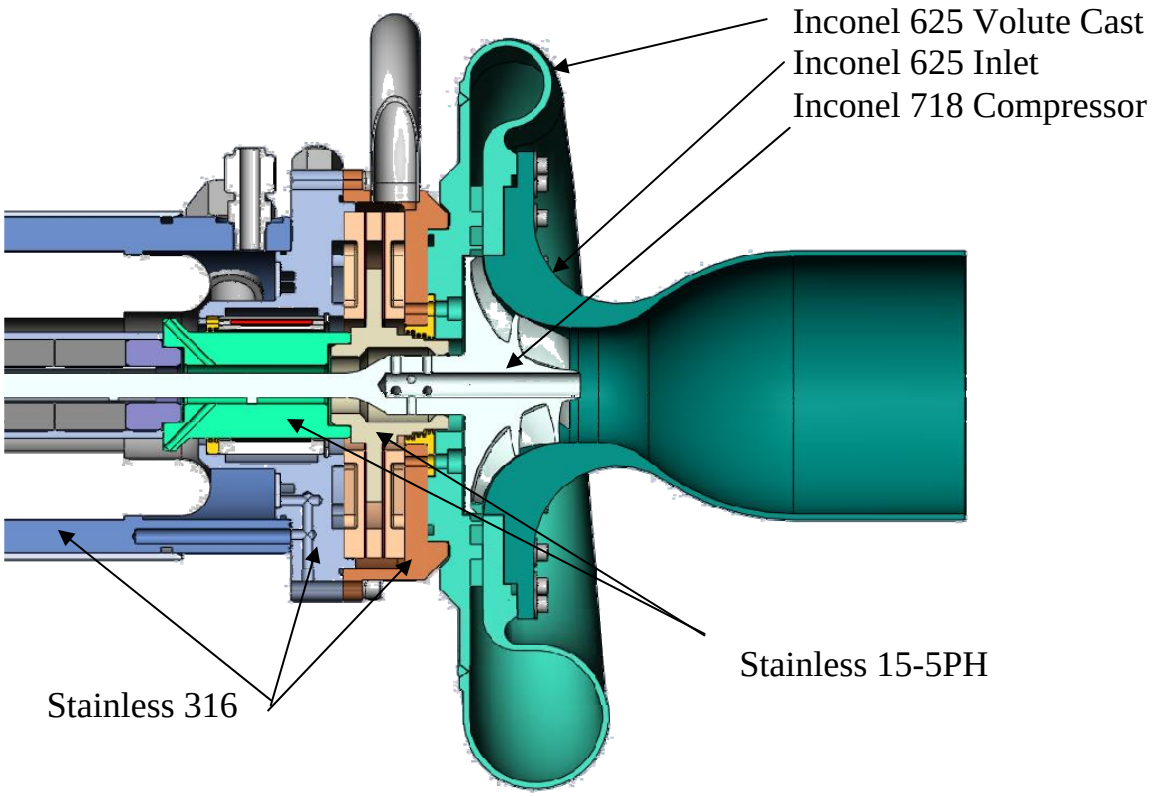

Figure 42: TAC Compressor End Close Up

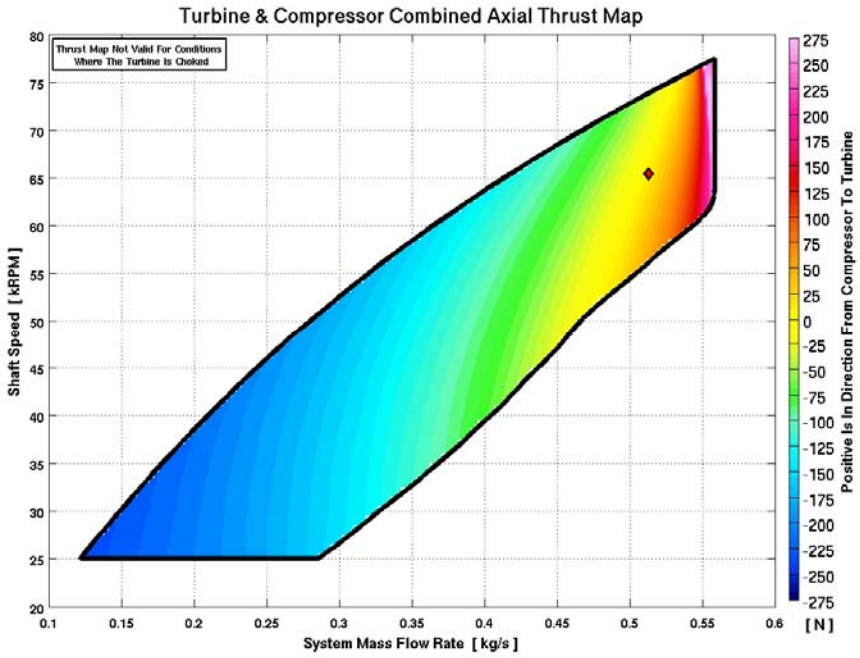

Figure 43: Combined Turbine and Compressor Axial Thrust Map

Compressor	**0.5**	**kg**
Turbine	**0.46**	**kg**
Main Housing	**3.45**	**kg**
Compressor Volute	**3.3**	**kg**
Alternator Stator	**4.45**	**kg**
Turbine Plenum	**4.85**	**kg**
Alternator Rotor/Bearings	**0.919**	**kg**
Endplates/Seals	**5.5**	**kg**
Guide vanes, Bolts, Piping	**6.67**	**kg**
Total Weight	**30.1**	**kg**

Table 4: TAC Weight Breakdown

8.2 Foil Bearings

The TAC is supported on foil bearings. It is the intent to utilize foil bearings from a Capstone C30 Microturbine. The CO2 environment for these bearings is considerably different than that of the microturbine so bearing loss and cooling data is difficult to verify. For this reason a small scale experiment was performed to quantify the foil bearing losses on air and CO2.

A Capstone natural gas compressor was modified by removing the pumping elements and adding a flywheel mass. This mass simulates the weight of the TAC and should more closely approximate the bearing losses. A pressurized piston arrangement was used to load the thrust bearing. This was limited to approximately 50 N of force. A photograph of the test rig is shown in Figure 44.

The test rig was operated to 30 krpm on air and 35 krpm on CO2 at 20 psi pressure. The results are shown in Figure 45. The measured power was from the DC supply feeding the controller. Efficiency estimates for the controller and the motor are approximately 85%, so the foil bearing power loss is approximately 85% of the value in the plot. The data repeated nicely and had a power law profile that was curve fit. This data was extrapolated to provide an estimated bearing loss for the TAC thermal analysis and cooling flow.

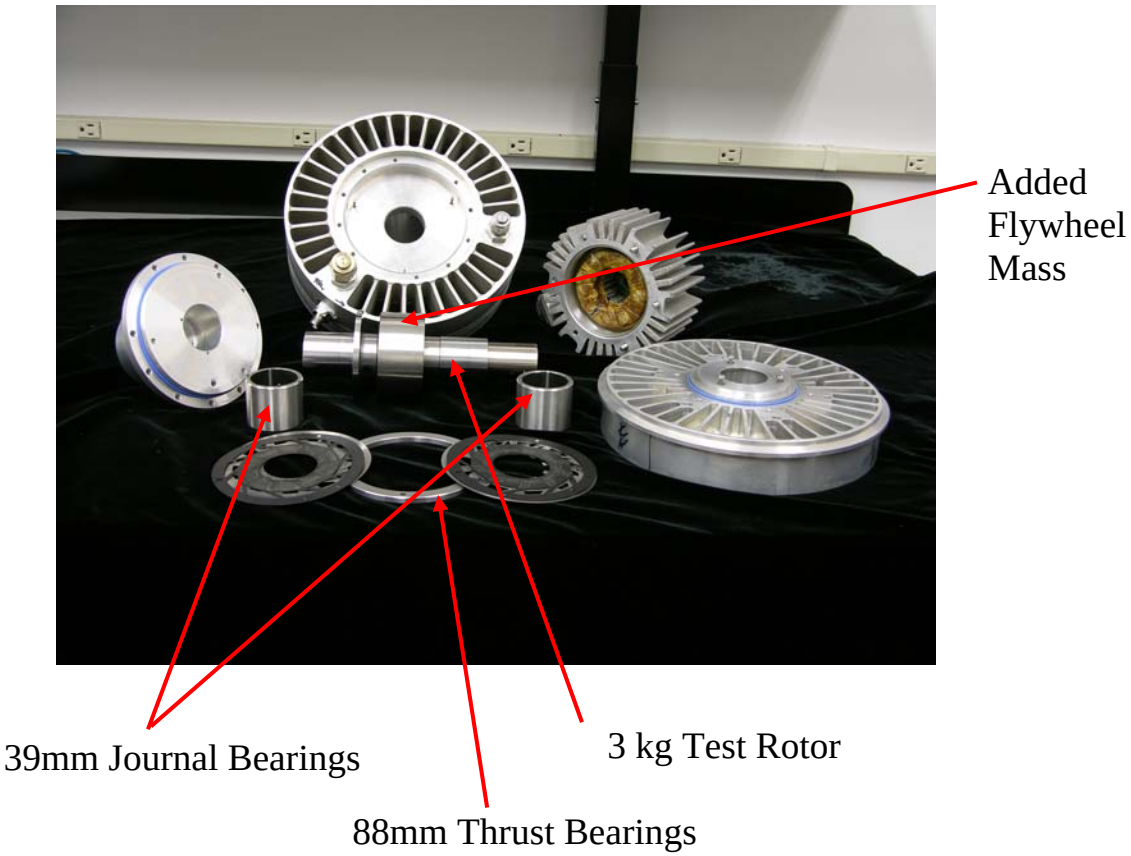

Figure 44: Foil Bearing Experimental Hardware

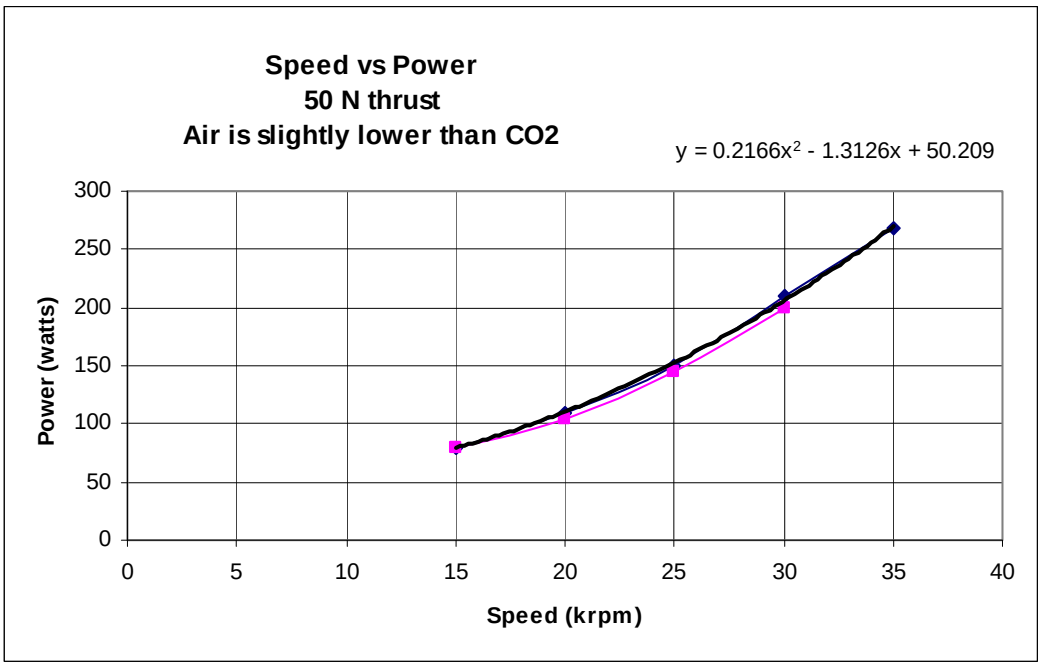

Figure 45: Foil Bearing Power vs. Speed (Power is from DC Supply)

8.3 Cooling Flow

The TAC is cooled by two primary flows, the compressor inlet flow and a cooling water jacket. The cooling flows cool the bearings and alternator cavity. The cooling jacket is designed to cool the stator core and copper losses, with the auxiliary compressor flow removing heat from the bearings and windage. The auxiliary compressor flow is primarily from a hollow compressor wheel inlet that is pumped by radial passages in the generator cavity on both ends of the stator. This raises the generator cavity pressure to direct flow to the generator and also through the bearings. The water cooling passages are shown in Figure 46. The predicted pressures in the TAC at full operating pressure are shown in Figure 47. The secondary flow passages are shown in Figure 48 with the predicted flow rates for proper cooling shown in Figure 49.

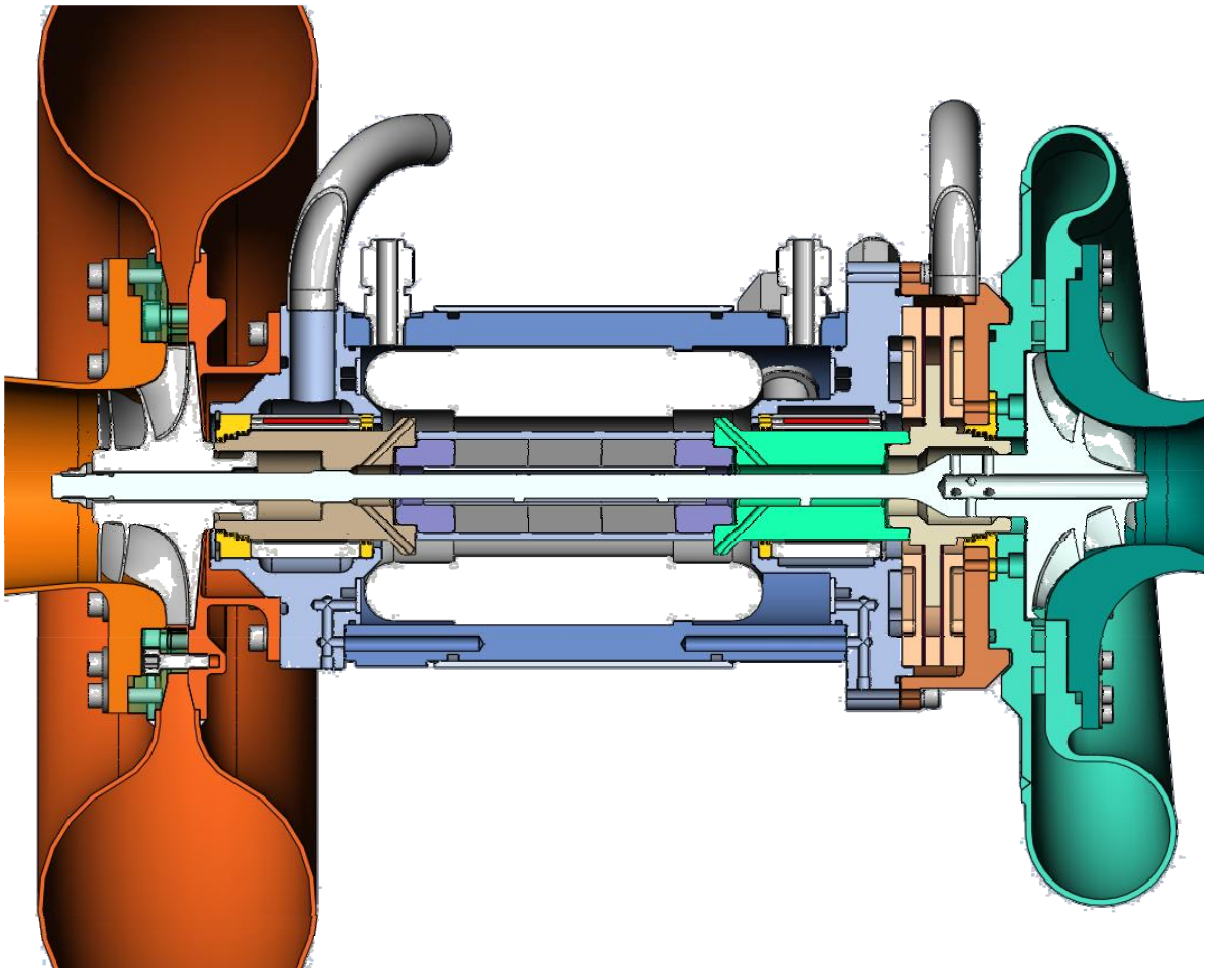

Figure 46: Water Cooling Passages

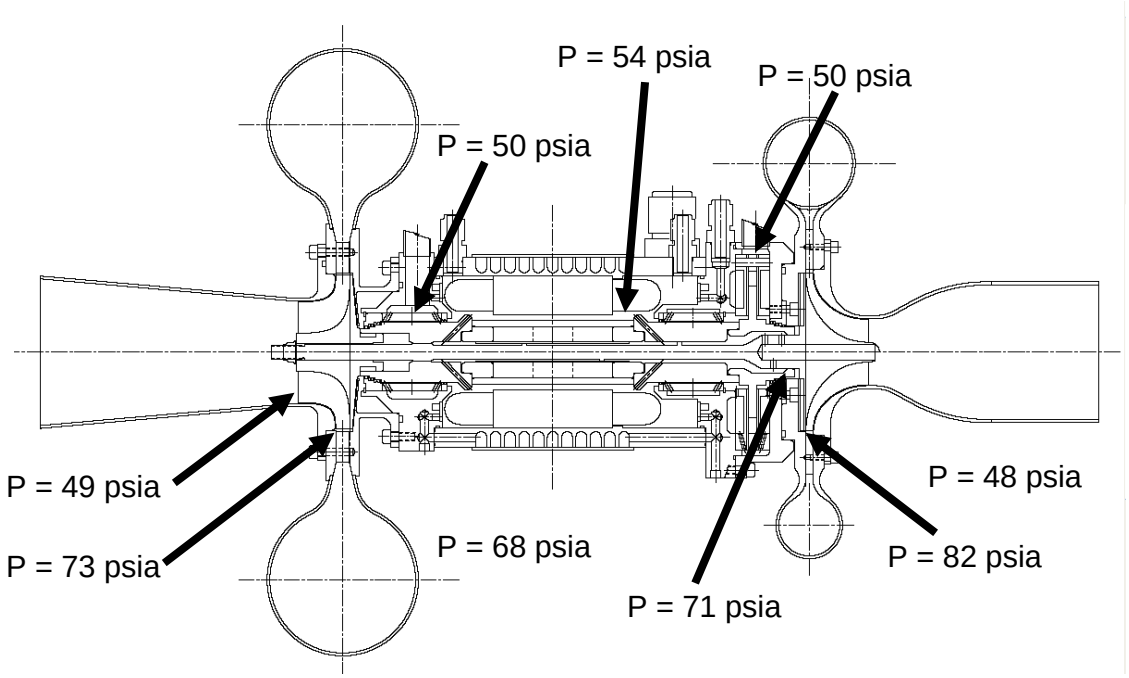

Figure 47: Predicted Cavity Pressures at Operating Speed

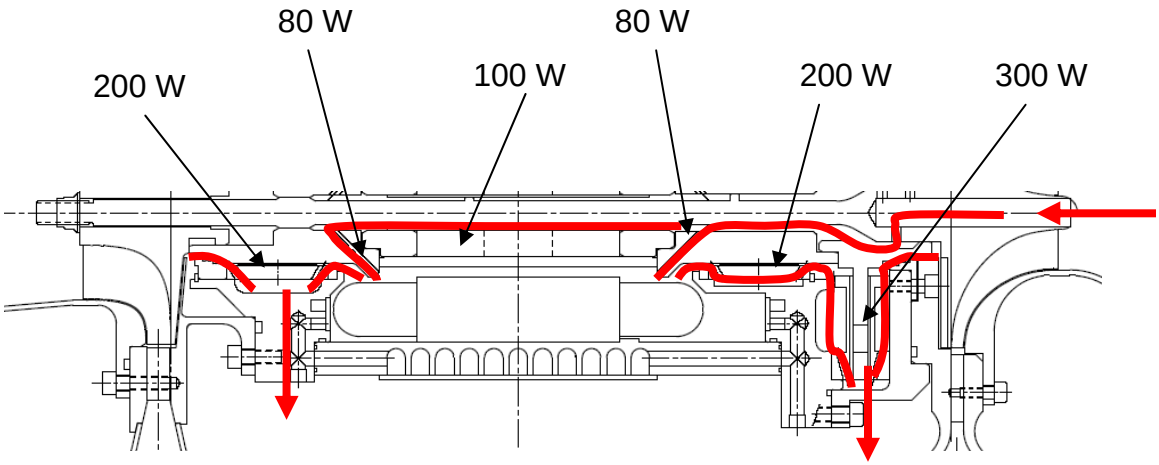

Figure 48: Power Loss and Gas Cooling Flow Passages

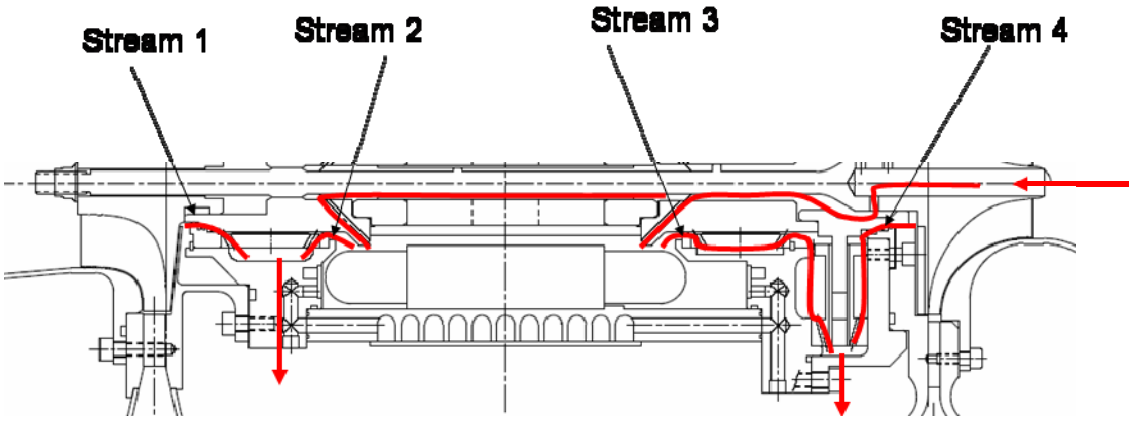

Stream Number	1	2	3	4
Seal Type	6 stagger	3 straight	3 straight	6 stagger
Seal Rad Clr (mm)	.127	.127	0.127	0.127
Seal Leakage (g/s)	3.17	4.5	4.5	4.8
Inlet Temp (K)	810.92	383	383	455
Power Input (W)	100	411	430	150
Exit Temp (K)	838.7	483	483	483

Figure 49: Cooling Mass Flows, Temperatures, Heat Loss

The mass flows are controlled by the labyrinth seals. It is recommended that the final labyrinth and cavity flow be adjusted to provide adequate cooling when the unit is initially tested. Minimizing the mass flow, which is a parasitic loss, will maximize the system efficiency. Controlling the generator temperature is the primary criteria for proper mass flow through the compressor bypass routes.

8.4 Rotor Dynamic Assessment

The rotor with foil bearings is very stiff and resistant to bending. The foil bearings are compliant. This combination results in rigid body modes that are at very low shaft speeds. As seen in Figure 50, the 1st two rigid body modes are below 15,000 rpm. The bearing liftoff speed has been identified at about 9,000 rpm. This dictates that the minimum operating speed should be above 15,000 rpm and ideally would be 20-25 krpm.

The 1st bending mode is calculated conservatively at 81,000 rpm. The bending mode can be modified by increasing the retention tube that surrounds the magnets. A thicker tube will increase the weight, but also increase the bending mode frequency. Since the operating frequency is approximately 65,000 rpm, 81 krpm is adequate for operation.

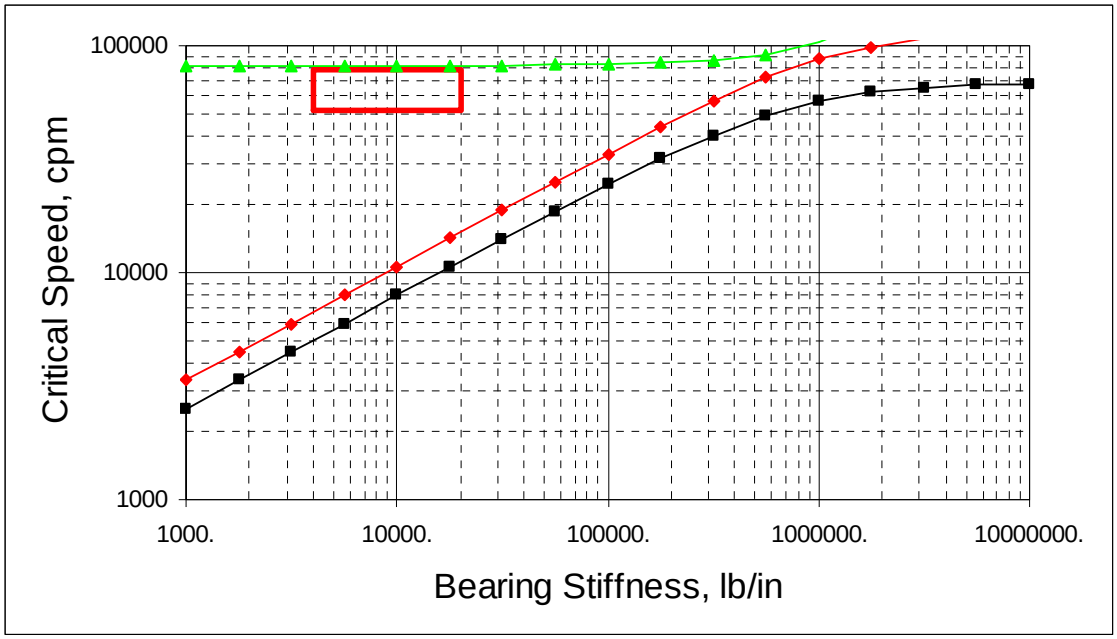

Figure 50: Un-dampened Critical Speed Map

9. Power Controller

The power controller serves several functions. It provides a boost converter function to increase the 120 VDC load supply voltage as specified by NASA to 450 VDC (selected by Barber-Nichols Inc.) to operate the generator at 400 VAC as specified by NASA. Another function is to use the alternator as a motor to start the Brayton cycle power converter. The power controller also converts any power available from the alternator by active rectification to the 450 VDC bus and the buck regulate the power to 120 VDC for the load. The power controller also has fault handling capability. It engages a set of temporary resistors in the event of shaft over speed.

9.1 Power Controller Packaging

The power controller is packaged in a 19 inch rack mount. It is a 4U size and can be air or water cooled, water cooling is preferred. The control rack layout is seen in Figure 51 and Figure 52.

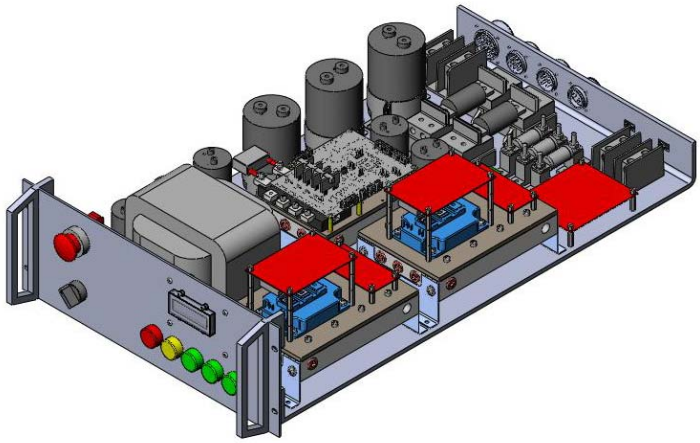

Figure 51: Power Controller (Isometric View)

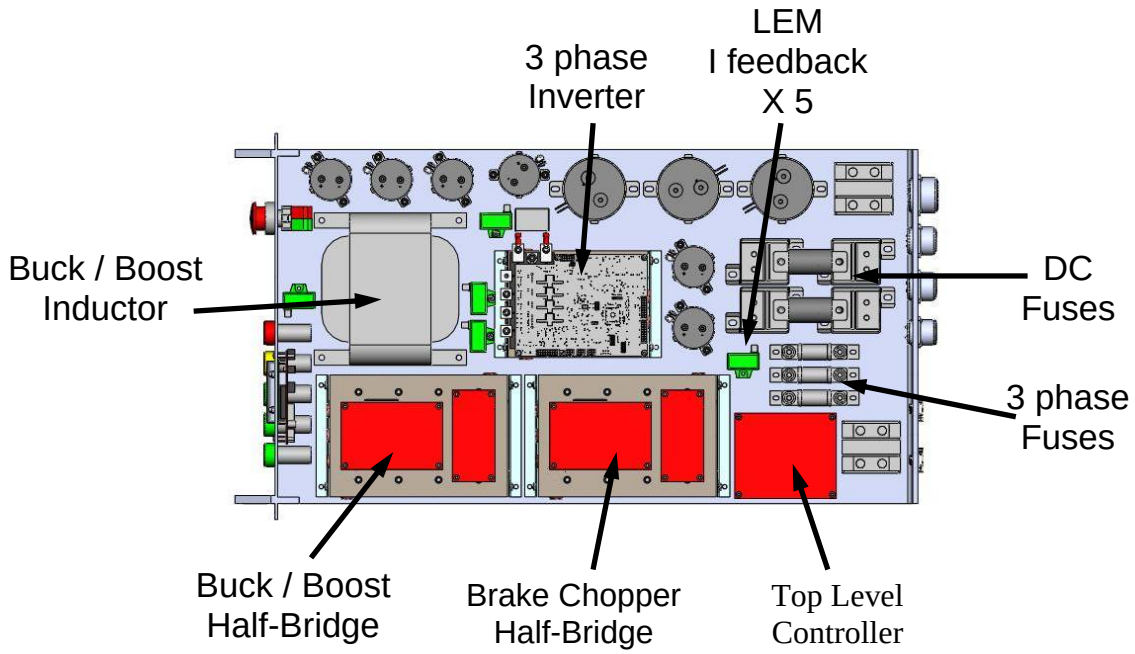

Figure 52: Component Locations for Power Controller (Top View)

9.2 Power Controller Schematic and Simulation

The power controller utilizes a full bridge IGBT package that contains a full-bridge three-phase drive and an auxiliary switch placed across the DC bus that is used as a brake. The top level schematic with function blocks is shown in Figure 53.

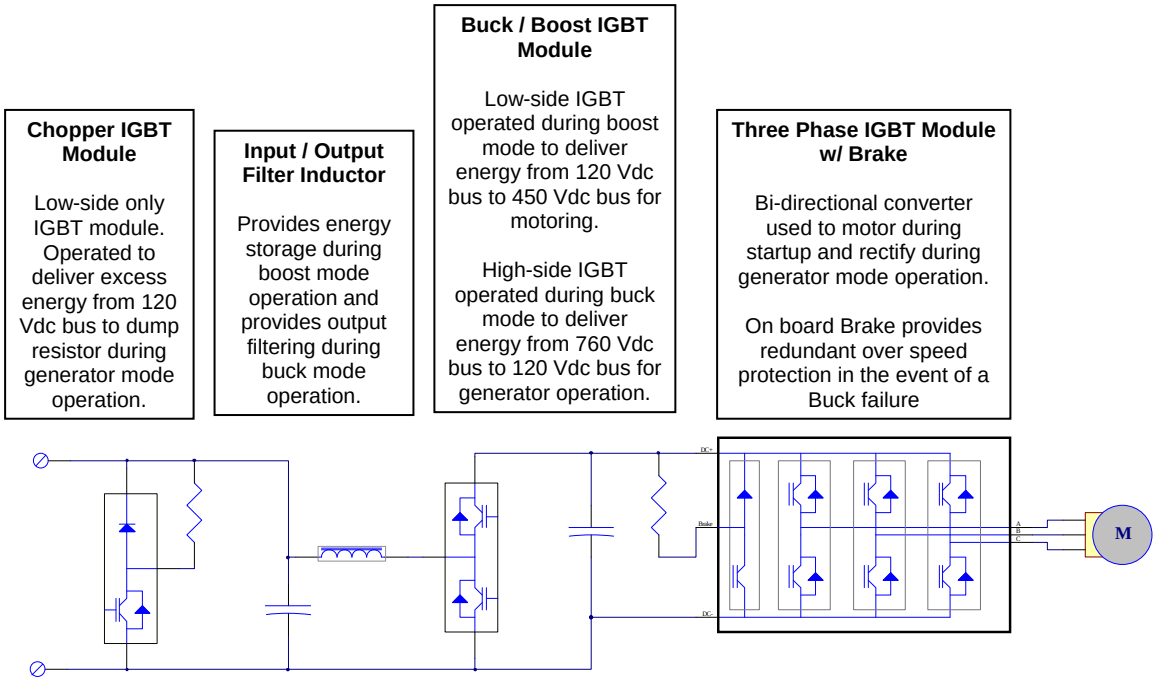

Figure 53: Top Level Control Schematic

The power converter simulation models can be broken down into the motor generator operational section and the boost converter section. The motor generator controller section is shown in Figure 54. The boost converter section is shown in Figure 55.

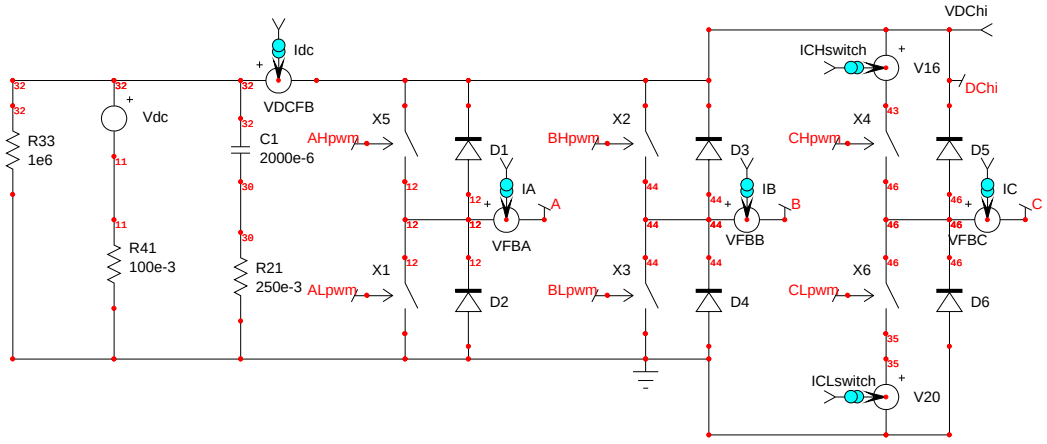

Figure 54: Motor/Generator Controller Simulation Circuit

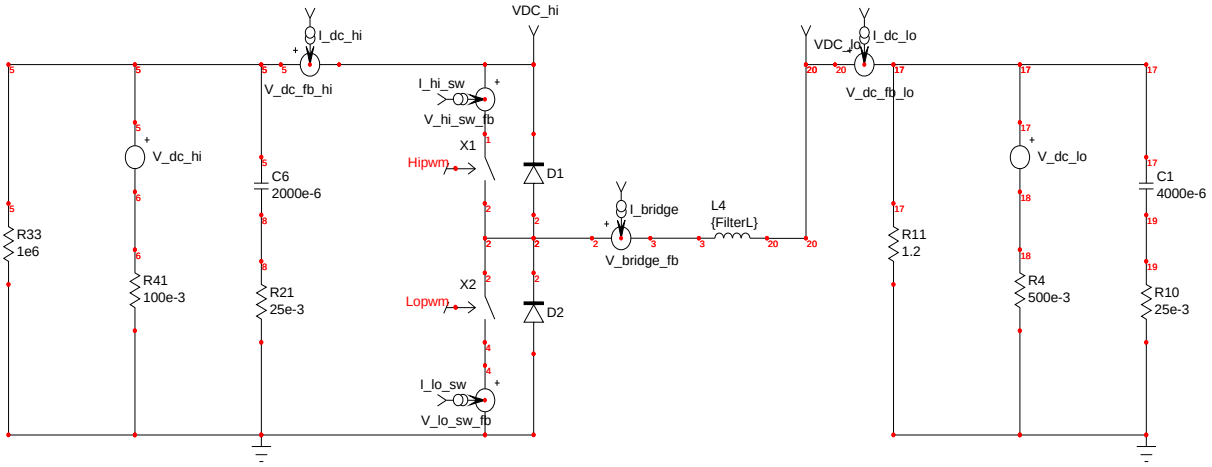

Figure 55: Boost/Buck Converter Controller Simulation Circuit

The motor controller simulation circuit is used to identify waveforms and predict performance for the motoring and generating modes of operation. Figure 56 shows the motoring mode simulation results and waveform. Figure 57 shows generating mode simulation results and waveforms.

- **Motor Mode Simulation @ 600 Hz**
  - 5A +/- 2.5A Switch Points on Phase IGBTs
  - I leg = 2.0 Arms, 1.55 kW In
  - Phase-Phase Vpk = 333V
  - 450 Vdc source on Hi DC bus

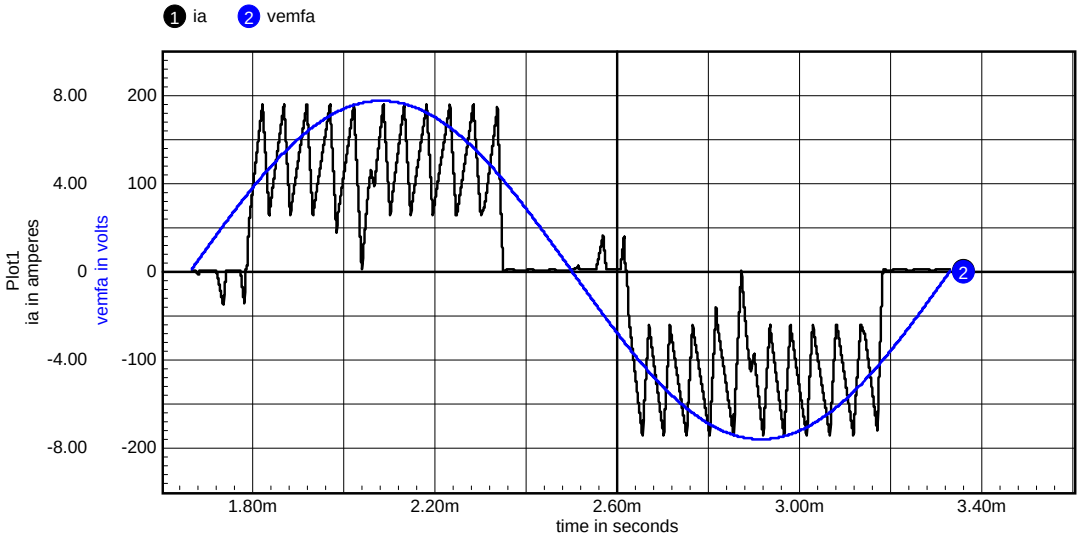

Figure 56: Motoring Mode Simulation

- **Generator Mode Simulation @ 1050 Hz**
  - **30A +/- 5A Switch Points on Phase IGBTs**
  - **I leg = 22.9 Arms, 15.85 kW out**
  - **Phase-Phase Vpk = 583V**
  - **760 Vdc sink on Hi DC bus**
  - **Sensorless Generator operation viable**
  - **"speed-loop" winding added for redundancy**

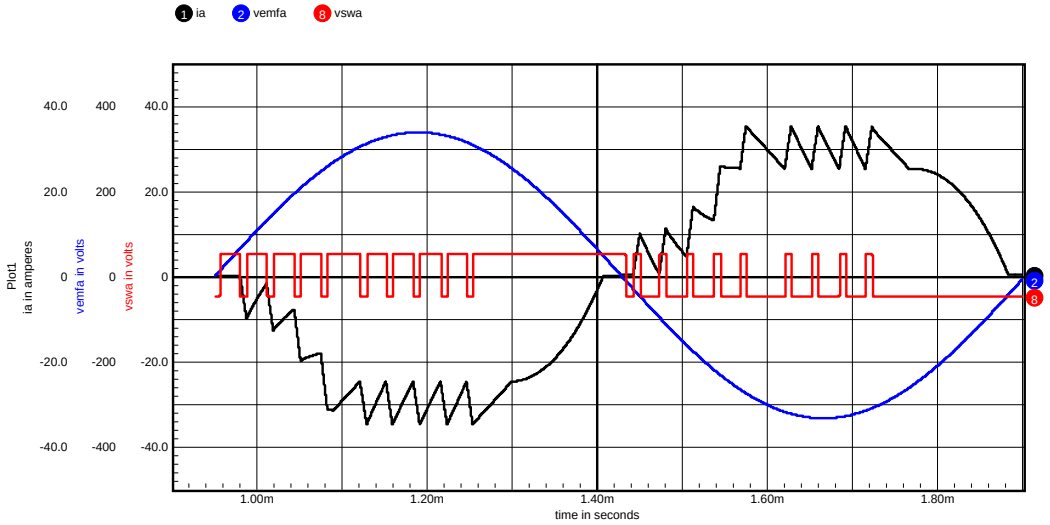

Figure 57: Generating Mode Simulation

The buck-boost converter simulation is used to predict operating waveforms and also size components. The converter uses an inductor to store energy for the boost operation. The simulation also identifies the proper DC bus capacitor size for load step simulation. The boost mode is used at low power to motor the shaft to approximately half speed. The simulation is performed at the predicted power and speed level for cold startup operation. After the unit is motored to half speed, heat can be applied and the machine will operate from a power consumer to a power supplier.

The buck simulation is performed at full power. The buck simulator takes the rectified high voltage and converts it to regulated 120 VDC low-voltage. The specification dictates 6% DC bus ripple maximum (120 +/- 6 VDC). The simulation identified the minimum bus capacitance to satisfy the specification. No load step specification was supplied, however, a larger than necessary capacitor was added to allow 50% load drop testing to be performed. Figure 58 shows the boost mode simulation while Figure 59 shows the buck mode simulation.

- **Boost Mode Simulation**
  - **12.5 +/- 7.5 Switch Points on Lo IGBT**
  - **125 Vdc source on Lo DC bus**
  - **135 ohm load on Hi DC bus @ 450 Vdc**
  - **I Hi = 3.5 A, I Lo = 12.5 A**
  - **1.58 kW in, 1.56 kW out, Total loss = 1.27%**

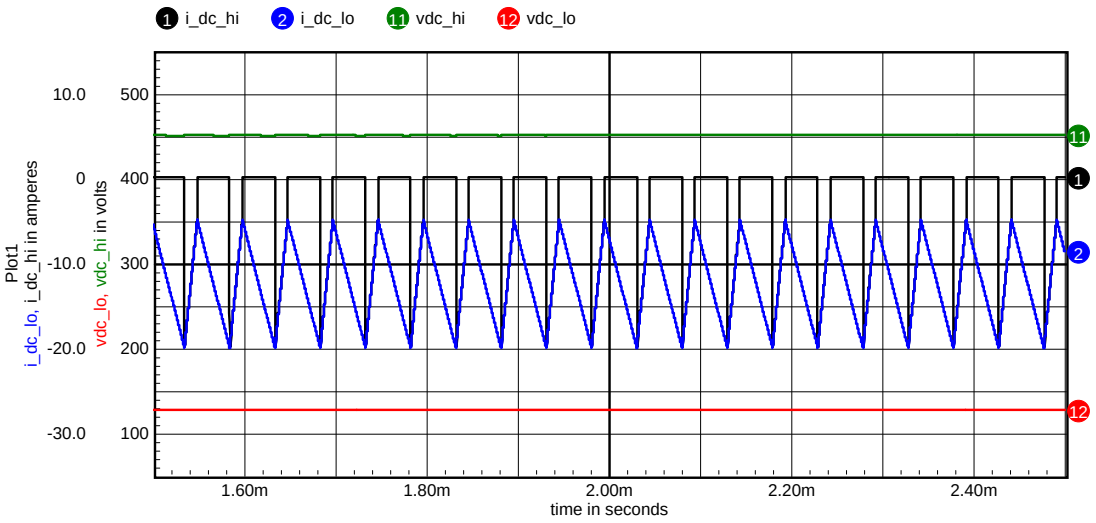

Figure 58: Boost Mode Simulation

- **Buck Mode Simulation**
  - **100A +/- 10A Switch Points on Hi IGBT**
  - **760 Vdc source on Hi DC bus**
  - **1.2 ohm load on low DC bus @ 120.3 Vdc**
  - **I Hi = 16.6 A, I Lo = 100 A**
  - **12.55 kW in, 12.03 kW out, Total loss = 4.1%**

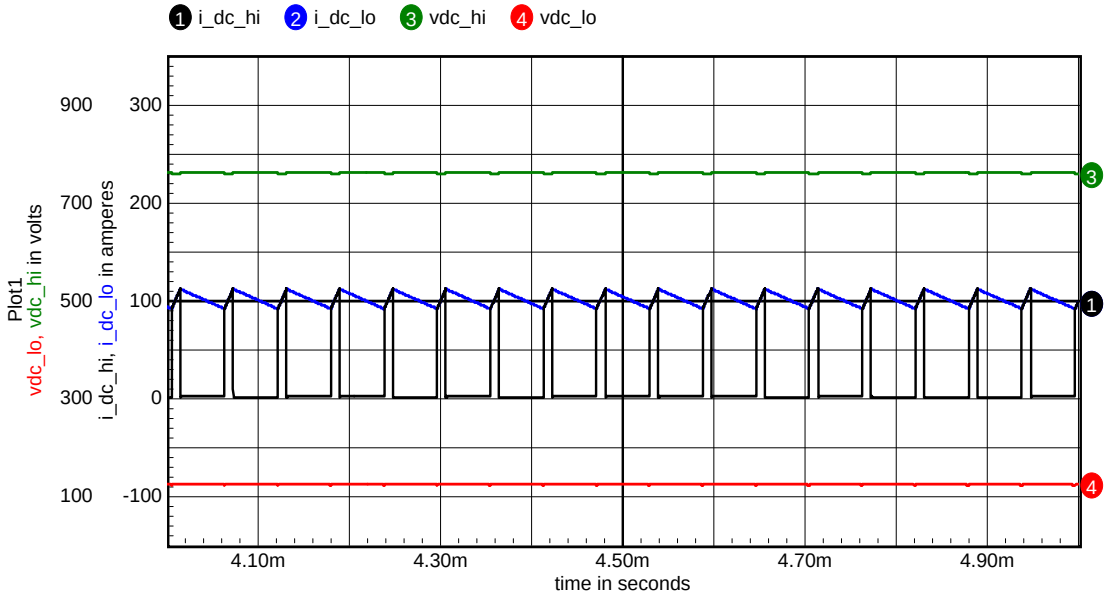

Figure 59: Buck Mode Simulation

10. Power Converter

The power converter consists of the TAC, NaK Heater, Recuperator, and a Gas Cooler. Two types of NaK heaters were assembled into a converter. A shell tube NaK heater and a plate fin NaK heater. The shell tube NaK heater power converter was larger and heavier than the plate fin exchanger. The shell tube NaK heater design was supplied by a company with molten salt heat exchanger experience, while the plate fin was design was supplied by a company without NaK experience.

The plate fin NaK exchanger construction is much more compact and lightweight and was also identified and proposed during in the 1960's and 1970's SNAP reactor program. Regardless of the pedigree of the heat exchanger manufacturer, the design of the NaK exchanger should use the knowledge base generated from the SNAP reactor program relative to materials of construction. The performance and construction risk is regarded as less important than the risk of a structural failure and subsequent leak. From this standpoint, the fixed tube sheet exchanger with multiple tube welds is more risky than a brazed and welded plate-fin heat exchanger.

10.1 Power Converter with Shell/Tube NaK Heater

The power converter layout with the shell/tube heat exchanger is shown in Figure 60.

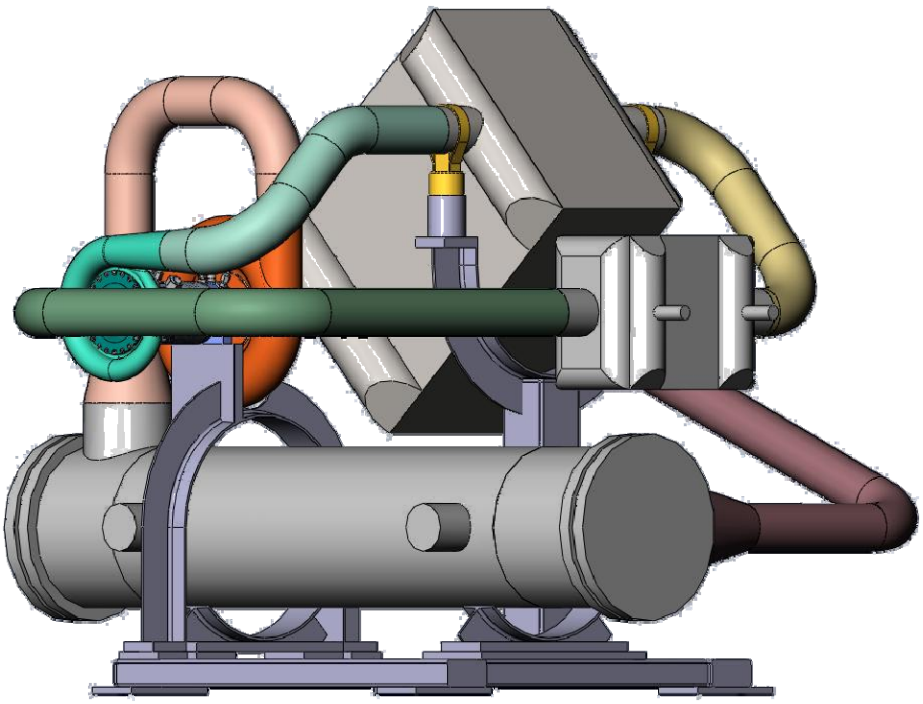

Figure 60: Power Converter with Shell/Tube NaK Exchanger

The power converter with the shell/tube exchanger has an estimated weight of 780 kg. The volume identified in the system layout is approximately 1500mm x 1550mm x 1442 mm. The layout in three views is shown in Figure 61.

The power converter stress analysis is done in a manner to simulate the system from a cold 200 K startup to operating temperature. The operating temperature differs by component. The stress analysis is done with the goal of matching thermal growth by matching thermal growth areas. This enables the loop to be welded pipe construction and eliminate any bellows. Bellows would complicate the system and have piping pressure drop implications reducing performance. The thermal boundary conditions and steady state operating thermal condition is shown in Figure 62. The system primary stress regions are shown in Figure 63. As the piping undergoes thermal growth, the TAC piping interfaces must be analyzed for stress. The results are shown in Figure 64.

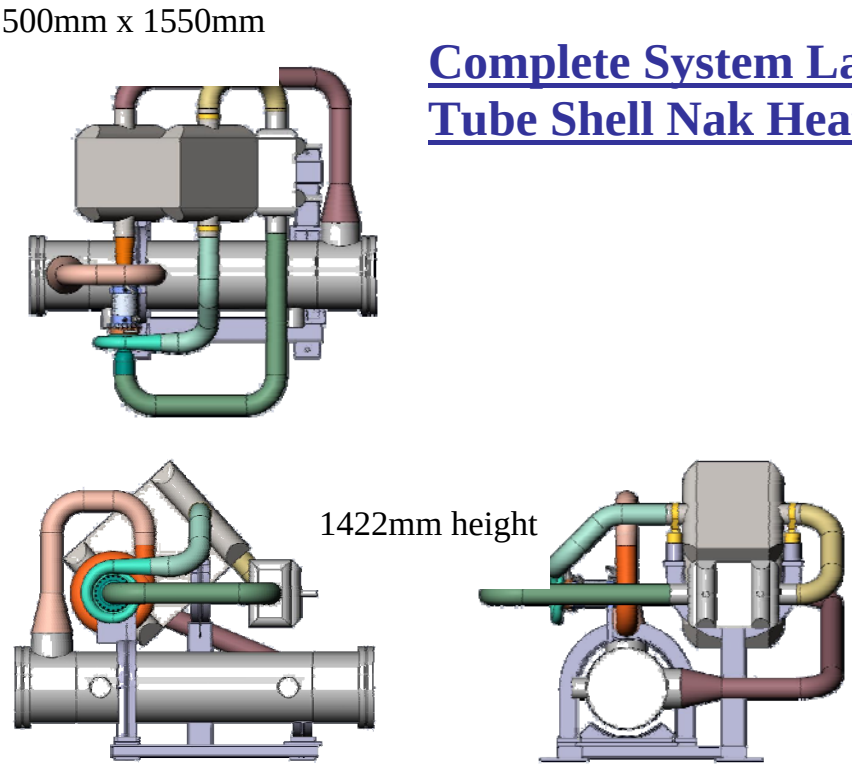

Figure 61: Power Converter for Shell/Tube, Three Views

- Analyzed via steady-state thermal analysis (assumed slow thermal ramp from cold initial condition)
- Forced Convection (5887 W/m^{2}C) applied to piping (simulates internal flow)

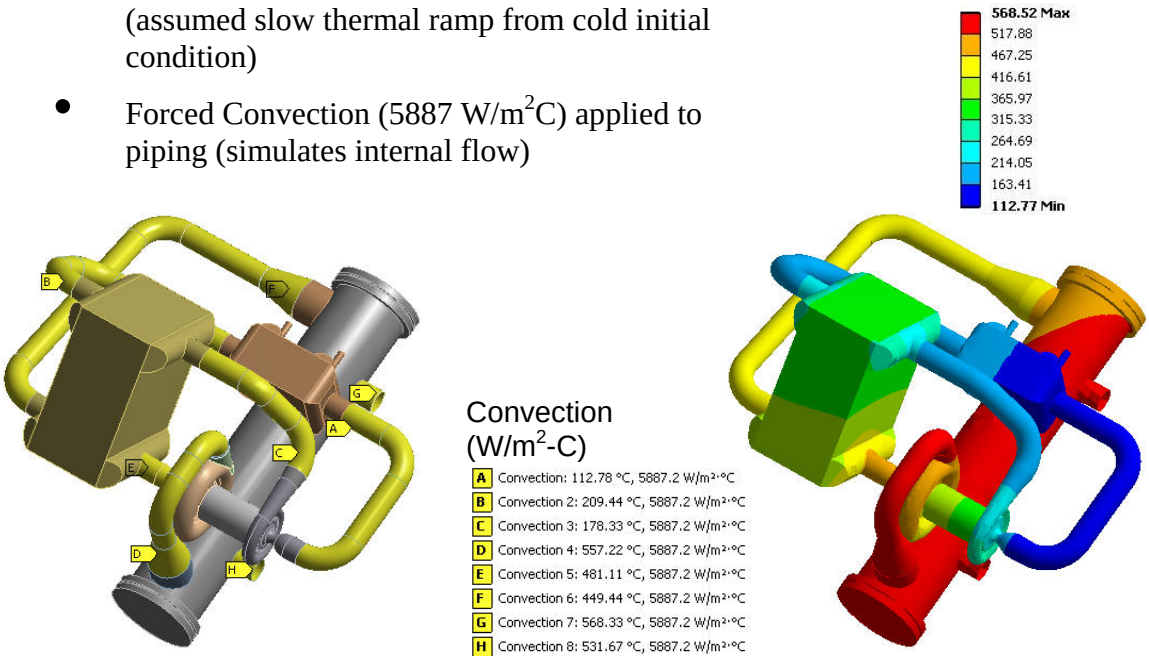

Figure 62: Static Thermal Conditions for Shell/Tube Power Converter System

Static - Stress in Piping due to Weight & Thermal Growth Shell/Tube Heat Exchanger System

- Structural Analysis (Thermal Loads + Weight) of 3D Shell Model
  - **Materials, thicknesses, component stiffness' representative of full 3D model**
  - **Max piping load = 152 MPa (FSy = 1.86)**
- Forces & Moments calculated at Turbomachinery nozzle interfaces

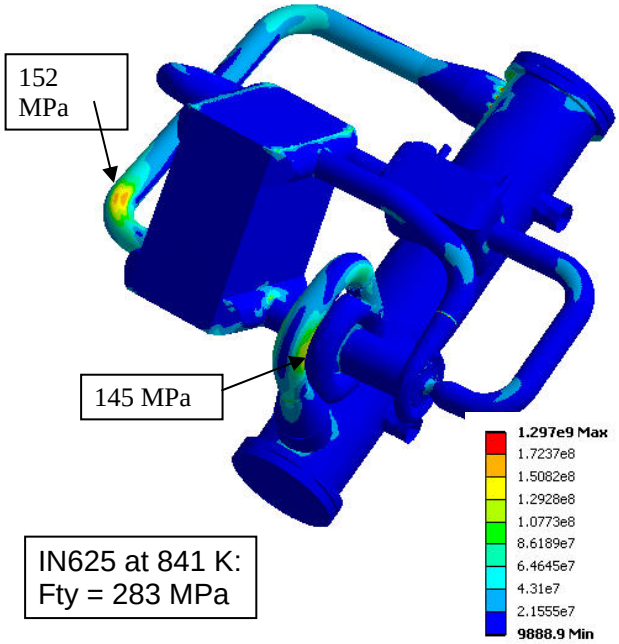

Figure 63: Shell Tube Stress Regions

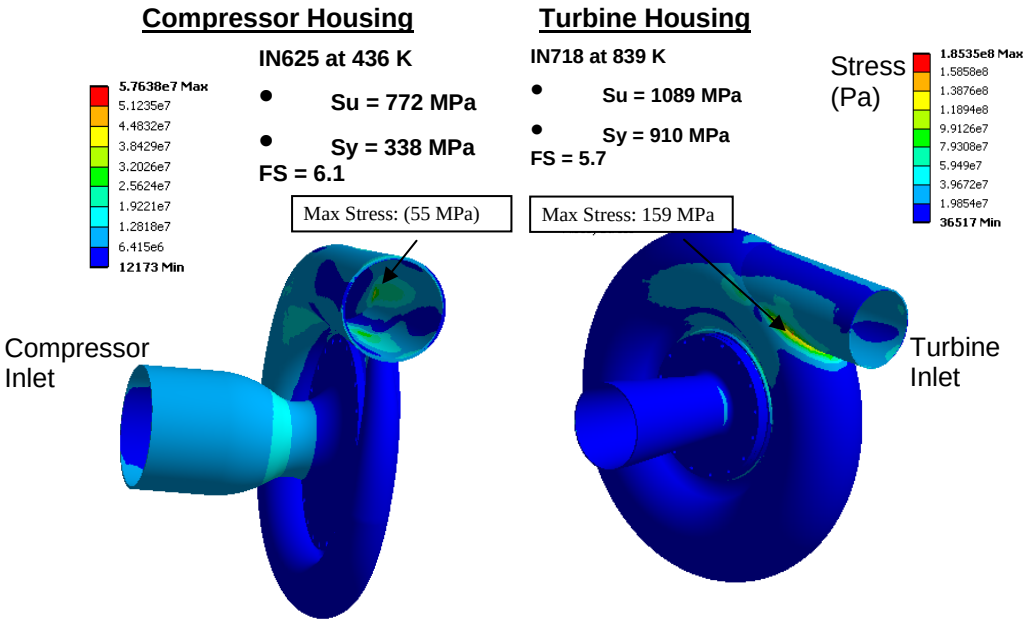

Figure 64: Piping Interface Loads on TAC

10.2 Power Converter with Plate/Fin NaK Heater

The power converter designed with the plate fin heat exchanger is more compact and more importantly has considerably less weight. The overall dimensions are approximately 1200mm x 1200mm x 1200mm with an overall weight estimate of 260 kg. The isometric solid model of the power converter is shown in Figure 65. A three view of the same configuration is shown in Figure 66.

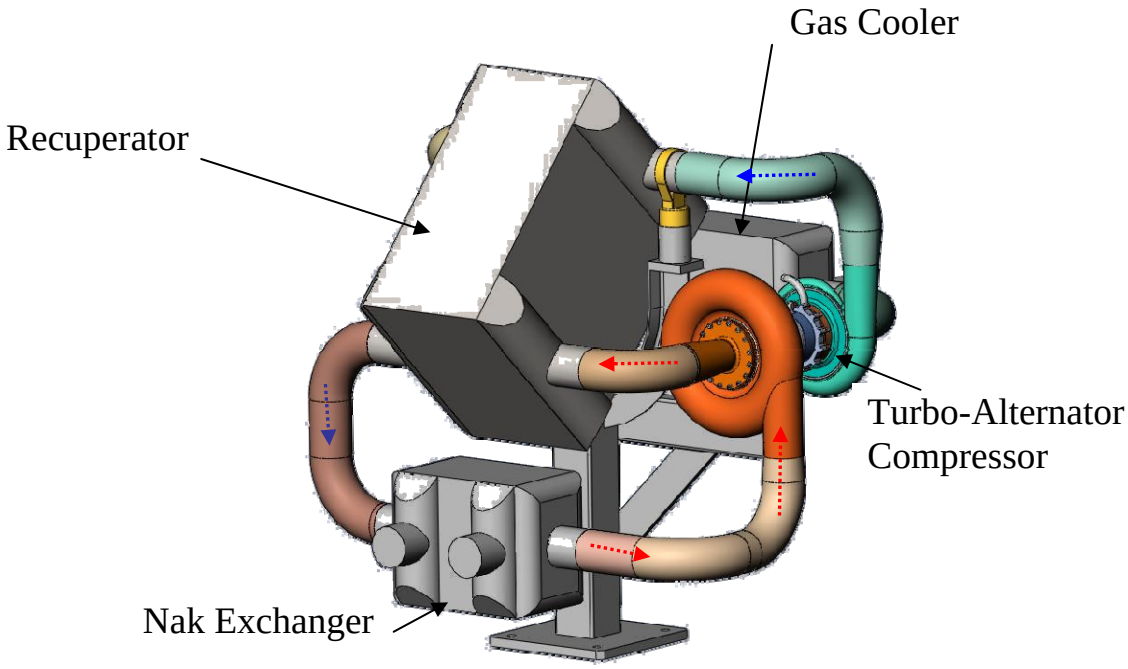

Figure 65: Power Converter with Plate/Fin NaK Heater

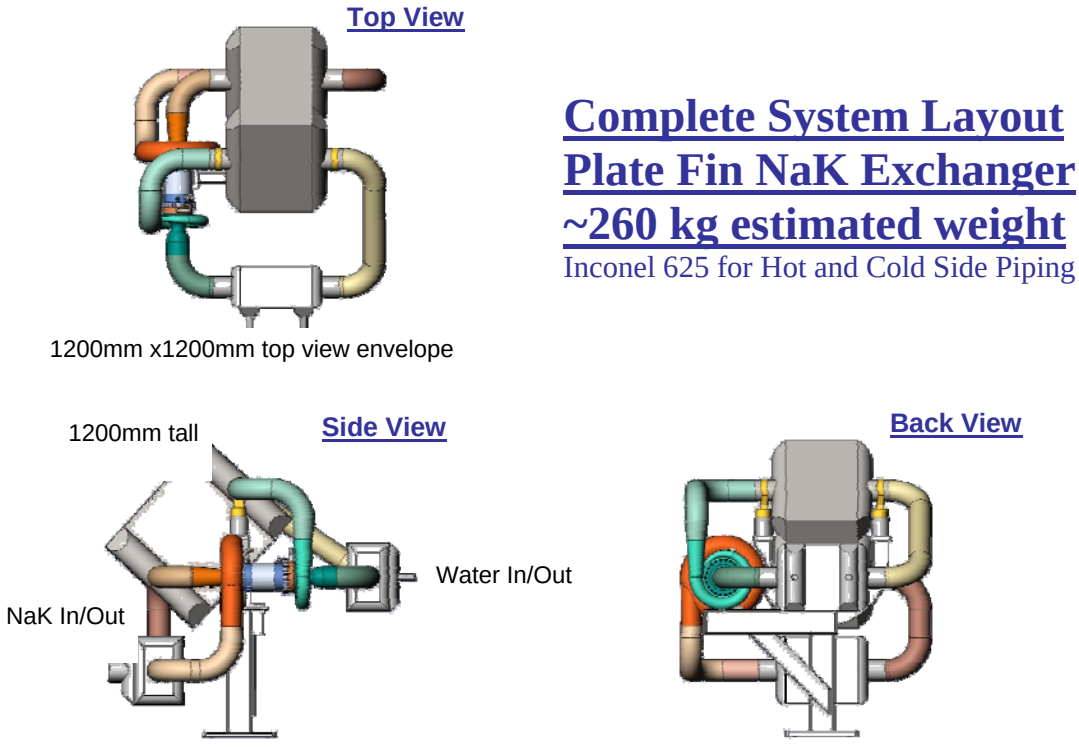

Figure 66: Power Converter Three View with Plate/Fin NaK Heat Exchanger

The thermal model is constructed in the same manner as the shell/tube heat exchanger. The boundary conditions are supplied to distribute the temperature in a manner that reflects the actual operation, Figure 67. The thermal information is used to find the thermal stresses for the power converter, Figure 68. The thermal stresses for the converter focused on the TAC result in Inconel 625 being used for the piping to avoid bellows. The TAC compressor and turbine also use Inconel to allow high stress safety factor, Figure 69.

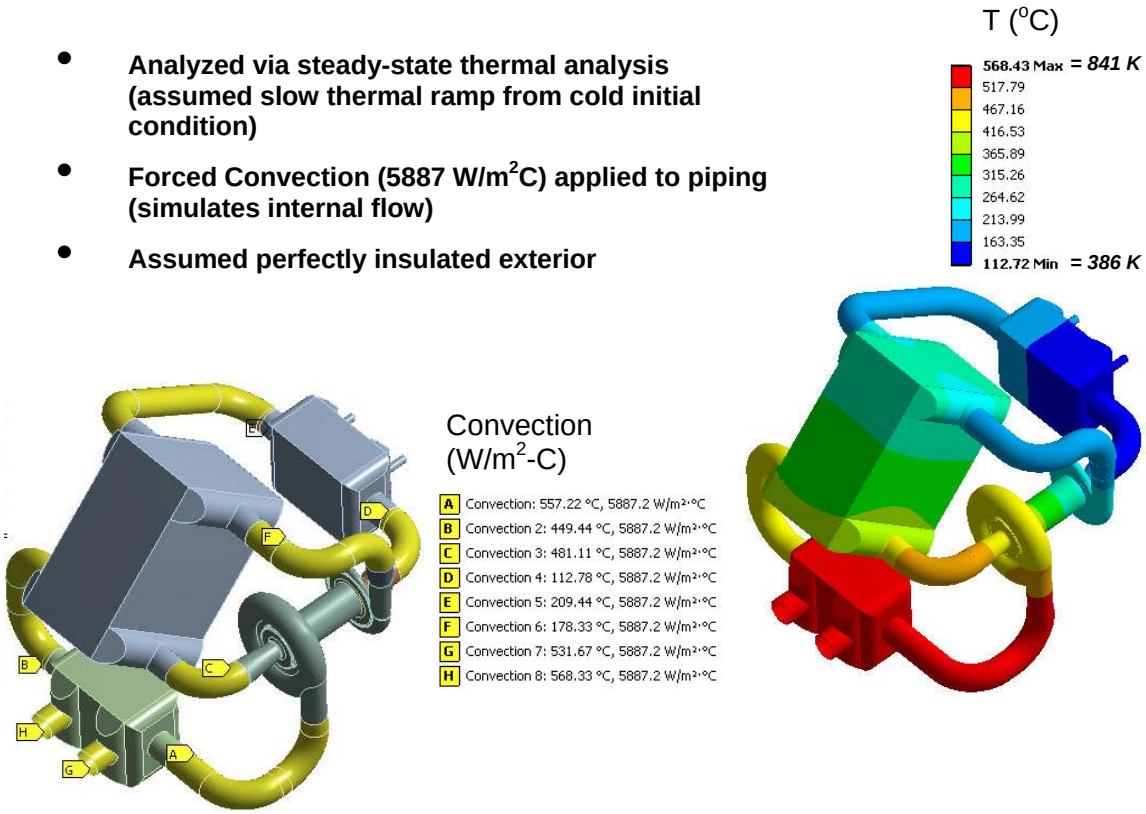

- **Analyzed via steady-state thermal analysis (assumed slow thermal ramp from cold initial condition)**
- **Forced Convection (5887 W/m^{2}C) applied to piping (simulates internal flow)**
- **Assumed perfectly insulated exterior**

Figure 67: Plate/Fin Power Converter Thermal Analysis

- Structural Analysis (Thermal Loads + Weight) of 3D Shell Model
  - Materials, thicknesses, component stiffness' representative of full 3D model
  - Max piping load = 103 MPa (FS = 2.7)
  - Max (Compressor Exit) Nozzle load = 207 MPa
- Forces & Moments calculated at Turbomachinery nozzle interfaces
  - Applied to 3D Compressor / Turbine Models

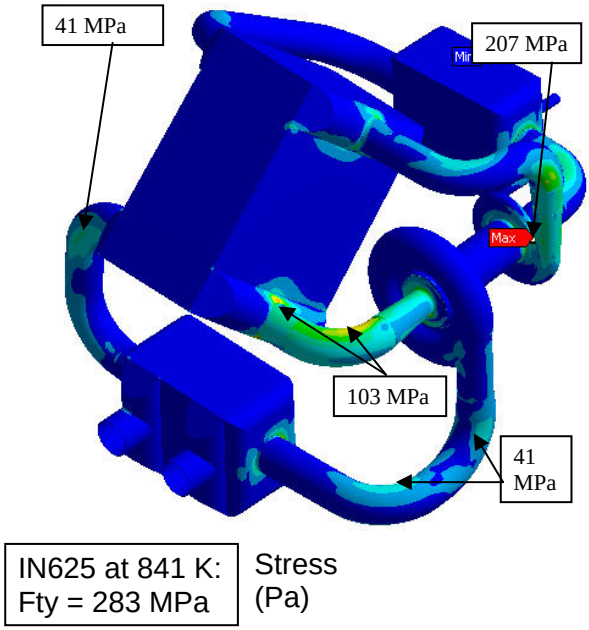

Figure 68: Plate/Fin Power Converter Stress Results

Compressor Housing

In625 at 436 K

- Su = 772 MPa
- Sy = 338 MPa

Max stress = 172 MPa

FSyt = 1.96

Turbine Housing

IN718 at 839 K

- Su = 1089 MPa
- Sy = 910 MPa

Max stress = 103 MPa

FSyt = 8.8

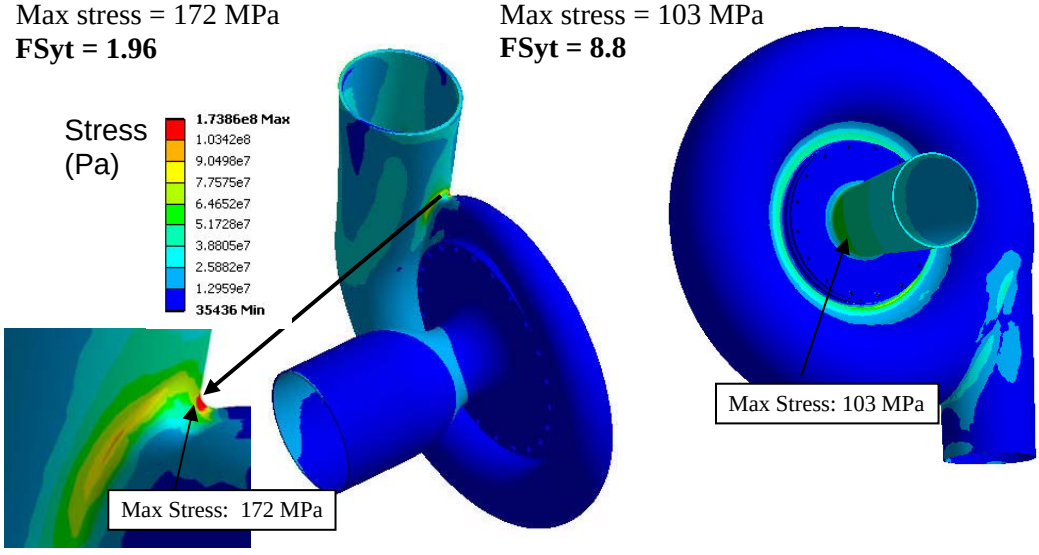

Figure 69: Plate/Fin Power Converter TAC Resultant Stress Results

The power converter ideally is insulated for the thermal vacuum environment. The insulation considered is multi-layer insulation. A very conservative method of calculation and the results are outlined in Figure 70. It indicates that 30-50 layers of MLI would be sufficient to minimize the radiated heat loss to a low level. The analysis considers the entire surface of the hot side of the loop as a black body radiating to the environment and does not consider the benefit of the radiation effect from the cold side of the equipment.

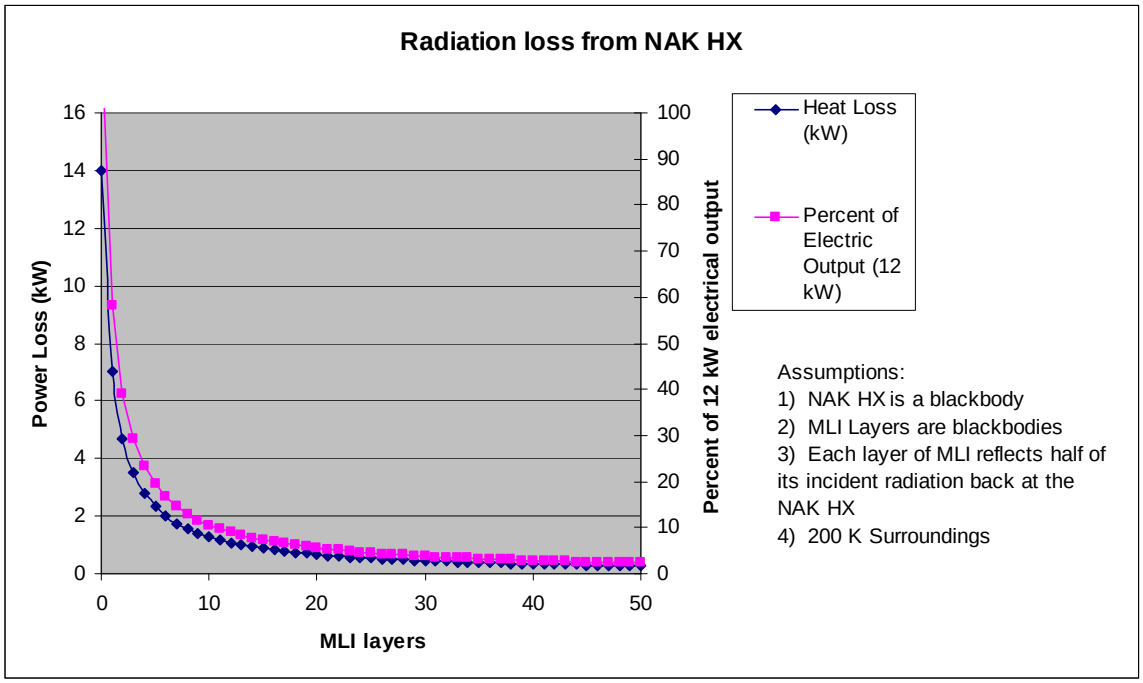

Figure 70: Insulation Analysis

11. Control Console and Data Acquisition, and Fill System

11.1 Control Console and Data Acquisition

The data control console operates the power converter and also functions as a data acquisition system. The control is set up on a programmable logic controller that is FPGA based and manufactured by National Instruments. The data control console is programmed using National Instruments LabVIEW software. The control console is programmed as a state machine. It has a startup mode, operating mode, shutdown mode, and fault handling mode. The control console has a graphical interface as shown in Figure 71. All of the pertinent pressure and temperature measurements are acquired, displayed and stored. The NaK pump and water pump could also be controlled using this as a master system controller. The control console communicates and controls the TAC power controller and monitors the health and fault status of all aspects of the power converter. Strip chart displays, both fixed and customizable are supplied, Figure 72.

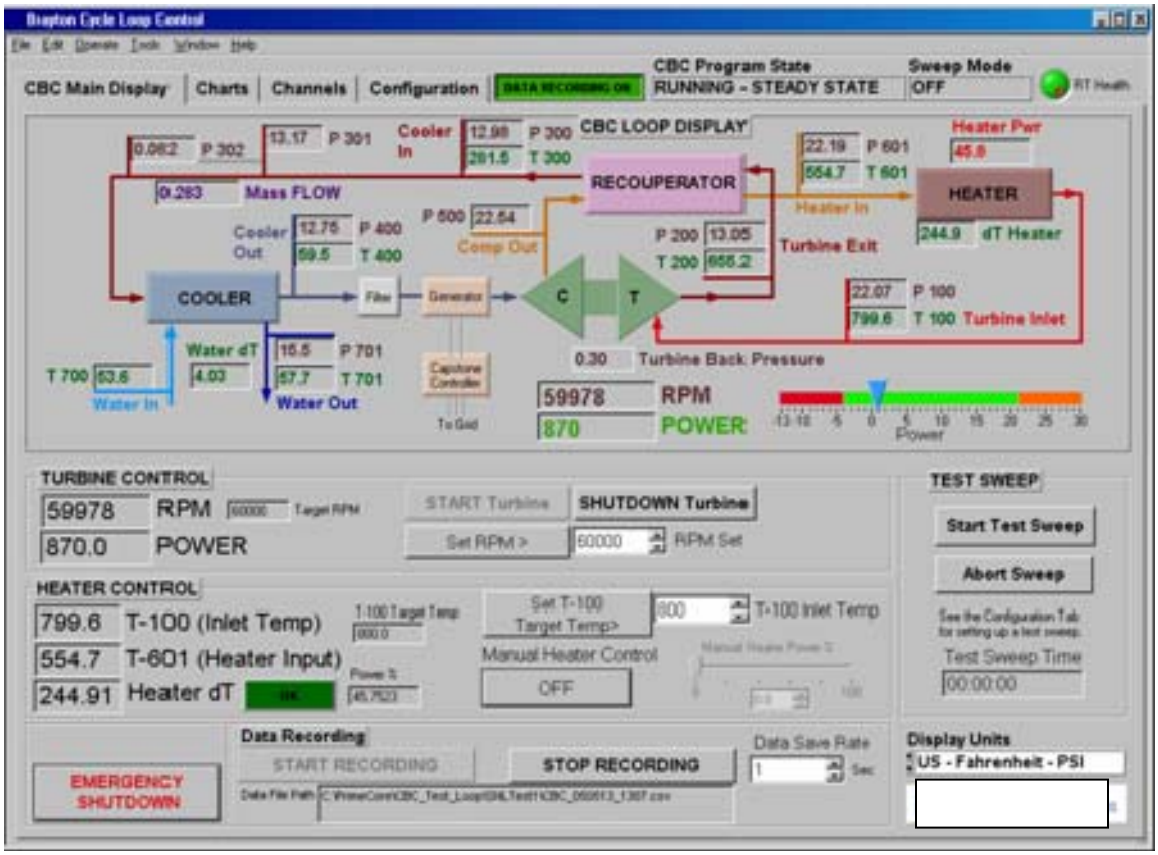

Figure 71: Control Console Screen Example

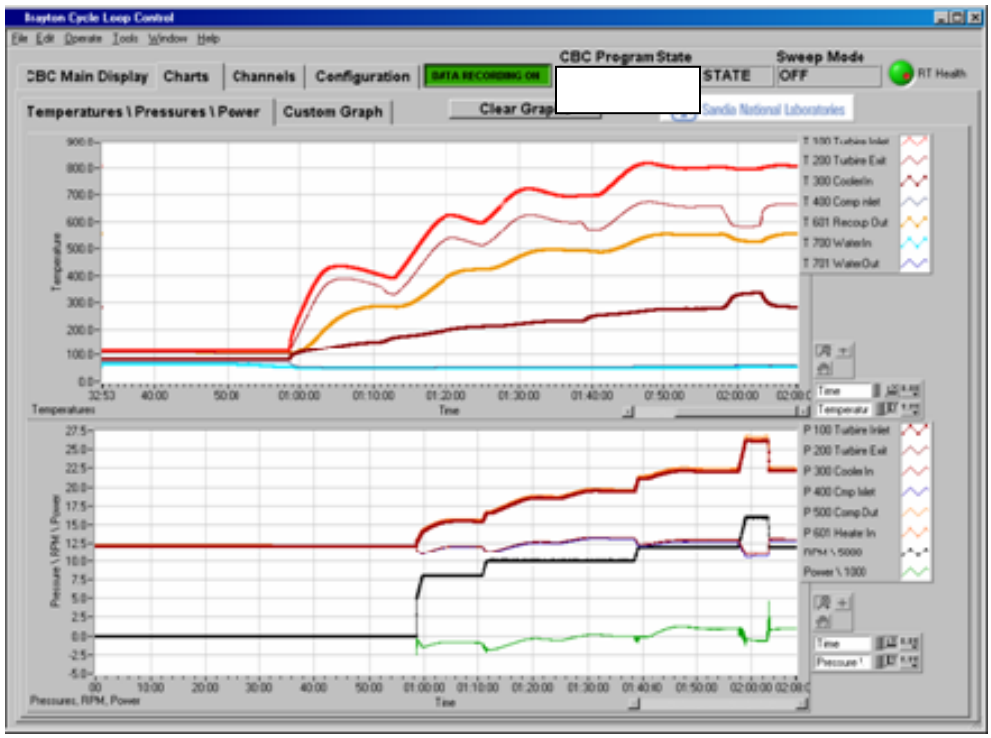

Figure 72: Strip Chart Recording Example

11.2 Fill System

The fill system is used to control the gas fill for the Brayton system. The diagram (Figure 73) shows the major components for this system. A vacuum pump is supplied to evacuate the power converter prior to gas fill. The system is filled with a standard CO2 gas bottle. It is supplied with a regulator and valves for flexible operation, either manual evacuation and fill, or automated through the control console.

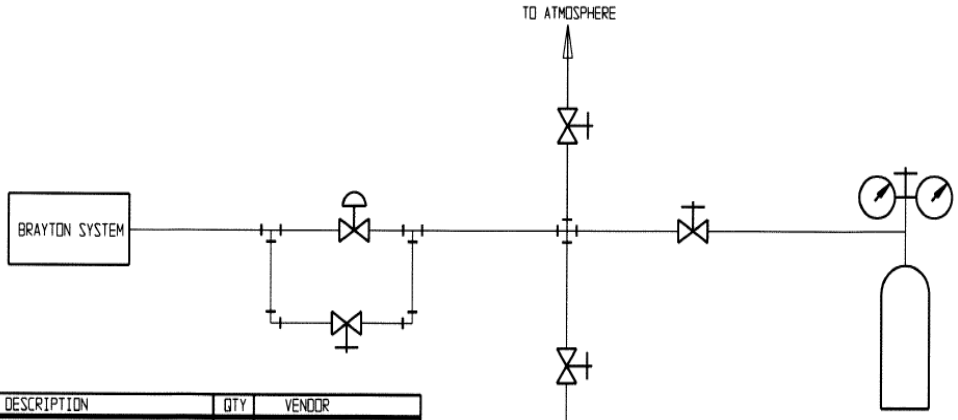

PART NUMBER	DESCRIPTION	QTY	VENDOR
SS-45S8-33CD	SOLENOID VALVE	1	SWAGELOK
SS-810-3	FTG, 8TU X 8TU X 8TU	2	SWAGELOK
SS-810-9	FTG, ELBOW 8TU X 8TU	2	SWAGELOK
SS-810-4	FTG, 8TU X 8TU X 8TU X 8TU	1	SWAGELOK
SS-8P6T	BALL VALVE	4	SWAGELOK
A371319D2P	VACUUM PUMP	1	EDWARDS
7897A39	REGULATOR	1	MCMASTER
7986A61	GAS BOTTLE	1	MCMASTER
	1/4 OD TUBE 316 SS	A/R	
NW16X50SWG	NW FITTING TO SWAGELOK	1	LDS VACUUM SHOPPER
NW10-16-ASR-V	ADAPTER NW10 TO NW16	1	LDS VACUUM SHOPPER
7919A51	ADAPTER 9/16 TO 1/4 NPT	1	MCMASTER
SS-810-7-4	ADAPTER 8TU TO 1/4NPT	1	SWAGELOK

Figure 73: Fill System Diagram and Equipment List

12. Summary

A set of prioritized goals were given in the specification. The design as presented is reviewed against these published goals.

- **Close relevance to future flight designs, including the potential for 8 year service life**

The power converter, as designed, is very similar to other existing power generation systems that have been designed by Barber-Nichols Inc. and others. The foil bearing

TAC type systems have shown to have very high reliability and life in excess of 80,000 hours.

- **Credible development path and maturation approach exist to achieve TRL 6 by FY 2012 with a reasonable cost**
- **Low development cost and risk**

The technology is mature and can be applied to the unique specification for the power converter. The temperatures and power level have led to a very conservative design that can be achieved with an easy development path with reasonable cost. No distinct technology challenges exist that need to be developed.

- **Design extensible to Mars (materials and design strategies compatible with mars environment)**

The equipment and materials used in this equipment are all stainless steel construction. The compatibility with the Mars environment should be robust.

- **High thermal-to-electric efficiency**

The power converter system strives to achieve over 18% thermal to electric efficiency. This is a high efficiency for a 12 kWe Brayton Cycle power converter with the specified high and low temperature range.

- **Minimum complexity**

The power converter complexity is low. Only a single moving part is used. The design is derived from highly reliable air-cycle type machinery used in commercial aviation.

- **Low mass and volume**

The system at 260 kg is within the boundaries of prior space based power systems in terms of kg/kWe. The system was designed to be compact and fit in a cube of 1.2 m size

- **Close relevance to future flight designs, including the potential for 8 year service life**

The design is similar to other Brayton Cycle power conversion systems that have been proposed in the past. The 8 year life has been considered in this design and is considered low-risk.

REPORT DOCUMENTATION PAGE	Form Approved OMB No. 0704-0188

1. REPORT DATE *(DD-MM-YYYY)*	2. REPORT TYPE	3. DATES COVERED *(From - To)*
01-06-2010	Final Contractor Report	

4. TITLE AND SUBTITLE
Closed Brayton Cycle Power Conversion Unit for Fission Surface Power Phase I Final Report

5a. CONTRACT NUMBER
NNC08CA64C

5b. GRANT NUMBER

5c. PROGRAM ELEMENT NUMBER

6. AUTHOR(S)
Fuller, Robert, L.

5d. PROJECT NUMBER

5e. TASK NUMBER

5f. WORK UNIT NUMBER
WBS 463169.04.03.01.02

7. PERFORMING ORGANIZATION NAME(S) AND ADDRESS(ES)
Barber-Nichols Inc.
6325 West 55th Avenue
Arvada, Colorado 80002

8. PERFORMING ORGANIZATION REPORT NUMBER
E-17020

9. SPONSORING/MONITORING AGENCY NAME(S) AND ADDRESS(ES)
National Aeronautics and Space Administration
Washington, DC 20546-0001

10. SPONSORING/MONITOR'S ACRONYM(S)
NASA

11. SPONSORING/MONITORING REPORT NUMBER
NASA/CR-2010-215673

12. DISTRIBUTION/AVAILABILITY STATEMENT
Unclassified-Unlimited
Subject Category: 20
Available electronically at http://gltrs.grc.nasa.gov
This publication is available from the NASA Center for AeroSpace Information, 443-757-5802

13. SUPPLEMENTARY NOTES

14. ABSTRACT

A Closed Brayton cycle power conversion system has been developed to support the NASA fission surface power program. The goal is to provide electricity from a small nuclear reactor heat source for surface power production for lunar and Mars environments. The selected media for a heat source is NaK 78 with water as a cooling source. The closed Brayton cycle power was selected to be 12 kWe output from the generator terminals. A heat source NaK temperature of 850 K ± 25 K was selected. The cold source water was selected at 375 K ± 25 K. A vacuum radiation environment of 200 K is specified for environmental operation. The major components of the system are the power converter, the power controller, and the top level data acquisition and control unit. The power converter with associated sensors resides in the vacuum radiation environment. The power controller and data acquisition system reside in an ambient laboratory environment. Signals and power are supplied across the pressure boundary electrically with hermetic connectors installed on the vacuum vessel. System level analyses were performed on working fluids, cycle design parameters, heater and cooling temperatures, and heat exchanger options that best meet the needs of the power converter specification. The goal is to provide a cost effective system that has high thermal-to-electric efficiency in a compact, lightweight package.

15. SUBJECT TERMS
Closed Brayton cycle power conversion; Fission surface power; Power conversion systems

16. SECURITY CLASSIFICATION OF:			17. LIMITATION OF ABSTRACT	18. NUMBER OF PAGES	19a. NAME OF RESPONSIBLE PERSON
a. REPORT	b. ABSTRACT	c. THIS PAGE			STI Help Desk (email:help@sti.nasa.gov)
U	U	U	UU	73	19b. TELEPHONE NUMBER *(include area code)* 443-757-5802